2021 年 3 月、関西大学審査学位論文

Novel Ionic Liquid-Type Lubricant for Magnetic Disk Media

イオン液体を用いた磁気ディスク用潤滑剤に関する研究

Kouki Hatsuda

初田　弘毅

博士論文要旨

初田弘毅

<<論題>>　Novel Ionic Liquid-Type Lubricant for Magnetic Disk Media

<<概要>>

ハードディスク装置は記録容量の増加に伴い、磁気ヘッドの素子部と磁気ディスクのスペーシング（Head-Media Spacing、HMS）が年々減少している。ディスク上に塗布されている潤滑剤は両末端に水酸（OH）基を有するパーフルオロポリエーテル（perfluoro polyether、PFPE）が用いられている。潤滑膜の平均厚みは現在の 10Å から更に低減することが求められおり、ディスク表面から分子レベルの高さを小さくする必要がある。また、次世代記録方式として熱アシスト磁気記録方式（Heat-Assisted Magnetic Recording、HAMR）の実用化が検討されている。HAMR ではディスク表面が瞬間的に数百℃まで加熱されるので PFPE 潤滑膜の揮発が懸念される。我々はイオン液体の高い熱安定性に着目して磁気ディスク用途への展開を検討した。イオン液体はアニオン（負に荷電したイオン）とカチオン（正に荷電したイオン）の組み合わせからなり、アニオンとカチオン間の静電相互作用により高い熱安定性を有する。HAMR 用途において高い熱安定性は有利であり、分子高さの低減についてもイオン液体は分子サイズが小さくとも揮発が抑えられるので有利であると考えた。そこで、このイオン液体を磁気ディスク用途に使うという設計コンセプトを実験的にイオン液体が磁気ディスク用潤滑剤として有望であると確認した。

<<各章の要旨>>

第１章は、PFPE 型潤滑剤の開発背景と磁気ディスク用潤滑剤への要求特性を説明する。

第２章は、初期検討としてハードディスク業界で従来使われている Fombline Z-Tetraol2000s(Solvay)とイオン液体を比較評価して相違点を明確にした。イオン液体は新規に OH 基とパーフルオロエーテルを有したものを合成した。単分子膜厚はイオン液体が 12Å、Z-Tetraol2000s が 18Å であった。ピンオンディスク装置により凝着力と摩擦力を測定した結果、イオン液体は凝着力が Z-Tetraol2000s に比べて小さくなることがわかった。一般的には凝着力は分子間相互作用（Van der Waals 力）に依るところが大きいがイオン液体は静電気的な反発力の為に低い凝着力になったと考えられる。

第３章は、前章の結果を踏まえてさらにイオン液体の分子設計を行った。ディスク表面に対する分子配向性の制御を期待して分子内の OH 基の導入位置の違う２つのイオン液体を合成した（IL-1、IL-2)。単分子膜厚はイオン液体 IL-1 が 6Å、IL-2 が 12Å であり、PFPE 鎖の太さが 7Å であるため、物理限界レベルまで膜厚を薄くすることが可能となった。同じくピンオンディスク装置により凝着力を測定した。その結果、イオン液体が表面と水平に配向している（IL-1）方が低凝着力を示し、分子配向と凝着力の相関を明確にできた。

第４章は、HAMR を模したレーザー照射装置を用いて、潤滑膜の耐熱性を比較した。レーザーの電流値が 140mA の場合、PFPE の蒸発量は一意にボンド比率に依存し、ボンド比率が大きいほど蒸発量は小さくなった。つまり PFPE のなかでは最もボンド比率が高い UV 処理した Z-Tetraol（ボンド比率：96%）が最も蒸発量が小さい。イオン液体はボンド比率に依存せず蒸発量は小さく、Z-Tetraol(ボンド比率：96%)と同等もしくは同等以上であることがわかった。

結論：設計コンセプトである分子高さの低減、レーザーに対する耐性についてイオン液体が優れることが実験的に確認できた。極薄膜物性としてイオン液体はボンド比率が小さいが、拡散速度は遅く耐熱性に優れている。この点が PFPE 潤滑剤と大きく違う点であり、イオン液体はケミカルにディスク表面と結合している成分は少なくともイオン結合という従来にない結合を持ち込むことで磁気ディスクの潤滑剤として必要なピックアップ、ヘッド摩耗、耐熱性を満たす可能性が示唆された。これらのことからイオン液体は HAMR 用潤滑剤として PFPE よりも優れていると考えられ、その実用化を期待される。

以上

Novel Ionic Liquid-Type Lubricant for Magnetic Disk Media

Kouki Hatsuda

Table of Contents

Abstract

1. Introduction ---------- 4

2. Preliminary Study ---------- 18

3. Application of IL for Ultra-Low HMS ------ 34

4. Application of IL for HAMR ---------- 49

5. Conclusion and Outlook ---------- 61

6. Acknowledgement ---------- 64

7. Reference ---------- 65

Abstract

With the increasing areal density of magnetic recording media, head–media spacing (HMS) has continued to decrease. Consequently, with decreasing HMS, the lubricant thickness should be smaller than the current thickness (10 Å). Accordingly, a heat-assisted magnetic recording (HAMR) system has been developed. When the temperature of the top surface of the magnetic disk media increases up to 600 °C, lubricant depletion due to evaporation or thermal decomposition occurs, which causes severe tribological problems. Thus, a new type of lubricant based on ionic liquids (ILs), which consists of anions and cations, is developed. Owing to the electrostatic interaction between anions and cations, ILs have a high thermal stability irrespective of the molecular weight. It is anticipated that these characteristics are considerably advantageous not only for the HAMR but also for reducing the HMS thickness. The objective of this study is to experimentally verify the design concept of IL-type lubricants.

First, ILs comprising a perfluoroether and a hydroxyl group were synthesized, their basic properties were studied and compared with those of Z-Tetraol 2000s (Solvay). The monolayer thicknesses were 12 and 18 Å for IL and Z-Tetraol 2000s, respectively. The microscopic friction and adhesion properties were measured using the pin-on-disk tester. The IL exhibited friction comparable to that of Z-Tetraol, however, its adhesion remained low even when it was thin. These properties suggested the feasibility of low-head flying without experiencing any tribological problems.

Second, two OH groups were designed to further increase the confinement to the disk surface. For IL-1, two OH groups were located at both terminal ends of the cation, whereas those for IL-2 were located at only one side of the cation, their monolayer thicknesses were 6 and 12 Å, respectively. The perfluoroether chain of IL-1 exhibited a laying orientation on the disk surface because the 6 Å thickness was equal to the diameter of perfluorochains, whereas that of IL-2 pointed upward. The ion pair of IL-2 was estimated to be covered by the perfluoroether chain such that the polar surface energy of IL-2 was smaller than that of IL-1.

Third, far-field laser irradiation was performed to evaluate the lubricant depletion for HAMR. For perfluoropolyethers (PFPEs), the depletion increased with the bond ratio, whereas IL only exhibited minimal depletion regardless of its bond ratio because of its ionic interactions.

Based on the above studies, the design concept, that is, small monolayer thickness and high thermal stability, was experimentally confirmed. Furthermore, the friction and adhesion properties were comparable and better, respectively. The foregoing improvements were achieved with the low bond ratios of ILs. Large mobile lubricants can effectively reduce the head wear, and a high bond ratio is usually required for film stability. Presumably, the ILs adsorb on the disks not only via the hydroxyl groups, but also through ionic interaction. This manner of bonding differs from the chemical bonding of conventional PFPEs. Owing to ionic interaction, the tribological performance can be improved even at low HMS and HAMR. Accordingly, it is concluded that ILs are promising for both low HMS and HAMR.

1. Introduction

1.1 Role of hard disk drive (HDD) on information society

The Internet of Things (IoT) refers to electric devices (e.g., sensors) that connect to the internet and enable us to make our world smarter and more responsive. It has significantly improved human lives and impacted businesses in all industries. Billions of IoT devices communicate real-time data without human involvement as they collect and share information; globally, tremendous amounts of data are generated each day. The International Data Corporation (IDC) forecasts that the summation of all global data will increase from 33 ZB in 2018 to 175 ZB by 2025. The shipping of more than 22 ZB of storage capacity across all storage media types must be completed between 2018 and 2025 to keep up with storage demands. Approximately 59% and 26% of the capacity should come from the hard disk drive (HDD) industry and flash technology, respectively. However, as video and audio streaming becomes more popular, the use of other optical storage, such as DVDs or Blu-ray discs, has decreased [1]. The storage for PCs or smart phones uses solid-state drives (SSDs) instead of HDDs, which are preferred by computing data centers in enterprises and cloud providers because these are the most cost-effective storage media to date. Near-line storage, which is a type of storage between online (for frequently accessed data) and offline (for infrequently accessed data) storage, has a potential application for HDDs. Along with the growing demand for data storage in enterprises and cloud providers, the use of near-line storage is a compromise between the cost of recording volume, electric power consumption, and large storage capacity. Online storage, which requires rapid input/output for operational computing, is suitable for SSDs. Offline storage, which, historically, stores data in magnetic tapes, is suitable for data archiving and long-term backup. The demand for HDDs as near-line storage remains high because they are anticipated to afford large storage capacities.

1.2 Importance of head–media spacing for high areal density

The head–disk interface (HDI) has constantly evolved to achieve a consistent growth in areal density. The HMS is the most important HDI parameter related to areal density: the areal density increases as the HMS decreases. A schematic of a slider head as it flies over a disk is shown in Fig. 1-1.

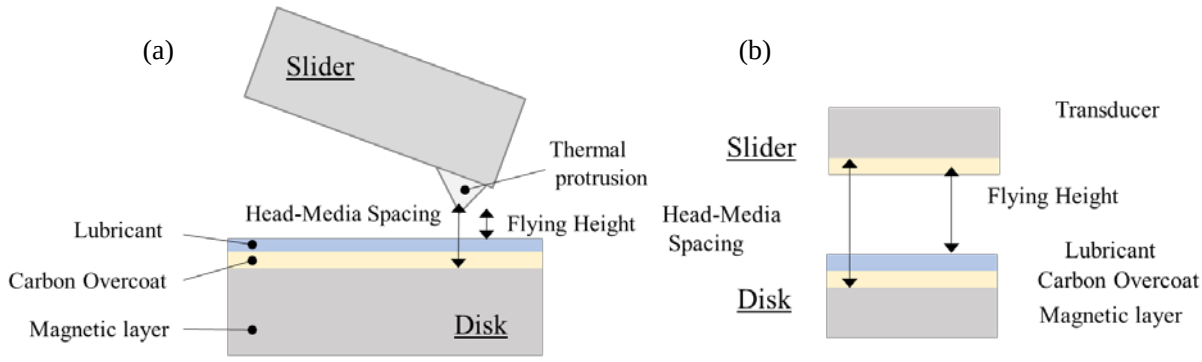

Fig. 1-1 Schematic of (a) head flying over a disk and (b) HMS component

HMS is the distance between the top of the disk's magnetic layer and slider head's transducer along with the sum of

the disk overcoat thickness, lubricant thickness, flying height, and head overcoat thickness. A small HMS enables the magnetic bit length to have a small physical dimension. To attain good writability and strong read-back signal, a low flying height is ideal; however, this increases the occurrence of unwanted slider–disk contact. Although the HMS has consistently decreased over the years, the continued development in the tribological design of HDI has maintained the reliability of HDDs. According to the ASTC report (2012), an HDD with 4 Tb/in^2 of areal density will be introduced in 2020. The current HMS target is 4–5 nm, which would lead to a lubricant thickness of 0.8 nm. Moreover, because the current lubricant thickness is approximately 1.0 nm, a reduction of 0.2 nm is necessary. 0.2 nm seems is significant for the areal density with an extremely limited HMS budget and thus exigent for lubricant design [2].

1.3 Historical perspective for lubricant function in HDI

In the last several decades, lubricants for magnetic disk media have been developed to provide a more reliable HDI. The PFPE is commonly used in this application because of its unique characteristics, such as chemical inertness, hydrophobicity, and liquid state over a wide temperature range [3].

(a) Fomblin Z-Dol (Solvay formerly Ausimont): As shown in Fig. 1-2 (a), this is a PFPE whose basic chemical structure includes a OH group at both terminal ends.

(a) Fomblin Z-Dol

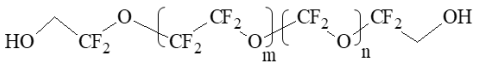

(b) Phosfarol A-20H

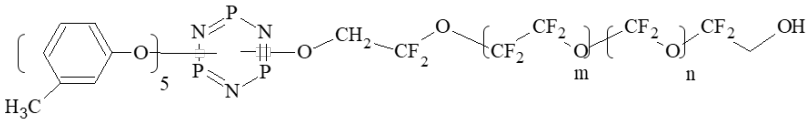

(c) Fomblin Z-Tetraol

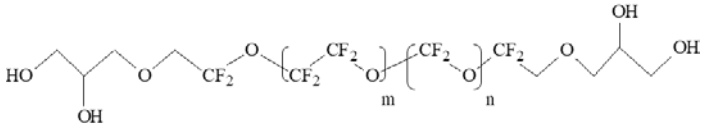

Fig. 1-2 Chemical structures of PFPEs

In the 1980s, the contact start/stop (CSS) mode was employed for the head gimbal assembly of HDDs. In the CSS mode, the slider head was dragged over the disk surface at the start/stop of operation while the heads in the HDDs flied above the magnetic disk during normal operation.

(b) Phosfarol A-20H (Moresco Co., Ltd): The aforementioned start/stop motions cause severe wear on the disk surface; to reduce this wear, a new type of PFPE has been developed. Between the two terminal ends, only one is substituted from the OH group to phosphazenes, which have a ring structure consisting of nitrogen and phosphorus. Phosphorus is one of the chemical components of an extreme pressure agent. The Dow chemical company and Moresco Co., Ltd. (formerly Matsumura oil Co., Ltd) commercialized it with the trade names X1P and A20H,

respectively. The lubricant formulation used in X1P or A20H is effective for reducing wear. The chemical structure of Phosfarol A-20H is shown in Fig. 1-2 (b).

(c) Fomblin Z-Tetraol (Solvay): This lubricant has two OH groups each for both terminal ends (Fig. 1-2 (c)). The total number of OH groups is larger than that of Z-Dol; hence, Z-Tetraol can more strongly adsorb on the disk surface than Z-Dol. The bond ratio is the parameter that quantifies the lubricant molecules in a lubricant layer that adsorb on the disk surface. Decreasing the molecular weight is advantageous for a low flying height; however, it causes a problem related to lubricant evaporation. A high bond ratio is necessary to solve problems related to evaporation, spin-off, and pick-up; the bond ratio without any treatment involved is called natural bond ratio. The natural bond ratios of Z-Tetraol and Z-Dol are 80% and 45%, respectively.

Ultraviolet (UV) treatment: UV process is performed after lubed process in disk manufacturing. With UV treatment, the bond ratios of Z-Tetraol and Z-Dol are 90% and 60%, respectively. The bond ratio exhibits a 10–15% increment compared with the natural bond ratio. For the PFPE lubricants of magnetic disk media, it was assumed that the bonding mechanism of UV involved the OH groups being attacked by the photoelectrons emitted from the carbon overcoat, thus enhancing the reactivity of OH groups to the surface [4–7].

Load/Unload technology: Since the mid-1990s, ramp load/unload technology has been employed as alternative to the CSS mode. For the ramp load/unload, the slider head moves off the disk before powering off and rests on the ramp located on the side closest to the disk. The ramp load/unload technology prolongs the life of the slider head because the head never comes into contact with the disk surface under normal operations; however, this does not mean that a lubricant is unnecessary. In practice, the head may occasionally come into contact with the rotating platter because of mechanical shock or other reasons. As stated, the lubricant thickness should be reduced to decrease the HMS, and the lubricant should maintain wear durability despite its decreased thickness.

Thermal flying height control (TFC) technology: Since the 2000s, the TFC technology of heads has been employed. The length of thermal protrusion changes dynamically which enable to control flying height. By applying this technology, the clearance between the magnetic head and disk surface can be reduced to a few nanometers. The thickness of lubricant films on magnetic disks should be reduced. Accordingly, a number of investigations were performed to reduce the thickness by a few angstroms. The thickness of the lubricant film is a non-negligible part of the HMS budget, and a lubricant thickness of several angstroms affects the areal density of magnetic recording [2]. To reduce the monolayer thickness of the lubricant on a magnetic disk surface, the PFPE confinement in the direction perpendicular to the disk surface has been investigated.

Touchdown Performance: Waltman et al. clearly indicated that low flying height of a slider head can be attained by reducing the lubricant film thickness, main chain molecular weight (MW), and main chain flexibility, given as follows [8]:

$$\Delta\text{clearance} \propto \frac{1}{\sqrt{\text{MW}}\,(\text{h})(\text{f})}$$

where MW is the molecular weight of the lubricant; h is the lubricant film thickness; f represents the main chain flexibility. This equation indicates that a larger clearance can be achieved with (1) smaller MW, (2) thinner film, and (3) stiffer main chain. The clearance between the flying head and outermost lubricant layer is experimentally

measured by acoustic emission (AE). As the flying head approaches the disk surface, the noise generated at the HDI is monitored as the AE signal. When the AE signal value suddenly increases, the slider head comes into contact with the disk media. Waltman et al. investigated the effect of each parameter on the touchdown clearance [8–11].

(1) Dependency on lubricant thickness: The touchdown clearance for various Z-Dol 4000 thicknesses was investigated. The numbers following the lubricant names (e.g., Z-Dol and Z-Tetraol) represent the MW of the PFPE; for example, in Z-Dol 4000, the MW is 4000. The touchdown clearance decreases as the lubricant thickness decreases. The touchdown clearance can be reduced by 0.8 nm with decreasing lubricant thickness from 15 Å to 7 Å, and the lubricant thickness can directly contribute to the HMS [8,10].

(2) Dependency on MW: Two different MWs of Z-Tetraol were prepared. The touchdown clearance of Z-Tetraol 1200 (thickness, 11.0 Å) is smaller than that of Z-Tetraol 2200 (thickness, 11.5 Å) by 0.8 nm. To clarify the effect of MW, the difference in lubricant thickness must be considered. According to the calculated result of Δclearance as a function of the film thickness for Z-Tetraol 2200, the difference in lubricant thickness between 11.0 and 11.5 Å corresponds to a 0.3 nm touchdown clearance. Thus, Z-Tetraol 1200 is superior to Z-Tetraol 2200 by approximately 0.5 nm in the touchdown clearance. By contrast, when the MW decreases, the evaporation loss increases because of the higher vapor pressure. Waltman et al. studied the correlation between the bond ratio and evaporation loss. The bond ratio varied because of disk aging under ambient conditions, i.e., no annealing or UV treatment was applied to the disk. For Z-Tetraol 1200, the amount of evaporation loss at 60 °C is suppressed by the higher bond ratio, i.e., the evaporated fraction after 20,000 min is 0.15 and 0.10 for 38 % and 63 % of the bond ratio, respectively. However, this still exceeds the criteria:0.05 which leading to degraded performance in the HDD due to the lack of lubricant film coverage. Thus, the use of a low-MW PFPE is not a practical solution because a trade-off relationship exists between the small monolayer thickness and evaporation loss [8,9].

(3) Effect of main chain flexibility: The Fomblin-type PFPE consists of $-CF_2O-$ (C1) and $-CF_2CF_2O-$ (C2) monomer units; the monomer units of the PFPE main chain are distributed in the random coil. As the C1/C2 ratio increases, the main chain becomes more flexible. Three different C1/C2 ratios of Z-Dols are prepared. To clarify the relationship between the main chain flexibility and Δclearance, only the C1/C2 ratio is varied at a constant film thickness and MW. Decreasing the C1/C2 ratio (i.e., the main chain stiffness increases) results in a larger Δclearance. This experimental result indicates that the main Z-Dol chain with a low C1/C2 ratio becomes compact [11].

Several companies competed in developing new types of PFPE lubricants. From among them, three representative PFPE lubricants are selected; the chemical structures of the three PFPEs are depicted in Fig. 1-3.

(d) D-4OH

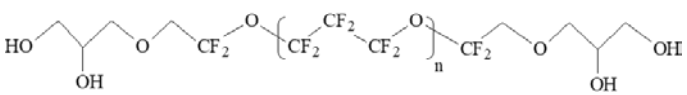

(e) TA-30

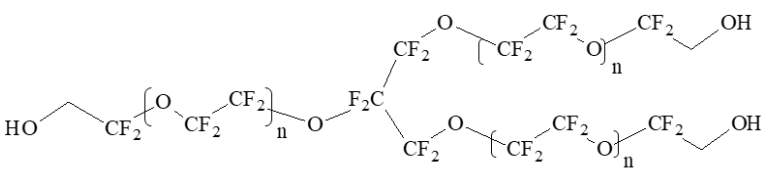

(f) Z-TMD

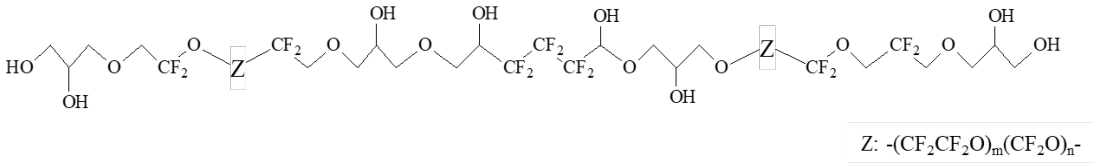

Fig. 1-3 Chemical structures of PFPEs

(d) D-4OH (Moresco Co., Ltd.): The chemical structure of D-4OH is shown in Fig. 1-3 (d). The main PFPE chain, also called the Demnum-type PFPE, consists of $-CF_2CF_2CF_2O-$ (C3). This PFPE, widely known as the material supplied by Daikin Industries, Ltd., is stiffer than the Fomblin-type PFPE. Compared to Z-Tetraol, the stiffer main chain in D-4OH resists the formation of a more globular conformation, thereby increasing the confinement to the disk surface [12]. Currently, D-4OH is one of the most popular lubricants in the HDD industry.

(e) TA-30 (AGC Inc. (formerly Asahi Glass Co., Ltd.)): TA-30 is a star-shaped polymer consisting of three linear PFPE chains with an OH group at each terminal end connected to a central core. Owing to its shape, TA-30 was tethered to the disk surface similar to a starfish, consequently reducing the lubricant thickness [13]. The TA-30 polymer is well designed considering the current lubricant requirement for magnetic disk media. Moreover, the perfluoroether unit is perfluoroethylene oxide, which is not only stable for a Lewis acid, but also stiffer than the Fomblin Z-type PFPE (i.e., copolymer of perfluoromethylene and perfluoroethylene oxides).

(f) Z-TMD (HGST Inc.): Z-TMD is one of the multidentate PFPE lubricants with several hydroxyl (OH) groups at the intermediate position along the PFPE main chain [14–17]. As stated, a trade-off relationship exists between the small monolayer thickness and evaporation loss that can be resolved by the multidentate-type PFPE. The MW of the main PFPE chain is sufficiently large to suppress the evaporation loss; hence, it is tethered to the disk surface because of the OH groups in the middle of the chain [18]. As a result, the Z-TMD exhibits a smaller monolayer thickness than the conventional PFPEs even with the same MW.

Fig. 1-4 summarize the lubricant development. With the continuous efforts of various engineers, the lubricant monolayer thickness has also continued to decrease. Fombline Z-Dol with large MW is utilized, and its monolayer thickness is large because of the high MW. Z-Tetraol is developed, and its monolayer thickness can be reduced because of the low MW. The four OH groups have the advantage over the two OH groups of Z-Dol in terms of bonding to the disk surface. A high bond ratio is essential to ensure the reliability of the HDI, especially for resolving the problems related to evaporation. D-4OH has the Demnum (C3)-type PFPE backbone. The Fomblin-type (C1/C2) PFPE has $-CF_2O-$(C1), making the main chain flexible, whereas the Demnum (C3)-type PFPE is stiffer. Thus, D-4OH at its monolayer thickness adopts a more compact main chain than the Fomblin-type Z-Dol or Z-Tetraol. The multidentate-type PFPE lubricant is the best lubricant that can successfully reduce the monolayer thickness. Its PFPE main chain has a high MW, however, it is tethered to the disk surface because of the OH groups located at the intermediate of the main chain.

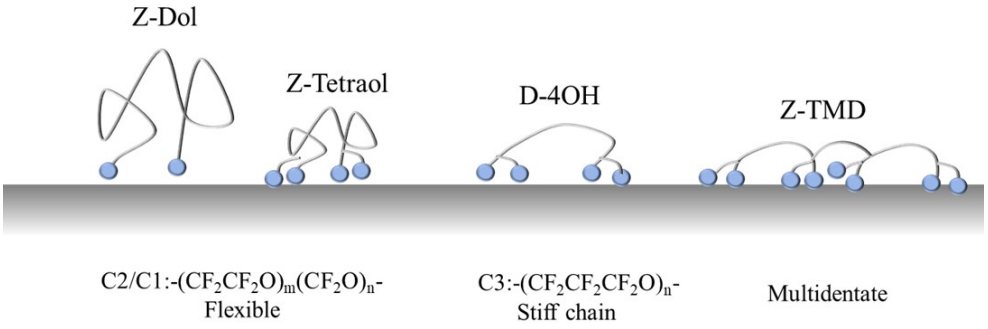

Fig. 1-4 Schematic of lubricant development on monolayer thickness
(blue circle: OH group, black line: PFPE chain)

1.4 Properties of lubricant film and method

The basic properties of the lubricant film are summarized in Table 1-1; these basic data are collected prior to the HDI evaluation. As the lubricant properties are correlated with the performance of the HDI specifications listed in the table, the HDI performance can be predicted based on these. The properties and their measurement metrology are described in this section.

Table 1-1 HDI evaluation items and related properties

	Lubricant properties	Unit	Method
1	Lubricant uniformity	Count	OSA
2	Thickness	Å	ESCA, FT/IR, Ellipsometer
3	Bond ratio	%	FT/IR, Ellipsometer
4	Surface energy	mJ/m^2	Contact angle meter
5	Monolayer thickness	Å	OSA, scanning Ellipsometer, Contact angle meter
6	Thickness loss	%	FT/IR, Ellipsometer

1. Thickness measurement

Thickness is considered as the most important lubricant parameter. For each property and evaluation item, data should be collected as a function of lubricant thickness to understand how the lubricant works on the disk media. For the PFPE, the lubricant thickness is measured by electron spectroscopy for chemical analysis (ESCA). From the narrow spectra of C1s, the C–H and C–F bands, which are attributed to the carbon overcoat and PFPE lubricant, respectively, are observed. The intensities of C–H and C–F are measured and used to calculate the thickness based on Beer's attenuation law of the underlayer (carbon overcoat) signals emitted by the overlaid layer (lubricant).

$$\text{Lubricant thickness} = d \times \exp\left(a\,(I_1/I_2) + 1\right)$$

where d is the effective electron escape depth; I_1 and I_2 represent the intensities of the lubricant C–F and carbon overcoat C–H, respectively; and a is the ratio of the C1s photoemission intensity from a bare disk [19,20]. Although ESCA is commonly employed to measure the absolute lubricant thickness, its use is inconvenient because it has a large-scale instrument with a vacuum chamber. Usually, Fourier transform infrared-reflection absorption spectroscopy (FT/IR RAS) is used with ESCA to measure the IR spectra of thin films. The absorbance at 1280 cm^{-1} attributed to the C–F stretching mode of the PFPE film is correlated with the lubricant film thickness [21]. After the absorbance of FT/IR RAS is calibrated by ESCA, only FT/IR RAS is used for measuring the lubricant thickness because of its simplicity and facility.

2. Lubricant uniformity

Lubricant uniformity is evaluated by an optical surface analyzer (OSA) supplied by KLA-Tencor; its commercial name is Candela. The OSA can rapidly provide the scanning image of the disk surface, facilitating the detection of the defects caused by lubricant particles or dewetting. If the surface image obtained by OSA exhibits many defects, this indicates that a slider head cannot fly stably. Particle-induced defects occur because of two reasons: the lubricant contains contaminant particles, and the lubricant aggregates or de-wets after its application on the disk surface. Filtration can reduce the quantity of particles from the outside, however, lubricant aggregation or dewetting is a problem resulting from the lubricant affinity to the disk carbon overcoat.

3. Bond ratio

The bond ratio indicates the amount of lubricant in the film that adsorbed on the disk surface. The PFPE lubricant physically and chemically adsorbs to the disk surface via the OH groups. If the bond ratio is low, then the performance in terms of thickness loss, spin loss, and lubricant pick-up may be inadequate. The bond ratio is determined by the ratio of film thickness after rinsing to that before rinsing. For the rinsing process, the lubricated disk is immersed in fresh solvent. Vertrel XF is frequently used as a rinsing solvent, and the bond ratio involves both physical and chemical bonding. In the case of the mixture of Vertrel XF and alcohol, the bond ratio only involves the latter.

$$\text{Bond ratio}(\%) = \text{h(as dip)}/\text{h(after rinsing)} \times 100$$

4. Surface energy

The surface energy is calculated from the contact angle using the extended Fowkes equation and divided into dispersive and polar components:

$$\cos\theta = -1 + \frac{2}{\gamma_l}\left[\left(\gamma_s^d \gamma_l^d\right)^{\frac{1}{2}} + \left(\gamma_s^p \gamma_l^p\right)^{\frac{1}{2}}\right]$$

where γs is the solid surface energy, γ_l is the liquid surface energy, indices d and p represent the dispersive and polar energies, respectively, θ is the contact angle. The information related to the interfacial force, coverage ratio, and monolayer thickness can be obtained using the surface energy (i.e., polar and dispersive energies) as a function of the lubricant film thickness. The dispersive energy of the blank disk (non-lubricated disk) is considerable large because the carbon overcoat surface is highly active. The dispersive energy decreases monotonically as the lubricant film thickness increases and approaches a saturated value when the disk surface is fully covered by the lubricant, the film

coverage is proportional to the dispersive energy. Accordingly, the coverage ratio is obtained as follows:

$$\text{Coverage ratio} = (\gamma^d(0) - \gamma^d(h))/(\gamma^d(0) - \gamma^d_{bulk})$$

where $\gamma^d(0)$ and γ^d_{bulk} represent the dispersive energies for the non-lubricated disk and the disk whose surface is fully covered by the lubricant, respectively; h is the lubricant thickness; and $\gamma^d(h)$ is the dispersive energy at the lubricant thickness (h). The dispersive energy originates from the van der Waals interaction. To design the air-bearing slider, the van der Waals force, which is quantitatively calculated using the Hamker constant based on the Lifshitz theory, should be considered:

$$\gamma_s^d(h) = \gamma_{bulk}^d + \frac{A^*}{24\pi(d_o + h)^2}$$

where A* is the Hamker constant; h is the lubricant thickness; and d_o is a constant. The values of A* and d_o are calculated by fitting them into the experimental data. The van der Waals force is the attractive interfacial force component that significantly affects the flying characteristics of the slider at a current flying height. A small Hamker constant indicates low disturbance under low-head flying.

The polar energy exhibits molecular orientation. As a function of the film thickness of PFPE lubricant, this energy exhibits oscillation, which is caused by molecular layering on the disk surface [12,13,22]. The minimum polar energy corresponds to the thickness of the monolayer because the quantity of the unbonded hydroxyl group should be minimized at the monolayer thickness. In addition to the polar energy as a function of lubricant thickness, two metrologies are presented in the succeeding section.

5. Monolayer thickness

The information on monolayer thickness is essential to design a reliable HDI. At the monolayer thickness, the coverage ratio is 100%, and the bond thickness approaches the saturated value, indicating that a portion of the mobile lubricant increase exceeds the monolayer thickness. This portion affects the lubricant reflowability or pick-up. As the HMS becomes narrower, many investigations related to the decreasing monolayer thickness have been performed. As discussed in Section 1.2, the multidentate-type PFPE lubricant seems to be most effective in reducing the monolayer thickness. Accordingly, it is relatively important to obtain the monolayer thickness as experimental evidence. In addition to polar energy as a function of lubricant thickness, there are two other metrologies. These are based upon two different phenomena: dewetting and terrace flow. First, dewetting is observed by OSA when the lubricant film thickness exceeds a critical dewetting thickness (i.e., monolayer thickness). The Q-polarized light wave of OSA provides the highest sensitivity to detect dewetting lubricant droplets. Second, terrace flow profiles are produced by measuring the spreading profile as a function of time. After a sufficient period, a shoulder in the spreading front corresponding to the lubricant monolayer thickness appears. According to [12], the monolayer thicknesses determined by three different methods were the same for D-4OH with three different MW values: 1500, 2100, and 3800. The derived monolayer thickness from three different method measurement is the same value for respective MW.

6. Thickness loss

Thickness loss results from evaporation. The initial thickness measured immediately after the lubricant is applied onto the disk is unity. Thereafter, the thickness is remeasured after various time spans. The thickness loss is calculated by the following equation:

$$\text{Thickness loss}(\%) = (h - h(t))/h$$

where h is the initial thickness; h(t) is the thickness after time, t. The storage temperature is usually estimated as 60 °C. The evaporation rate is determined by the thickness loss as a function of time. For the PFPE lubricant whose MW is less than 1500, the evaporation rate exceeds the criteria regardless of its bond ratio. In contrast, the PFPE lubricant whose MW exceeds 1500 continues to function well below the criteria on thickness loss. From the viewpoint of narrowing HMS, a smaller PFPE lubricant MW is advantageous because it increases the lubricant confinement on the disk surface, however, the thickness loss increases because of the high vapor pressure. Therefore, a trade-off between the small monolayer thickness and large thickness loss exists. To resolve this, the multidentate PFPE is developed, i.e., those PFPE chain is tethered to the disk surface such that the multidentate PFPE exhibits small monolayer thickness despite of high MW.

1.5 Specification of lubricant for Magnetic disk media

The specifications of HDI can be classified into four categories, as summarized in Table 1-2. With the lubricant having performed the key functions for durability at the CSS generation, the main current issue is the touchdown clearance. As the flying height narrows, contamination becomes even more critical because the adsorption of contaminants disturbs the stable head flying, hence, the important lubricant function is to protect the disk surface from contamination from the inner HDD environment. Each evaluation item is explained below. HDI tester are commercially available from Kubota Corporation, which enable to test flyability and durability.

Glide Noise: The status of flying can be monitored by the AE (acoustic emission) sensor as glide noise. When a slider head flies properly, the AE signal remains constant at the noise signal level. If a slider head encounters asperity on the disk surface, then the AE signal intensity exceeds the normal noise level.

Lubricant pick-up: Lubricant pick-up is a phenomenon wherein the lubricant on the disk media transfers to the flying head slider, causing a large distance variation between the flying head and disk. Currently, the flying height of the slider head is severally controlled, and the lubricant pick-up has to satisfy a strict set of criteria. For PFPE, the amount of pick-up is correlated with the mobile lubricant ratio. As the mobile lubricant decreases (i.e., the bond ratio increases), the amount of pick-up also decreases [16].

Touchdown clearance: The clearance between the flying head and outermost lubricant layer is quantified as the electric power (mW) of thermal protrusion. As the flying head approaches the disk surface, the noise generated at the HDI is detected as an AE signal. When the AE signal value suddenly increases, the slider head comes into contact with the disk media. At this moment, the touchdown power is determined, and the thinner lubricant thickness (large mechanical clearance) requires a longer protrusion of the TFC element.

Head wear and Altitude drag: Normally, durability deteriorates as the lubricant layer becomes thinner, however, it should be maintained despite such thickness. Thus, improving the durability of the lubricant layer itself is critical in lubricant development. Accordingly, the lubricant formulation or property is optimized to enhance the tribological

performance. Recent evaluation technology has enabled the quantification of durability performance. There are two evaluation items on HDI durability: head wear and Altitude drag test. The amount of head wear is measured using the TFC technology. When the pole tip of the head is worn, a longer protrusion is necessary for comparison with the initial state of the head. Head wear can be depicted based on the difference in touchdown power (mW). The Altitude drag test is a sliding test implemented under reduced pressure. It is an acceleration test for durability based on the fact that the slider head flies at a lower height under reduced pressure.

Spin loss: The spin loss is a phenomenon in which the lubricant on the disk scatters with high-speed rotation. This loss may be evaluated by comparing the lubricant thicknesses with and without the high-speed rotation over a sufficient period. The lubricant thickness can be measured by FT/IR or other metrologies, and the spinstand is used for high-speed rotation.

Contamination: The contamination problem has been around for a long time. Hydrocarbon contamination originates from the lubricating oil in the spindle motor and the suspension actuator pivot. Hydrocarbon-based lubricant oil is known to cause contamination in the HDI at elevated temperatures [23,24]. Siloxane is a well-known outgas material that can cause the slider head to crash because siloxane forms silica particles through friction heat at the HDI [25,26]. As stated above, this lubricant function is highlighted with current technology trend.

Corrosion: Both the lubricant and carbon overcoat contribute to protect the magnetic disk from corrosion. A defect in the carbon overcoat triggers corrosion under highly humid conditions. As the HMS becomes narrower, the carbon overcoat becomes thinner, accordingly, the anti-corrosion resistance of the overcoat should be maintained.

Table 1-2 HDI evaluation items and related properties

Category	Evaluation Items	Reevaluated Properties
Flyability	Glide Noise	Lubricant Uniformity
	Lubricant Pick-up	Bond Ratio
	Touchdown Clearance	Monolayer Thickness
Durability	Head Wear	Bond ratio, Coverage ratio
	Drag test	Coverage Ratio
	Spin Loss	Bond Ratio
Contamination	Hydrocarbon Exposure	Surface Energy
	Silicone Exposure	Surface Energy
Corrosion	Hot Wet test	Surface Energy, Ion Contamination

1.6 Next-generation magnetic recording systems

The recording density has been increased by reducing the size of the read/write head elements and magnetic grains of the media. However, the reduction in the size of the magnetic element has a physical limit, that is, the magnetic pole of the heads cannot generate sufficient magnetic field to write on the medium. Moreover, the magnetization of

the medium grain is not stable when there are temperature fluctuations inside the HDD. The limitation in increasing the recording density of HDDs is characterized by the competing requirements of scaling, thermal stability, and writability, which is known as the magnetic recording trilemma. To overcome this, two recording systems are developed: heat-assisted and microwave-assisted magnetic recording systems. For both systems, energy is locally provided to reduce the magnetic hardness only when writing data. As shown in Fig. 1-5, the HAMR and MAMR (microwave-assisted magnetic recording) heads are equipped with a laser diode and spin-torque oscillator (STO) to generate microwaves, respectively. New HDI requirements have arisen from the HAMR because of the heat applied on top of the disk surface [27,28]. In contrast, the MAMR seems to have no particular problem.

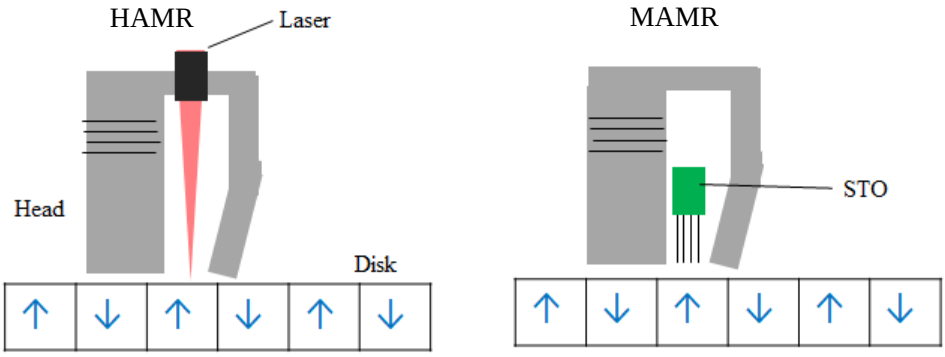

Fig. 1-5 Schematic of HAMR and MAMR

1.7 Ionic liquid features and previous investigations

Ionic liquids are organic salts composed of anions and cations. ILs transform to the liquid state at unusually low temperatures compare to inorganic salts. The melting point (m.p.) of NaCl is 801 °C, whereas that of ILs is less than 100 °C. Some ILs, such as the so-called room temperature ionic liquid (RTIL), even have an m.p. less than the room temperature. As shown in Fig. 1-6, ILs are larger molecular size and less ordered than NaCl. Consequently, the solidification of IL occurs at considerably lower temperatures than that of inorganic salts. Because ILs are of organic salt liquids, they possess many beneficial properties, such as electric conductivity, non-flammability, excellent thermal stability [29-31], and unique solubility. By exploiting these characteristics, their application in various industries is expected. Numerous papers have been published by scientists and engineers in this regard. The use of ILs as lubricant is one of the practical applications of these liquids.

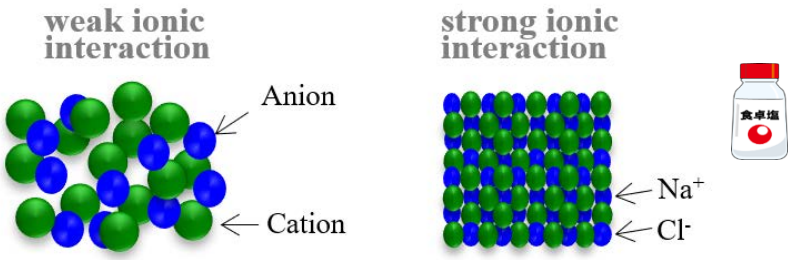

Fig. 1-6 Schematic of IL and Table salt (NaCl)

Since Ye et al. reported on the use of ILs as lubricants for space applications in 2001 [32], numerous researchers have investigated the tribological performance of ILs containing fluorinated anions, such as BF_4^-, PF_6^-, and

$(CF_3SO_2)_2N^-$. These ILs have exhibited superior antiwear and friction-reducing properties. In contrast, ahead of Ye's work, Kondo et al. previously studied protic ILs (PILs) from a different perspective. The objective was to develop lubricants for magnetic tapes [33–35]. In the magnetic tape industry, lubricants are typically applied onto the magnetic surface by dip coating to reduce the friction and wear due to the contact between the read/write magnetic head and media surface.

Several studies have been reported on the use of ILs as lubricants for the HDD media. The motivation of those studies is the use of ILs in the HAMR because of their high thermal stability. For the HAMR, the top surface of the magnetic disk media heats up to 600 °C over a few nanoseconds [27]. The lubricant depletes due to evaporation or thermal decomposition, causing severe tribological problems, hence, thermally stable lubricants are required as an alternative to the PFPE. Li et al. conducted an atomic force microscopy (AFM) study on various IL thin films and observed that a layering structure only occurs when the IL has an imidazolium ring in the cation. They attributed the IL layering structure of imidazolium to the π-π+ stacking between the IL and carbon overcoat surface on the magnetic disk and proposed that the structure is critical to the design of next-generation lubricants for magnetic disks [36]. Gong et al. evaluated the thin film properties of ILs and found that they have good lubricant uniformity on the disk surface. When heat was applied, the ILs exhibited a lower thickness loss than Z-Dol 4000 due to evaporation. Based on these experimental results, Gong et al. proposed the use of ILs as HAMR lubricants [37,38]. Kondo et al. synthesized a series of ILs with various lengths of alkyl chains in the cation and measured the friction coefficient of the thin film on the magnetic disk surface. They found that the friction coefficient decreased as the length of the alky chain increased, indicating that at a certain length, the alkyl chains function as a film boundary for preventing the direct contact between the two surfaces. Moreover, they measured the friction properties of the IL using an octadecyl group after heat treatment and concluded that the molecular design of ILs with long alkyl chains is effective for improving both the frictional performance and thermal stability [39–41]. Tani et al. developed a unique film boundary of PFPE using an IL (SNH2) consisting of PFPE carboxylate and diphenyether ammonium. They observed that SNH2 strongly adsorbed onto the magnetic disk surface and strongly interacted with the applied electric field during dip coating. When UV light was irradiated on the lubricant film, the cation in the IL dissociated from the disk surface, with the remaining PFPE carboxylate chemically adsorbing on the disk surface. The lubricant film obtained after UV treatment exhibited good stability compared with conventional PFPE under laser irradiation [42].

In contrast, few studies have examined low HMS. In this regard, Wang et al. investigated ultrathin IL films. Using atomic force microscopy (AFM), they confirmed that the IL monolayer thickness was only half of that of Z-Tetraol (MW: approximately 2000). The IL used in their study had an imidazolium cation and a fluorinated anion. The smaller monolayer thickness of the IL is attributed to the smaller molecular size of the material [43].

1.8 Lubricant development strategy and objective of this work

Based on the above discussion, there are two requirements for magnetic disk lubricants. First, as the HMS becomes narrower, the lubricant monolayer thickness should be smaller. Although a smaller MW of PFPE lubricants is effective for attaining better performance on TD clearance, the evaporation loss increases with the smaller MW. A trade-off problem exists between the TD clearance and evaporation. Considering evaporation loss, the lower limit of the PFPE MW is 1500. Generally, the boiling point is proportional to the MW of chemicals, that is, when the MW

decreases, the evaporation loss increases owing to the higher vapor pressure. In contrast, ILs exhibit a high thermal stability regardless of the MW because of the electrostatic interaction between anions and cations. Thus, the IL-type lubricants are expected to have a smaller monolayer thickness because their MW may be reduced without limit.

Second, ILs are expected to be applied to the HAMR system. The HAMR system is a promising next-generation magnetic recording technology for improving the areal density gains of hard disk drives. However, this technology introduces the critical head–disk interface problem associated with the use of near-field laser systems. The lubricant depletion due to evaporation or thermal decomposition becomes a severe problem. The depletion characteristics of PFPE-type lubricants have been investigated under various laser conditions, such as laser power, laser irradiation duration, and on/off laser irradiation duration. However, thermally stable lubricants are required as an alternative to PFPE because the aforementioned problem persists. Ionic liquids (ILs) are an attractive alternative because of their high thermal stability. Moreover, the contamination problem is more severe in the HAMR system [26]. When contaminant siloxanes adsorb onto the disk surface, they evaporate because of laser heating and condense on the slider head as smears. They accumulate on the head surface and affect not only the HDI reliability, but also the transmission efficiency of the laser light from the near-field transducer (NFT) of the HAMR head. To resolve this contamination problem in the HAMR, the disk surface should be fully covered with lubricant molecules, moreover, these molecules should be highly ordered to limit the lubricant adsorption site.

Along with the current development in HDDs, two lubricant requirements are expected. The author believes that both requirements can be simultaneously satisfied by ionic liquids. The objective of this work is to optimize ILs as lubricants for magnetic disk media and investigate their thin film properties in comparison with current PFPE-type lubricants.

1.9 Paper contents

Figure 1-7 shows the structure of this thesis. First, the background and objective of this study are stated. This chapter explains the necessity of developing new materials, and the HDD technology evolution and development of the PFPE-type lubricant are highlighted. The requisites for lubricants are described in detail, and it is presumed that the IL, as a new material, satisfies the current and will satisfy the future HDI requirements. Second, the basic properties of IL, as a novel material, are investigated for comparison with those of a representative PFPE-type lubricant, Z-Tetraol 2000s. The data on several frequently discussed parameters in HDD technology, such as lubricant thickness, bond ratio, and surface energy, are gathered. The IL exhibits a considerably different behavior compared with Z-Tetraol. In particular, the IL monolayer thickness is smaller than that of Z-Tetraol 2000s. Moreover, the IL exhibits a high polar surface energy and low adhesion force, which are independent of its thickness. Third, focusing on two major points (monolayer thickness and adhesion force), a new IL structure is proposed. The molecular orientation of the IL can be manipulated by the position of the OH group, such as multidentate PFPEs. This design concept of the IL is verified experimentally. Fourth, considering the HAMR application, the extent of lubricant depletion caused by a far-field laser on ILs and PFPEs is quantified. At the same time, data on basic properties, such as bulk TGA and bond ratio, are collected, and the correlation between the amount of lubricant depletion and these basic properties are examined. Finally, the paper is concluded by discussing the extent to which IL satisfies the lubricant requirements and its feasibility as a commercial product.

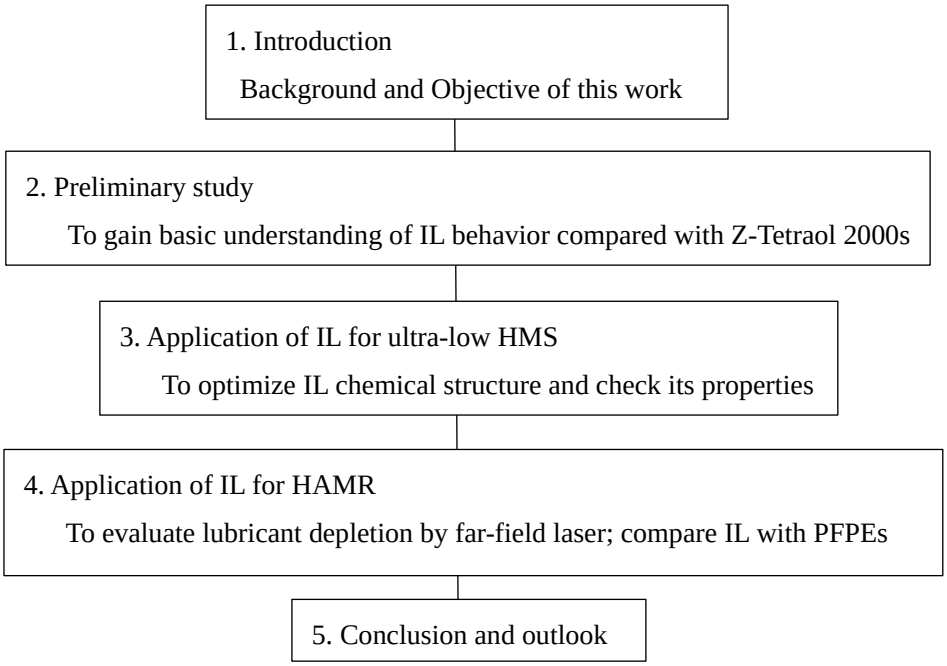

Fig. 1-7 Diagram of thesis content

2. Preliminary study

1. Objective of preliminary study

A novel IL is synthesized for magnetic disk media. The IL has a perfluoroether chain and an OH group, which are closely similar to the chemical design of the traditional PFPE-type lubricant. To gain a basic understanding of IL behavior, several ultrathin lubricant film properties, such as lubricant thickness, surface energy, and bond ratio, are measured; these parameters are consistently discussed in the HDD industry. Furthermore, the pin-on-disk microtribotester is used to compare the adhesion and friction force of IL with those of Z-Tetraol 2000s, which is a representative PFPE lubricant. Adhesion and friction force are key factors because they are related to flyability, head wear, and lubricant pick-up. As lubricant films become thinner, the basic understanding of the head–disk interface (HDI) is ever more critical to maintain HDD reliability.

2. Experiment

2.1 Lubricant Synthesis

The chemical structure of a novel IL synthesized by the author is presented in Fig. 2-1. For the cation moiety, the perfluoroether group and ethanol were introduced to the pyrrolidinium ring in the nitrogen atom. The anion was bis(nonafluorobutansulfonyl)imide. The MWs of the anion and cation were 580 and 704, respectively, hence, the total MW was 1,284. The details of the synthesis are described in [44]. The chemical structure and purity of the synthesized IL were checked using liquid chromatography and ion chromatography. Z-Tetraol 2000s (Solvay) was also checked for comparison. According to the F-NMR results of the PFPE backbone, its MW was approximately 2,300, and its m/n ratio was 5/6. Both lubricants are in the liquid state at room temperature. The viscosities at 25 °C were 1.2 and 2.4 Pa·s for the IL and Z-Tetraol, respectively. Themogravimetric analysis was performed under air flow; the 10% weight loss was measured at 365 °C and 261 °C for the IL and Z-Tetraol, respectively.

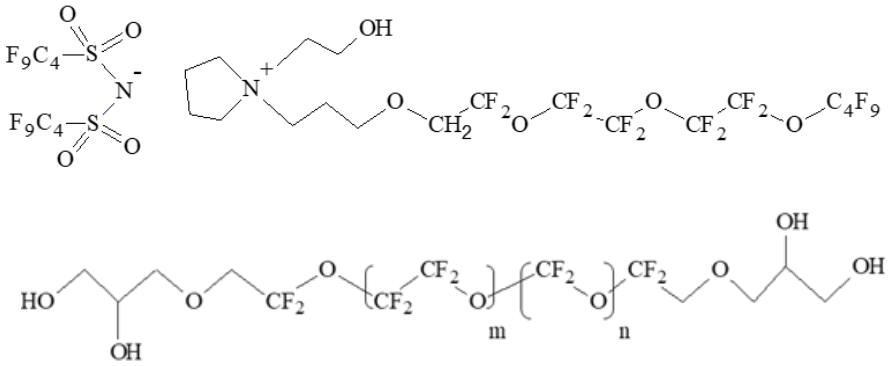

Fig. 2-1. Chemical structures of IL and Z-Tetraol 2000s

2.2 Thermogravimetry/Differential Thermal Analysis (TG/DTA)

Bulk thermal stability was evaluated using combined thermogravimetry and differential thermal analysis (EXSTAR TG/DTA 6200, Hitachi High-Tech Science Corporation). The measurements were performed in air purged from 30 to 600 °C at a heating rate of 10 °C/min. The temperature when the 10% weight loss was achieved was defined as

T_{d10}.

2.3 Sample preparation

Magnetic disks made of a glass substrate with a diameter of 2.5 in were used. The surface of each disk was nitrogenated with a diamond-like carbon overcoat. The average surface roughness (Ra) was approximately 0.2 nm. The magnetic disks were coated with each type of lubricant by dip coating. The lubricants were dissolved in Vertrel XF (Dupon-Mitsui Fluorochemicals Co., Ltd.). The lubricant film thickness varied with the concentration of lubricant in the solution. The disks were immersed in a solution of the lubricant for 180 s and pulled up with a speed of 1 mm/s. Ultraviolet irradiation and heat treatment were not performed. The lubricant film thickness was measured using a scanning ellipsometer (Five Lab Co., Ltd., MARY-102) equipped with a mechanical stage to enable the automatic measurement of any position over the disk. Immediately after dipping, the measured lubricant thickness was designated as “as dip thickness.”

2.4 Surface energy measurement

The contact angles were measured in the ambient atmosphere using a measuring instrument manufactures by Kyowa Interface Science Co., Ltd., DM-102. Droplets were applied to the lubricated surface of the disk using a capillary tube. The droplet volume was 2 mm^3, and the inner diameter was 0.8 mm. The contact angle data were determined 60 s after the droplet contacted the lubricant surface. The angles were measured on both sides of the droplet, and the three measurements were averaged. The surface energy was divided into dispersive and polar components, which were calculated by extending the Fowkes equation (Eq. (1)) from the contact angle data with water (γ^d_l=21.8 mJ/m^2 and γ^p_l=51.0 mJ/m^2) and hexadecane (γ^d_l=27.5 mJ/m^2 and γ^p_l=0 mJ/m^2).

$$\cos\theta = -1 + \frac{2}{\gamma_l}\left[\left(\gamma_s^d \gamma_l^d\right)^{\frac{1}{2}} + \left(\gamma_s^p \gamma_l^p\right)^{\frac{1}{2}}\right] \qquad (1)$$

where γ_s is the energy of the lubricated surface; γ_l is the liquid surface energy; index d represents the dispersive energy; index p represents the polar energy; and θ is the contact angle. The surface energies of the non-lubricated disk were 27.6 and 24.9 mJ/m^2 for γ_d and γ_p, respectively.

2.5 Bond ratio measurement

The bond thickness was the residual thickness after rinsing with the solvent Vertrel XF. The disk was immersed in Vertrel XF for 180 s, and the pulling up speed was 1 mm/s.

2.6 Terrace flow measurement

The lubricant was only applied to a part of the disk surface to observe the spreading of the front over time. The thickness profile of the films was measured using a scanning ellipsometer. The thickness profile measurements were made immediately after the lubricant film was applied. After a sufficient time had elapsed, the lubricant film had spread, thereafter, the shoulder corresponding to the monolayer thickness became observable. The disk was stored in a cassette and sealed using an aluminum package under partial vacuum to minimize contamination via the adsorption

of particles from ambient air [45].

2.7 Pin-on-disk microtribotester

The adhesion and friction forces were measured using a pin-on-disk microtribotester developed by the authors. The details of this microtribotester are described in [46,47]. A schematic of the tester is shown in Fig. 2-2.

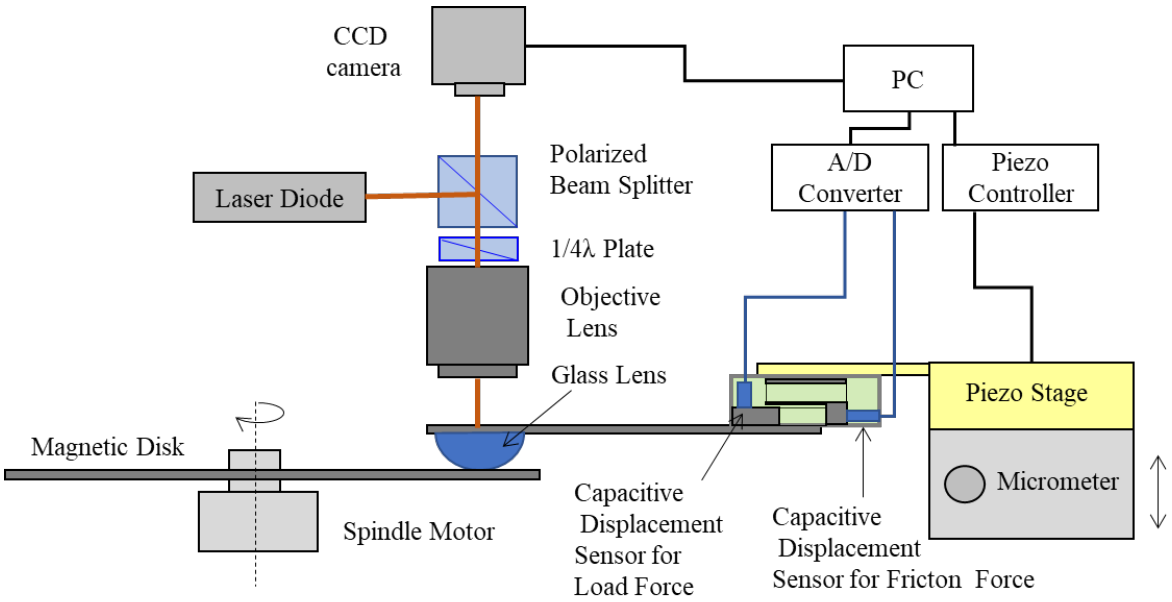

Fig. 2-2 Schematic of microtribotester used for measurement of adhesion and friction force

A magnetic disk was mounted onto the spindle. The pin was a glass semispherical optical lens (BK7) with an Ra value of 0.6 nm and a curvature radius of 1.82 mm, which is of the same order as the curvature radius of the actual slider head protrusion. A laser light was focused on the disk surface through an objective lens, and an optical lens was used as the pin. The reflected light was captured by a charge-coupled device camera to monitor the contact between the pin and disk surface with Newton's ring. The pin was approximately positioned onto the disk surface using a stage micrometer and precisely positioned using a piezo stage. The friction and load force sensors include force transducers consisting of parallel-leaf springs and capacitive displacement sensors (TECH ALPHA, FRS-713) to measure the strains in these springs. As the spindle rotated, the disk surface was moved up and down by the runout, caused by deformation because of the spindle hub clamping. The pin came into contact with the disk surface when the disk surface moved upward. In measuring the adhesion and friction forces, the pin was incrementally moved downward by the stepped movement of the piezo stage as the spindle rotated. The load force increased incrementally as the pin moved downward. The capacitive displacement sensor signal was converted to digital signals by a fast analog-to-digital converter, hence, the load force was monitored in real-time using a personal computer. The stepped movement of the piezo stage was stopped when the load force reached 0.5 mN. Rotations were performed several times at 0.5 mN to check the repeatability of the process, thereafter, the waveform data were obtained. The pin was loaded on the disk surface at a radius of 25 mm. The rotational speed of the disk was fixed at 6 rpm, corresponding to a relative velocity of 15 mm/s. All tests were conducted at a temperature of 28±2 °C and a relative humidity of

60±20%.

Figure 2-3 shows the schematic of the measurement of the adhesion and friction forces by the pin-on-disk microtribotester. The horizontal axis represents the time, and the right vertical axis represents the friction force. The left vertical axis represents the total force of the applied load and adhesion force.

When the pin was in contact with the disk surface from the leading slope to the maximum height, the applied load increased (load application region), following the pull-in at the touchdown of the probe. Then, the load decreased from the top to the trailing slope (load release region). The adhesion force was observed when the pin took off from the disk surface. At the point where the release force reached the magnitude of the adhesion force, take-off suddenly occurred (pull-out region).

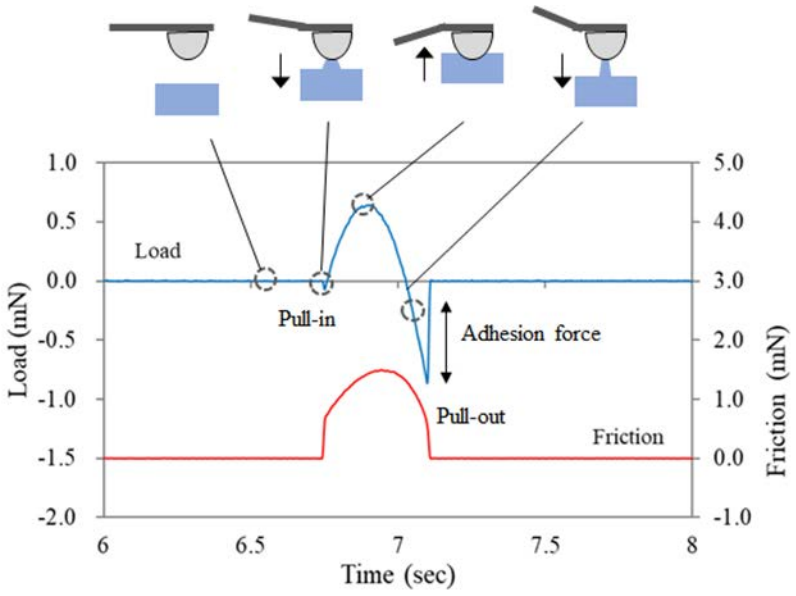

Fig. 2-3 Schematic of adhesion force and friction force measurements by pin-on-disk microtribotester

3. Results

3.1 Thickness profile

The lubricant thickness was measured as a function of the lubricant solution concentration, as shown in Fig. 2-4. All thickness values were obtained using ellipsometry. For both Z-Tetraol and IL, the thickness increased by increasing the dip concentration, indicating that the IL thickness can be controlled by changing the dip concentration. The dependence of Z-Tetraol compared with that of the IL on the lubricant film thickness was more considerable. The 10 Å thick lubricant film of Z-Tetraol was obtained when the lubricant concentration was 0.03%, whereas for the IL, the same film thickness was obtained when the lubricant concentration was 0.05%. The adsorption of Z-Tetraol on the disk surface was slightly strong owing to the four OH groups. Z-Tetraol lubricant exhibited a plateau from 0.05% to 0.06%, corresponding to the lubricant thickness of 18 Å. Based on the terrace flow method, the monolayer thicknesses were 12 and 18 Å for the IL and Z-Tetraol, respectively. Thus, the aforementioned plateau implied the completion of a monolayer formation followed by a multilayer formation.

The adsorption process is typically investigated through graphs known as adsorption isotherms. During the abovementioned plateau, the lubricant molecules condensed throughout the disk surface. Contrary to the results of

Z-Tetraol, a plateau was not clearly observed for the IL lubricant. However, the increase from 0.04% to 0.06% was relatively slow, hence, the corresponding IL monolayer thickness may be approximately 10 Å.

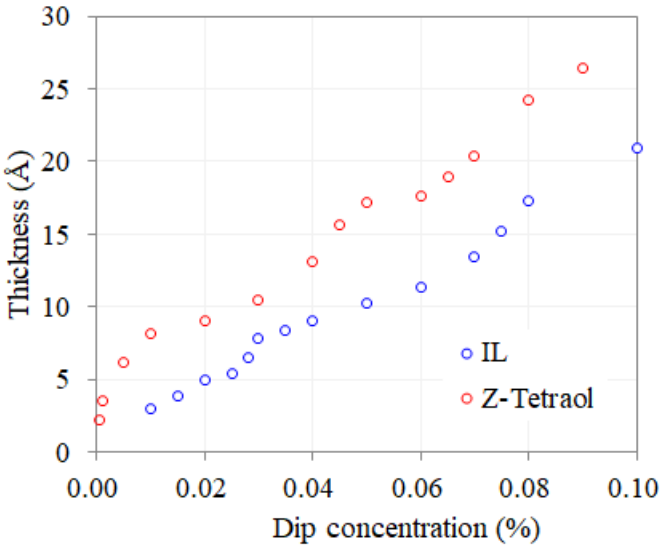

Fig. 2-4 Lubricant thickness as a function of dip concentration for the IL and Z-Tetraol

3.2 Film Characterization by FT/IR RAS

The Fourier transform infrared-reflection absorption spectroscopy (FT/IR RAS) methodology provides insights into the chemical structure and molecular orientation of the thin film because the electric field vector of the grazing incident beam is polarized perpendicular to the surface. Moreover, only the vertical vibration mode interacts with the surface, and the band is intensified. Figure 2-5 shows the FT/IR spectra of the IL and Z-Tetraol lubricants. Absolute thickness values were measured by an ellipsometer. For both the IL and Z-Tetraol lubricants, the band at approximately 1260 cm^{-1}, which was caused by the C–F vibration mode, increased monotonically with the film thickness, as shown in Fig. 2-6. This trend allowed the FT/IR to be used for thickness characterization.

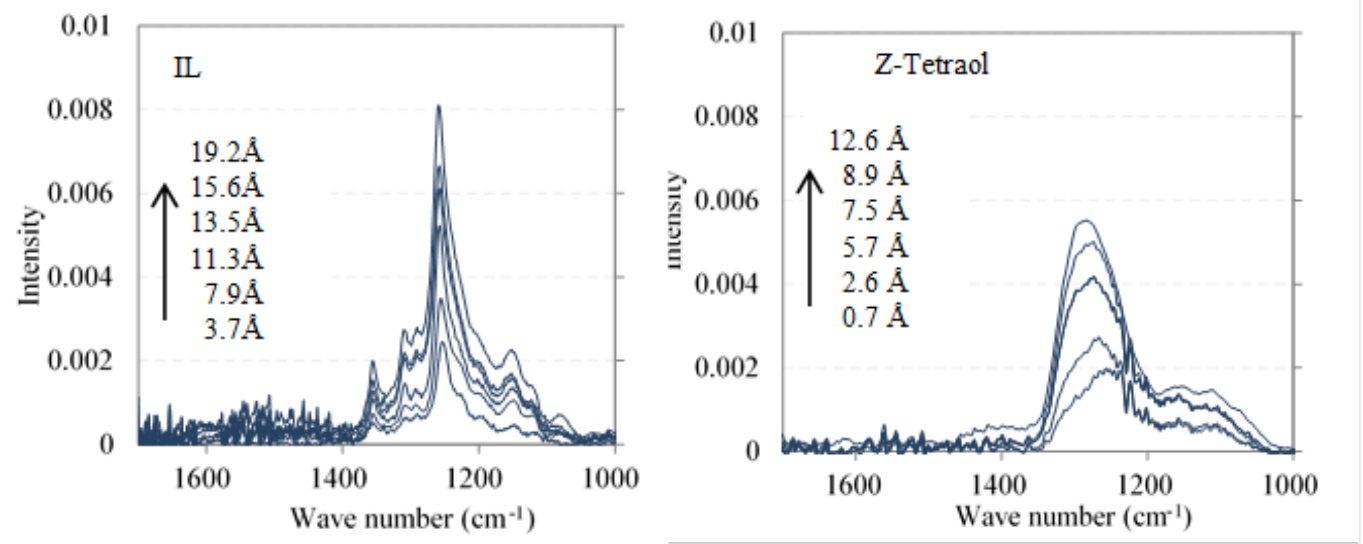

Fig. 2-5 FT/IR RAS spectra as a function of dip concentration for IL and Z-Tetraol

The IL bandwidth was smaller than that of Z-Tetraol at approximately 1260 cm^{-1}. The Z-Tetraol backbone was a random copolymer of $(CF_2CF_2O)_m(CF_2O)_n$, which generated many vibration modes owing to the perturbation of a neighboring random perfluoroether unit. In contrast, the IL perfluoroether merely consisted of $(CF_2CF_2O)_2$, forming its band sharp. For the IL, several peaks were observed, reflecting its relatively complicated chemical formula, the peaks at 1309 and 1355 cm^{-1} were assigned to N (of the pyrrolidinium ring) and SO_2, respectively. Although several researchers have published reports on the orientation of adsorbed fluorinated molecules onto the substrate using FT/IR RAS [48–50], a clear explanation about the molecular orientation based only on Fig. 2-5 has not been obtained.

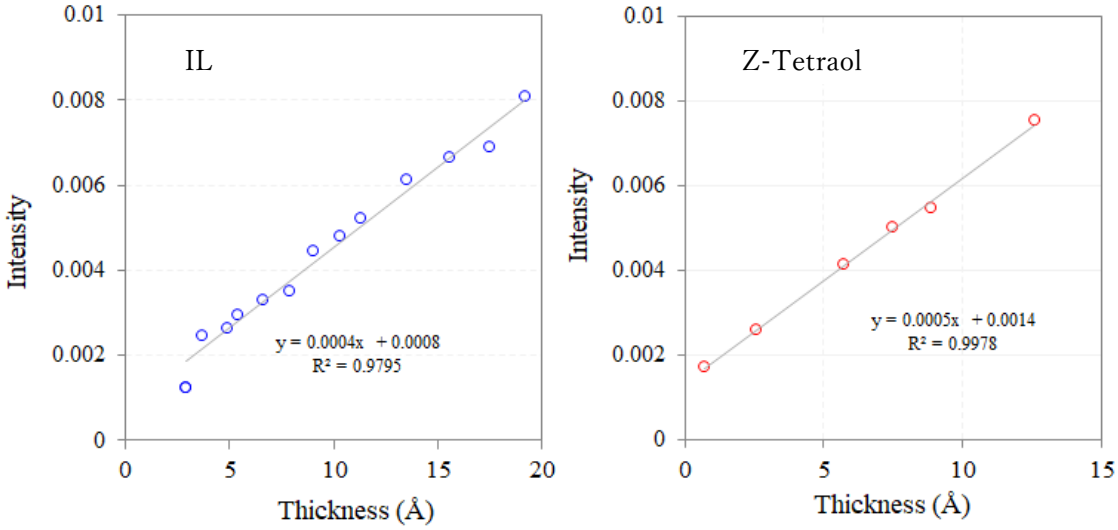

Fig. 2-6 Correlation between peak intensity and lubricant thickness

3.3 Terrace flow

As shown in Fig. 2-7, the terrace flow profiles determine the monolayer film thickness. The Z-Tetraol monolayer thickness agreed well with that reported by Tagawa, whose results were derived from the same terrace flow method [18].

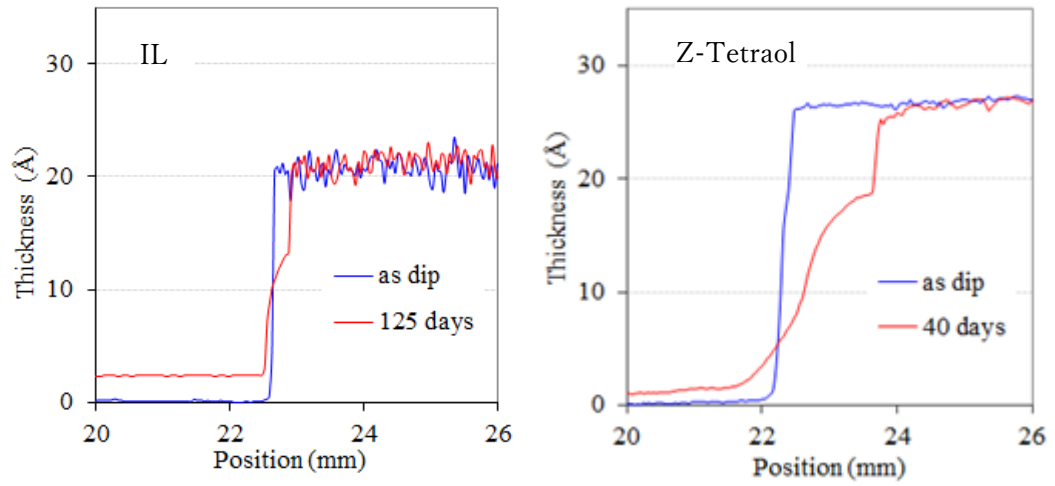

Fig.2-7 Terrace flow measurement result for the IL and Z-Tetraol

The 12 Å IL monolayer film thickness was larger than the PFPE chain cross-sectional diameter (8 Å) and smaller than the length of the perfluoroether segment (17 Å). Thus, the IL perfluoroether segment was inclined at a prescribed angle to the disk surface or was bent at the middle of the segment.

3.4 Bond thickness

Theoretically, the bond thickness increases with increasing lubricant thickness until the disk surface is fully covered by lubricant molecules. When the monolayer thickness is exceeded, the lubricant molecules do not bond to the disk surface, because of which the bond thickness levels off and a part of the mobile lubricant thickness increases with increasing lubricant thickness [51]. Figure 2-8 shows the bond thickness profile as a function of the film thickness of the IL and Z-Tetraol lubricants. The bond thickness increased monotonically with the film thickness and approached constant values of approximately 9 and 18 Å for the IL and Z-Tetraol lubricants, respectively. In comparing the monolayer thickness values, the 9 Å thick IL lubricant monolayer obtained with this bond thickness profile was slightly smaller than the 12 Å thickness from the terrace flow, whereas the 18 Å thick Z-Tetraol lubricant is equal to the thickness from the terrace flow.

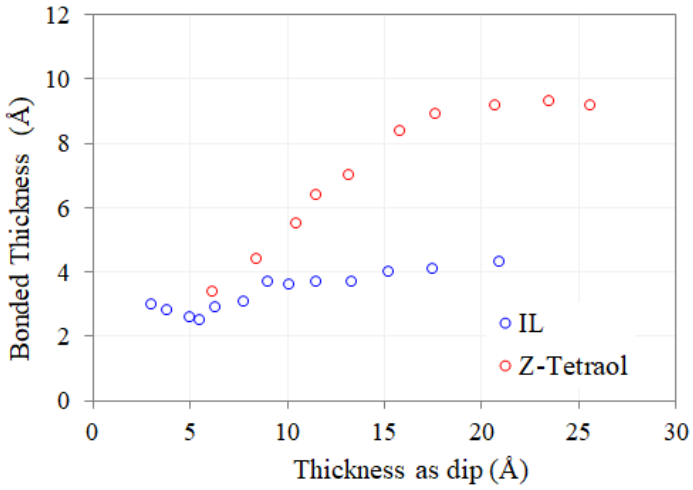

Fig. 2-8 Bond thickness profiles of IL and Z-Tetraol

3.5 Surface energy

Figure 2-10 shows the dispersive surface energy as a function of the film thickness of the IL and Z-Tetraol lubricants. The dispersive component decreased monotonically in both lubricants as the lubricant film thickness increased and approached a constant value when the disk surface was fully covered by the lubricant molecules. The dependence of the dispersive energy on the lubricant film is expressed by Eq. (2), as follows:

$$\gamma_s^d(h) = \gamma_{bulk}^d + \frac{A^*}{24\pi(d_o + h)^2} \qquad (2)$$

where h is the lubricant film thickness; d_0 is a constant; A* is the effective Hamker constant. Note that A* and d_0 were calculated by fitting them into the experimental data. The A* values were 2.4×10^{-19} and 3.1×10^{-19} J for the IL and Z-Tetraol lubricants, respectively; the d_0 values were 3.4 and 4.0 Å for the IL and Z-Tetraol lubricants, respectively. For both A* and d_0, the IL values were as small as those of Z-Tetraol. Therefore, the adhesion force

should not be significantly large [12,13]. These characteristics are expected to provide a reliable HDI under a low-flying head. Tani et al. demonstrated that the coverage ratio, α(h), can be derived from Eq. (3) [47]:

$$\alpha(h) = \frac{\gamma_s^d(0) - \gamma_s^d(h)}{\gamma_s^d(0) - \gamma_{bulk}^d} \qquad (3)$$

where $\gamma^d_s(0)$ is the dispersive energy value of the non-lubricated disk surface. The film coverage is proportional to the dispersive energy. As shown in Fig. 2-9, the coverage ratio as a function of the film thickness is calculated by fitting the dispersive energy curve. The coverage ratio curves of the two lubricant types were considerably similar although the IL monolayer thickness was smaller than the Z-Tetraol monolayer thickness by 6 Å. The coverage ratio increases with the decreasing quantity of the non-lubricated area. It is affected by several parameters, such as the length and orientation of the lubricant molecular.

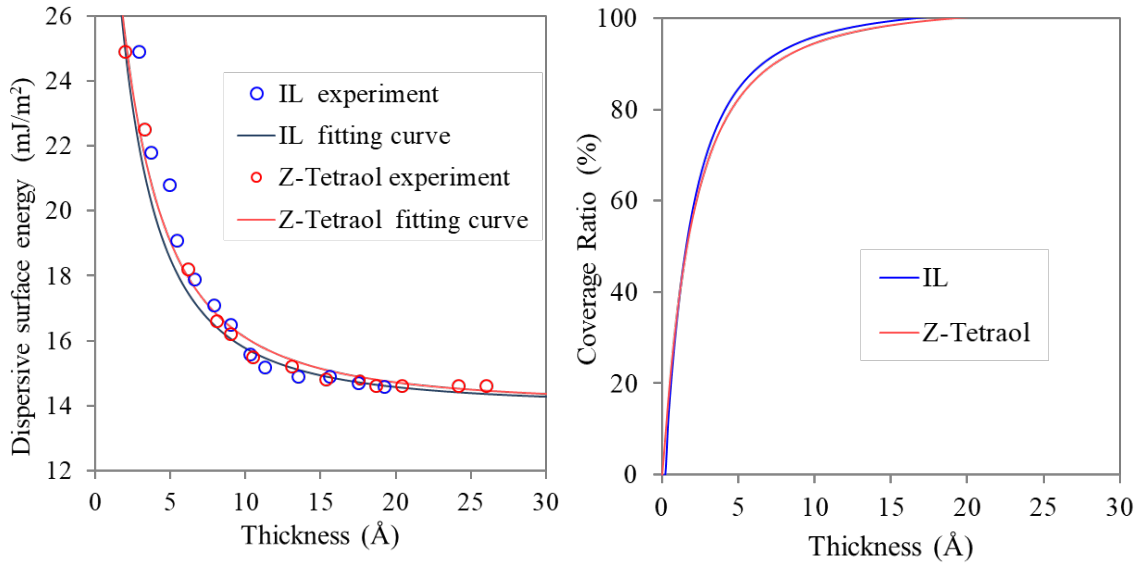

Fig. 2-9 Dispersive surface energy data and coverage ratio as a function of lubricant film thickness and fitted theoretical curve

The corresponding polar surface energy is also shown in Fig. 2-10 as a function of the film thickness. For Z-Tetraol, the minimum point of the polar component was at approximately 20 Å. Waltman et al. reported that the oscillation, as a function of the conventional PFPE film thickness, is caused by the molecular layering on the disk surface [12,13,22]. First, the minimum point of the polar component corresponds to the thickness of the monolayer because the quantity of the unbonded hydroxyl group should be minimized at the monolayer thickness. In contrast, the polar energy of the IL is considerably higher than that of Z-Tetraol. The polar component of the IL increased until its thickness reached 11 Å. This thickness may have initially increased the quantity of IL molecules on the disk surface before decreasing and thereafter remaining constant from 14 to 19 Å. The sudden drop to 13 Å approximately corresponds to the monolayer thickness of the IL shown in Fig. 2-7. Presumably, the decrease in polar surface energy was caused by the molecular orientation of minimizing the polar groups at the top of the lubricant surface.

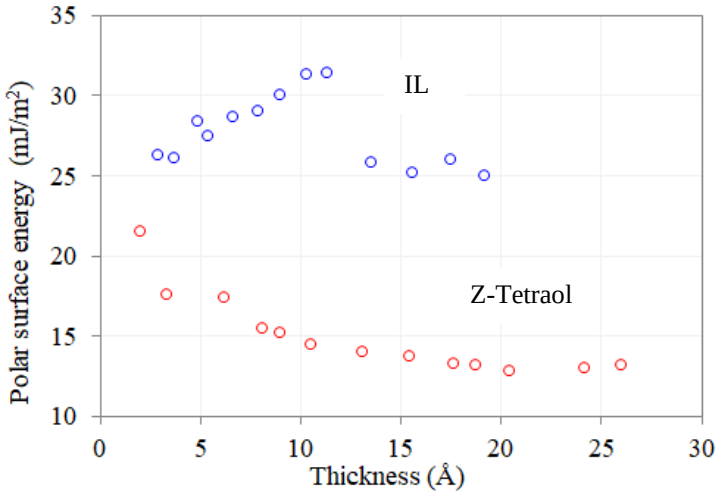

Fig.2-10 Polar surface energy data as function of film thickness of IL and Z-Tetraol lubricants

3.8 Friction and Adhesion force

The representative friction and adhesion measurements are presented in Figs. 2-11 and 2-12, respectively. The horizontal axis represents the time, and the right vertical axis represents the friction force. The left vertical axis represents the total force corresponding to the applied load and adhesion force. By comparing the IL with Z-Tetraol, two significant differences were identified. (1) The IL's friction coefficients at the maximum applied load (approximately 0.5 mN) were relatively high compared with those of Z-Tetraol throughout the thickness. (2) The IL's adhesion force was relatively small compared with that of Z-Tetraol regardless of the lubricant thickness.

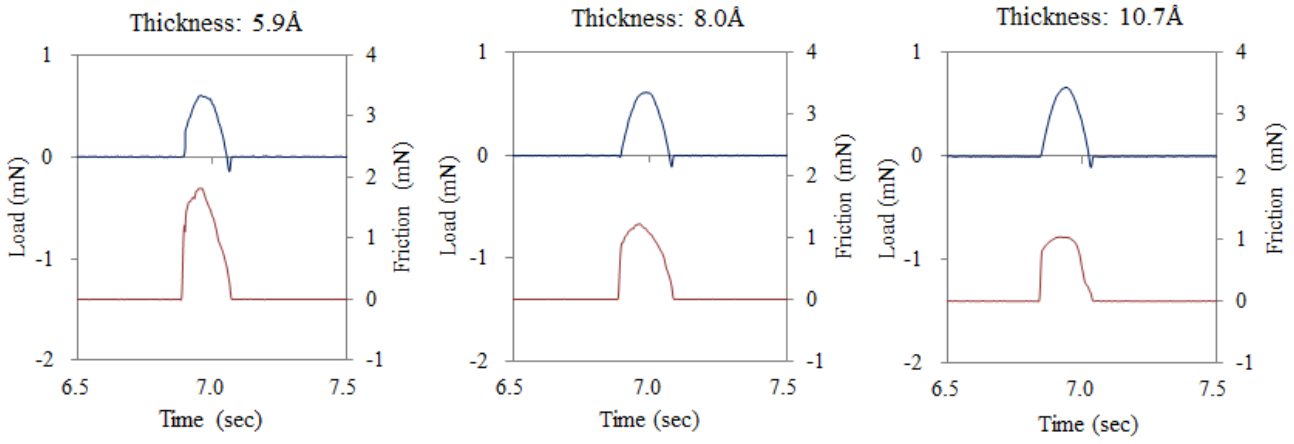

Fig. 2-11 Representative friction and adhesion measurement results at various thicknesses of IL

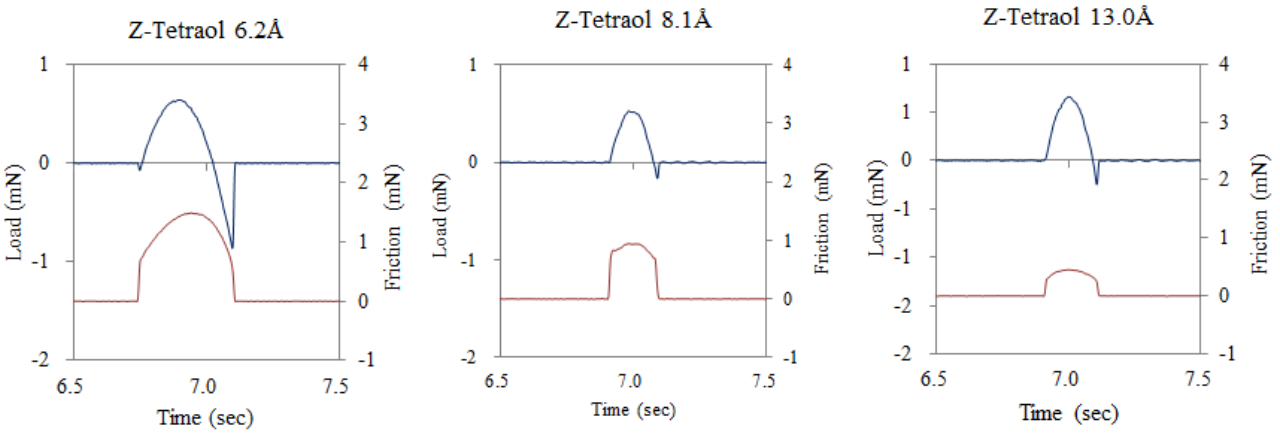

Fig. 2-12 Representative friction and adhesion measurement results at various thicknesses of Z-Tetraol

First, the IL's friction coefficients at the maximum applied load (approximately 0.5 mN) were relatively high compared with those of Z-Tetraol throughout the thickness, as shown in Fig. 2-13. The coverage ratio should be a critical parameter for friction because the friction coefficient of the underlying non-lubricated carbon layer is more than 20 times greater than that of the lubricant [47]. As stated above, the coverage ratios of the two lubricant films were considerably similar. Thus, the coverage ratio did not cause this difference in the friction coefficient. One of the reasons is the bond ratio. The IL's bond ratio was considerably lower than that of Z-Tetraol. For the IL, the presence of mobile molecules was dominant at the contact area between the pin and disk surface. The IL film was deformed or expelled when the load was heavily applied because it was not bonded to the disk surface. Therefore, the pin and disk surface might have been in a local solid-to-solid contact, which would have produced high friction. Z-Tetraol provided a sufficiently high bond ratio with the four hydroxyl groups. These bonded lubricant molecules covered the underlying carbon surface and reduced the severe contact between the pin and disk surface.

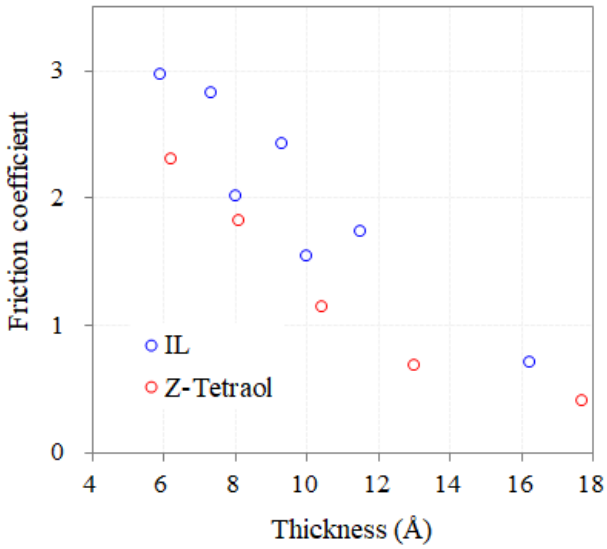

Fig.2-13 Friction coefficient at maximum applied load as a function of lubricant thickness

Second, the IL's adhesion force was relatively small compared with that of Z-Tetraol. To quantify the adhesion force, the experimental data were fitted using Eq. (4) based on the Johnson–Kendall–Roberts (JKR) model:

$$\begin{aligned} \mathrm{W} &= W_o + W_a \\ &= W_0 + 3\gamma\pi\mathrm{R} + \sqrt{6\gamma\pi R W_0 + (3\gamma\pi R)^2} \\ F &= \mu(W_0 + W_a) \end{aligned} \qquad (4)$$

where W is the total load force; W_0 is the applied load; W_a is the load force caused by the adhesion force; R is the curvature radius; γ is the total surface energy based on the sphere and plane models. Fig. 2-14 shows the friction curve as a function of load force and corresponding motion of the pin and disk. The gray line represents the fitting curve of the JKR model. The fitting curves are extrapolated to zero value on the friction force axis. The friction force, F_0, at the applied load of 0 mN and adhesion force were derived from the fitting curves based on Eq. (4). The experimental friction curves for the IL and Z-Tetraol lubricants are shown in Fig. 2-15.

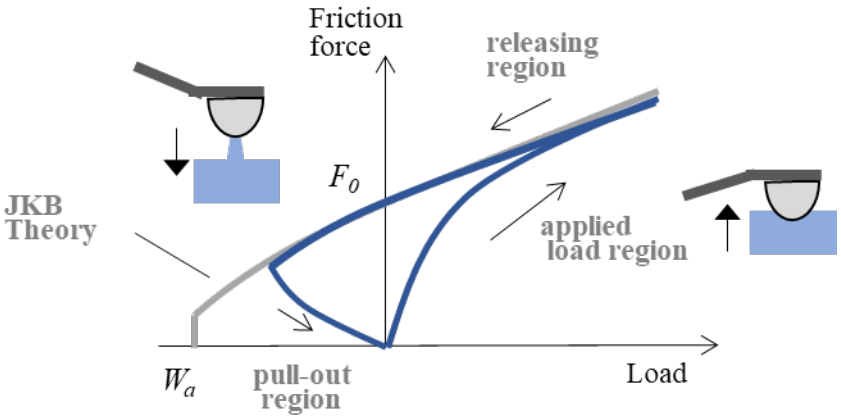

Fig. 2-14 Explanation of friction curve and JKR simulation

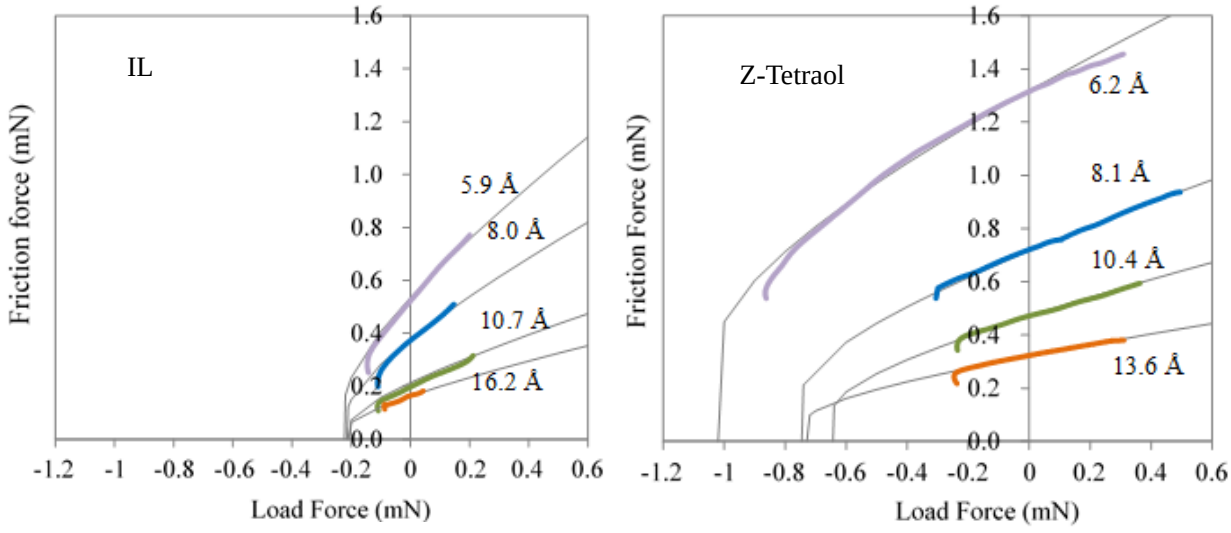

Fig. 2-15 Friction curves at various thicknesses of IL and Z-Tetraol lubricants

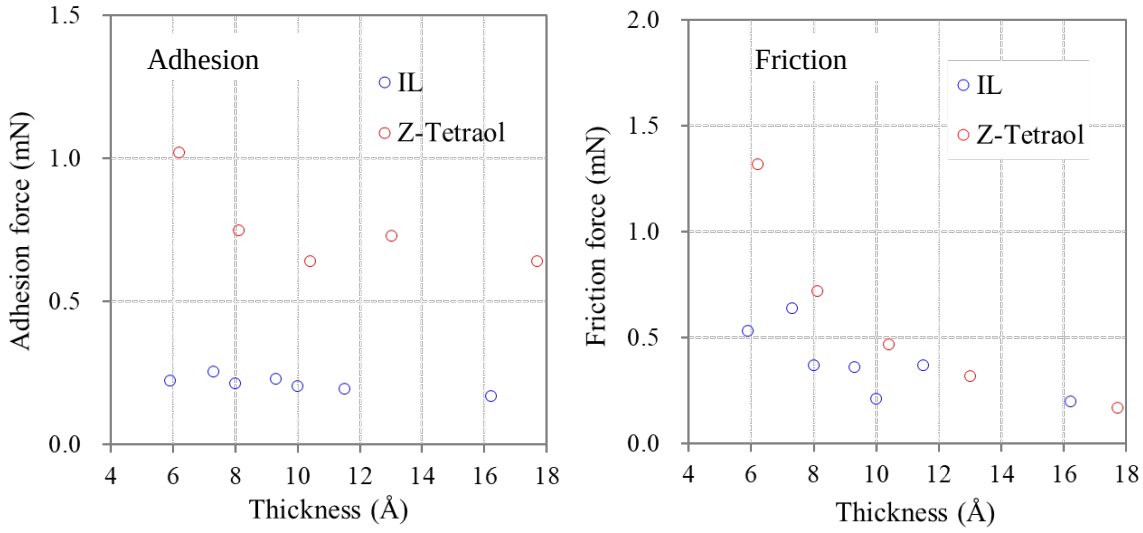

Fig. 2-16 Adhesion force and friction force as a function of thickness for IL and Z-Tetraol

Fig. 2-16 shows the adhesion and friction forces as a function of the lubricant thickness. For Z-Tetraol, the friction force decreased monotonously as the lubricant thickness increased; the adhesion force decreased until the corresponding lubricant thickness reached approximately 10 Å and remained flat above this value. Compared with the adhesion force of Z-Tetraol, that of the IL lubricant was small within the lubricant thickness range corresponding to the adhesion force. The friction force of the IL, F_0, was slightly smaller than that of Z-Tetraol.

4. Discussion

For Z-Tetraol, the derived monolayer thickness from the terrace flow measurement is 18 Å, which is identical to the saturated bond thickness and the thickness corresponding to the 100% coverage ratio. In contrast, the monolayer thickness of the terrace flow measurement is 12 Å, however, the saturated bond thickness is 9 Å, and the thickness corresponding to 100% of the coverage ratio is 18 Å. To explain these differences in the IL monolayer thickness values, it is necessary to discuss the molecular configuration.

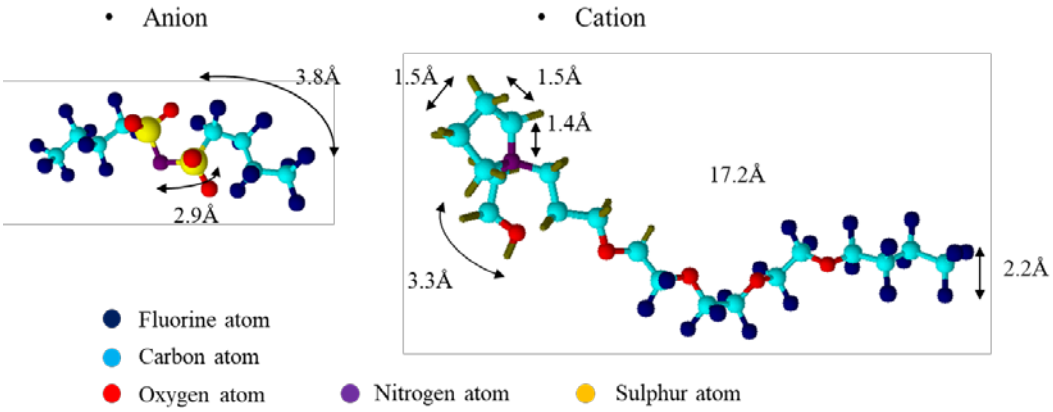

Fig. 2-17 Molecular modeling calculation for IL

First, the IL molecular modeling simulation was performed via ACD/3D Viewer (Advanced Chemistry Development, Inc.) to determine the length of each segment for the IL. The result of the molecular modeling simulation is shown in Fig. 2-17. The longest segment is perfluoroether with a length of 17 Å, whereas the fluorocarbon chain of the anion is 4 Å. The 12 Å of IL monolayer thickness was less than the perfluoroether chain thickness (18 Å), hence, the perfluoroether segment was inclined at a prescribed angle to the disk surface.

Second, the manner of adsorption is discussed. Figure 2-18 shows the thickness loss caused by the heat treatment at 100 °C for 5 h for two of each. The thickness losses of the IL lubricant are comparable to those of Z-Tetraol although the natural bond ratio (NBR) of the IL lubricant is lower than that of Z-Tetraol. The mobile lubricants of PFPEs readily evaporate. For PFPEs, the high bond ratio is necessary to attain high thermal stability. The IL exhibits high thermal stability despite its low bond ratio, suggesting that ionic interactions are involved in their adsorption on the disk surface. As a bulk, it is well-known that the anions and cations of the IL interact electrostatically, resulting in high thermal stability. Figure 2-19 shows the TGA results for each lubricant. The IL is superior to Z-Tetraol in terms of bulk thermal stability. This result proves the strong ionic interaction in ILs. However, the ionic interaction with the disk surface is weak compared with the chemical bond or hydrogen bond of Z-Tetraol because the bond ratio of Vertrel XF rinse is low. Nevertheless, the ionic interaction is sufficiently strong to maintain the thermal stability of the ultrathin film.

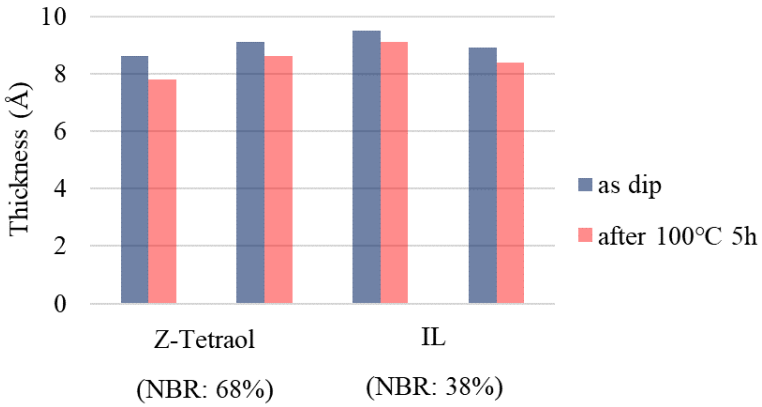

Fig. 2-18 Initial lubricant thickness and thickness after heat treatment at 100 °C for 5 h

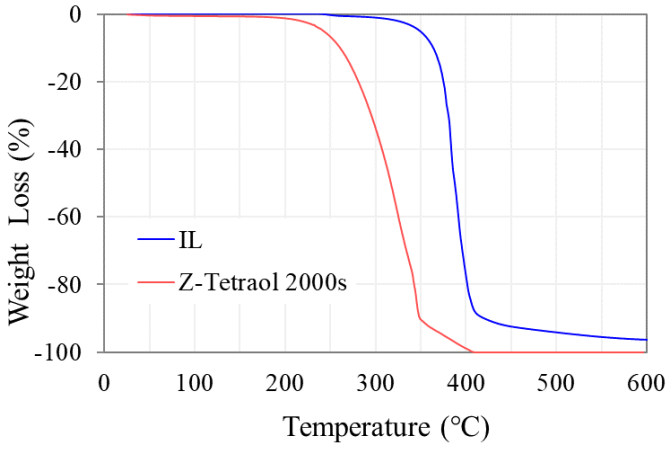

Fig. 2-19 TGA measurement results for each lubricant

Considering the two problems above, molecular configurations are proposed, as shown in Fig. 2-20. For the IL in this study, the inclination angle of the perfluoroether chain is varied because the terminal end of the perfluoroether chain is not bonded to the disk surface as Z-Tetraol. Based on the molecular modeling simulation, the perfluoroether chain is 17 Å; using sin(θ)=12 Å/17 Å, θ is approximately 45°, as shown in Fig. 2-20 (b). The molecular orientation is verified experimentally by the polar surface energy because it is determined by the outermost atomic group of lubricant layers. The polar surface energy may depend on the inclination angle. The perfluoroether chain works for distancing between the liquid (water) and ion pair. In the case of the molecular orientation shown in Fig. 2-20 (a), the perfluoroether chain prevents the water molecules from accessing its inner ion pair. At a higher thickness (approximately 18 Å), the polar surface energy is relatively low, and the dispersive energy is minimum. These results indicate that the inclination angle is high, and the packing density on the disk surface is high. The molecular weight of the IL is small compared with Z-Tetraol; hence, a larger amount of the IL molecules is necessary to cover the disk surface. In contrast, over a small thickness range (5–10 Å), the inclination angle is also relatively small, as shown in Fig. 2-20 (c), and the perfluoroether chain does not point upward. Thus, the polar surface energy increases as the amount of IL molecules, i.e., lubricant thickness, increases.

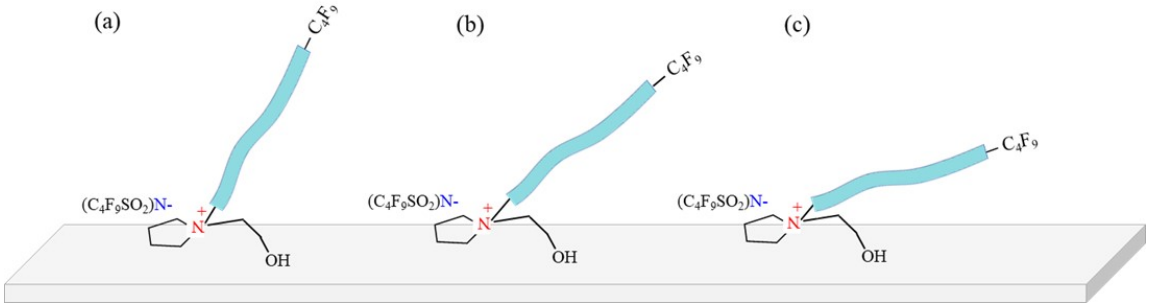

Fig. 2-20 Model of molecular configuration for IL

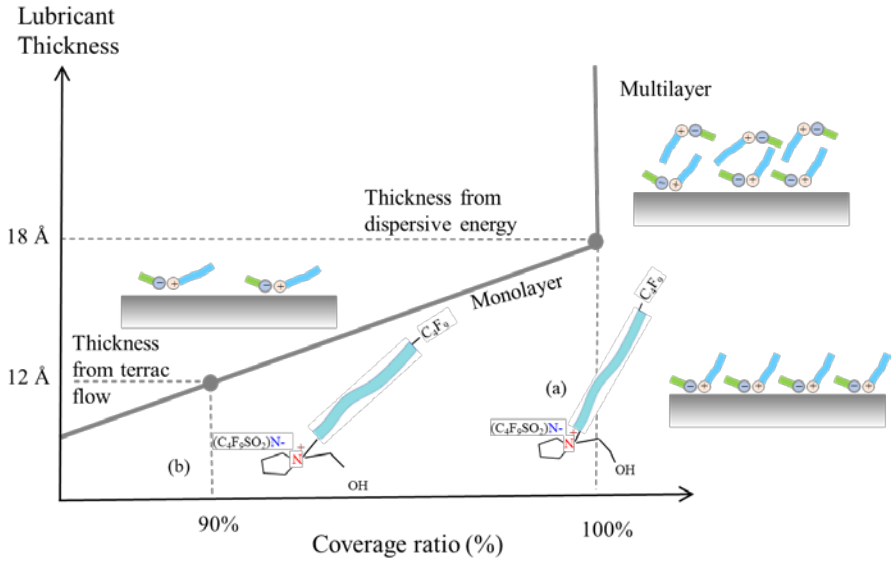

Fig. 2-21 Relationship between lubricant thickness and coverage ratio.

For the IL monolayer thickness, different values are obtained with the measurement methods such as terrace flow measurement, the saturated bonded thickness and the thickness of 100% coverage ratio. Presumably, these different values of the monolayer thickness may be attributed to change in the inclination angle of the perfluoroether chain. The relationship between lubricant thickness and coverage ratio is depicted in Fig. 2-21. When the lubricant thickness is 12 Å which is identaical to the monolayer thickness from the terrace flow, the molecular oriented like (b). ILs keep distancing each other, resulting in relatively small coverage ratio. In contrast, when the lubricant thickness is 18 Å which is identical to the monolayer thickness from dispersive energy, the molecular oriented like (a) and the inclination angle is high, and the packing density is high.

The adhesion force behavior of the IL is extremely unique. Normally, the adhesion force is high when thickness is less (5–10 Å) owing to the low coverage ratio.

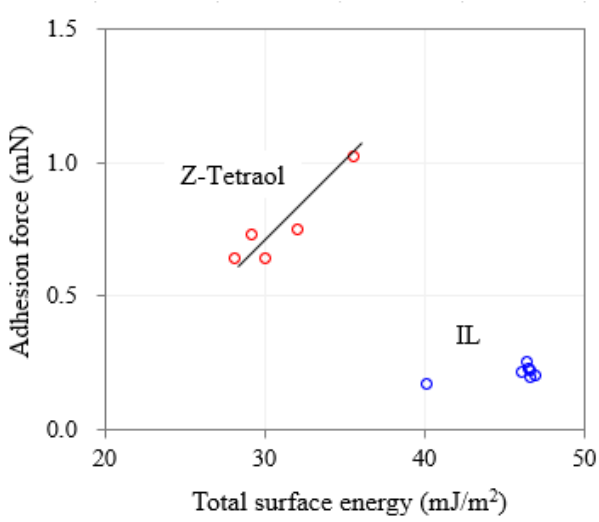

Fig. 2-22 Correlation between total surface energy and adhesion force

The lubricated disk with a low coverage has a high adhesion force because the non-lubricated carbon overcoat has a strong attraction force owing to van der Waals interactions. Figure 2-22 shows the adhesion force as a function of the total surface energy. The adhesion force of Z-Tetraol is proportional to the total surface energy because adhesion force is correlated interfacial force derived from the total surface energy. Tani et al. report previously the same trend for the relationship to the adhesion force and total surface energy [47]. In contrast, the adhesion force of IL is extremely low compared with that of Z-Tetraol despite of the high total surface energy. The origin of the adhesion force of the IL lubricant is not the same as that of the PFPE-type lubricant.

Considering the difference in chemical structure, the ion pair is the most plausible cause of the low adhesion force. Presumably, the ionic nature of the IL is considerably concentrated that the electric double-layer repulsion should be worked to the pin. The non-lubricated area (i.e., the carbon overcoat) has an attraction force because of a large Hamker constant. The presence of another force has been reported by several other research groups. The surface force of a nanoconfined IL between two parallel surfaces has been intensively investigated using a surface force apparatus [52,53] or AFM [54,55]. The surface force profile of the IL exhibited oscillations (alternating repulsion and attraction), resulting in a varied separation distance between the two surfaces; this surface force is referred to as solvation force. For a particular IL, the oscillation amplitude is larger; this is attributed to the stronger layering ability of IL. Recently,

the layering behavior of ILs at the interface has been intensively investigated. Some ILs form the molecular orientation at the interface, owing to the balance of its unique intermolecular interactions [56,57]. Considering the foregoing and the reports of other research groups, the microscopic adhesion force in this study is the sum of several interactions, such as van der Waals interactions, solvation forces, and electrostatic interactions. As a result of balancing these interactions to determine the adhesion force, a low magnitude of adhesion force is obtained.

However, Zhao et al. reported different microscopic adhesion results of ILs. They measured the microscopic adhesion in thin films (20 ± 2 Å) of Z-Dol 3800 and four imidazolium ILs by AFM. The lubricant thin film of Z-Dol 3800 exhibited the smallest adhesion force and highest water contact angle [58]. They concluded that the adhesion properties of ILs were correlated with its surface energy. Their results differed from those of the author of the present study. The experimental conditions had two differences: (1) the lubricant thickness of Z-Dol was 20 ± 2 Å, and (2) ILs without OH groups were used. The former caused the difference in the adhesion force of Z-Dol. The adhesion force of Z-Dol 3800 will reach a minimum value at its monolayer thickness (approximately 24 Å, as presented in the next chapter (Fig. 3-7)), which is comparable to 20 ± 2 Å. The minimum value of Z-Dol 3800 is one of the possible reason for smaller adhesion force compare to those ILs' value. The latter condition is relatd to the layering ability of the material. The OH groups in this study were used for controlling the molecular conformation, hence, the ILs with OH groups were expected to be more ordered than the ILs without OH groups on the disk surface. The layering ability of materials may be correlated to the interaction between two surfaces.

5. Conclusion

In this study, the ultrathin film properties of an IL-type lubricant were compared with those of Z-Tetraol (MW: 2300) as a conventional PFPE lubricant.

(1) The monolayer thickness of IL (12 Å), which was smaller than that of Z-Tetraol (MW: 2300), resulted from its small MW. It is expected that the thinner lubricant film on the magnetic disk will allow low-head flying.

(2) The bond thickness of the IL rinsed by Vertrel XF was smaller than that of Z-Tetraol because the IL only has a mono-hydroxyl (OH) group. Despite its low bond ratio, the IL exhibited a high thermal stability not only as a bulk, but also as an ultrathin film. This result suggests that the IL adsorbs on the disk surface via ionic interaction.

(3) Although the IL's polar surface energy was higher than that of Z-Tetraol owing to the ionic pair, its adhesion force was smaller than that of Z-Tetraol. A possible reason for this is the repulsion resulting from the ionic pair layering at the disk surface.

Considering that a further reduction in the HMS was necessary, a novel IL-type lubricant was developed. This study demonstrated the feasibility of using ILs as lubricant for magnetic disk media. Considerable amounts of critical data resulting from the unique characteristics of ILs were obtained. These data have never been collected even for conventional PFPE lubricants. Accordingly, further research and development work on IL-type lubricants are necessary to ensure the design and fabrication of highly reliable HDDs.

3. Application of IL for Ultra-Low HMS

1. Study objective

As the required HMS increasingly becomes narrower, lubricant thickness should also be smaller at the molecular level. The structure of multidentate-type PFPE involves technology in which pendent hydroxyl (OH) groups in the middle of the main chain tie down the main chain to the surface (Fig. 1–4). Owing to this technology, the lubricant monolayer thickness has become smaller than that of conventional PFPE lubricants, such as Z-Tetraol and Z-Dol. Among the multidentate PFPEs, Z-TMD has attained a thickness of 14 Å. It has eight OH groups, four of which are located at the intermediate positions along the main chain [13–17]. Tani et al. studied the monolayer thickness of several PFPE multidentate lubricants [18]. The smallest monolayer thickness of 11.5 Å was achieved by OHJ-DS (MW: 3900), which has three PFPE segments and four OH groups. The monolayer thicknesses were measured using the same terrace flow method. Designing the OH group position is effective for reducing the monolayer thickness, however, multidentate PFPEs have not yet reached their physical limitation in terms of thickness (i.e., 7 Å), which is derived from the cross-sectional diameter of the perfluoroether chain and calculated by molecular modeling simulation.

The positions of the OH groups in ILs are designed to further improve the monolayer thickness. It is expected that the molecular conformation of the designed IL is parallel to the magnetic disk surface according to the positions of the two OH groups in the IL. For IL-1, each of the two OH groups were placed at each terminal end. Figure 3-1 shows that the perfluoroether chain of IL-1 are tethered to the disk surface at both ends. In contrast, the two OH groups of IL-2 are placed on one side of the cation. The purpose of this study was to experimentally verify this lubricant design concept. Accordingly, the ultrathin film properties of the two ILs were examined by comparing them with Z-Dol, which had the same number of OH groups. In particular, the monolayer thickness, surface energy, adhesion force, bond ratio, and thermal stability as ultrathin films were compared and discussed.

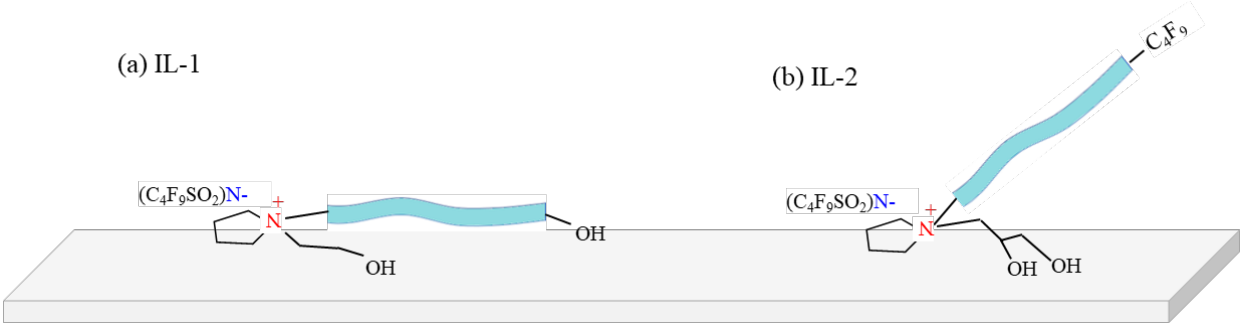

Fig. 3-1 Schematic of molecular conformations of IL-1 and IL-2 on magnetic disk surface: (a) IL-1 and (b) IL-2

2. Experiment

2.1. Lubricant

The chemical structures tested in this study are presented in Fig. 3-2. The author synthesized IL-1 and IL-2 (their

synthesis is described in the next section) to have the same anion and two OH groups in the cation. However, IL-1 had one group of OH at each terminal end, whereas IL-2 had two OH groups on one side of the cation. Z-Dol (Solvay) is a conventional PFPE lubricant with two OH groups. Z-Dols with three different MWs (Solvay) were used for comparison because they had the same number of OH groups as the developed ILs. Specifically, the MWs of Z-Dol 1500, 2000, and 4000 were 1500, 2200, and 3800, respectively. The MW of the PFPE backbone was obtained by fluorine nuclear magnetic resonance, and for further comparison, the thermal stability of Z-Tetraol 2000s (Solvay), which has four OH groups, was also tested.

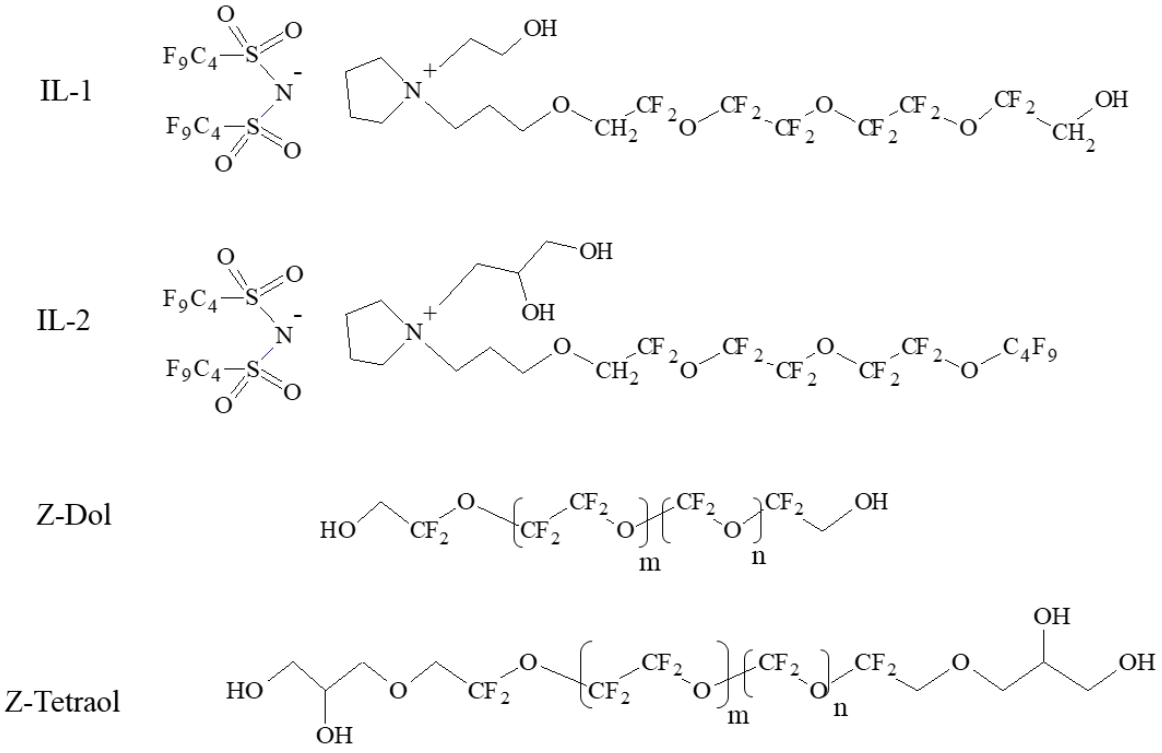

Fig. 3-2 Chemical structures of lubricants presented in this chapter

2.2 Synthesis details of ILs

As shown in Figs. 3-3 and 3-4, both ILs were synthesized in three steps. The starting material was perfluoroether alcohols with two OH groups, one at each terminal (1-1) and two OH groups at a single terminal (2-1) for IL-1 and IL-2, respectively. Compound 1-1 was 1H,1H,11H,11H-perfluoro-3,6,9-trioxaundecane-1,11-diol (SynQuest Laboratories Inc.), and compound 2-1 was fluorinated triethylene glycol monobutyl ether (Fluorochem Ltd.). In step 1, Br-terminated perfluoroethers (1-2 and 2-2) were synthesized from their respective perfluoroether alcohols by etherification with 3-bromopropyltosylate. For compound 1-2, only a single OH group was substituted with Br between the two OH groups. Because the two terminal OH groups in compound 1-1 had the same reactivity, a mixture of three different products was obtained after etherification: two terminals had OH groups (1-1), one terminal had Br, the other terminal had an OH group (1-2), and both terminals had Br groups. To isolate compound 1-2 from the mixture, silica-gel column chromatography was used. For compound 2-2, the reaction was simpler because it was not

necessary to leave half of the OH groups unreacted after etherification.

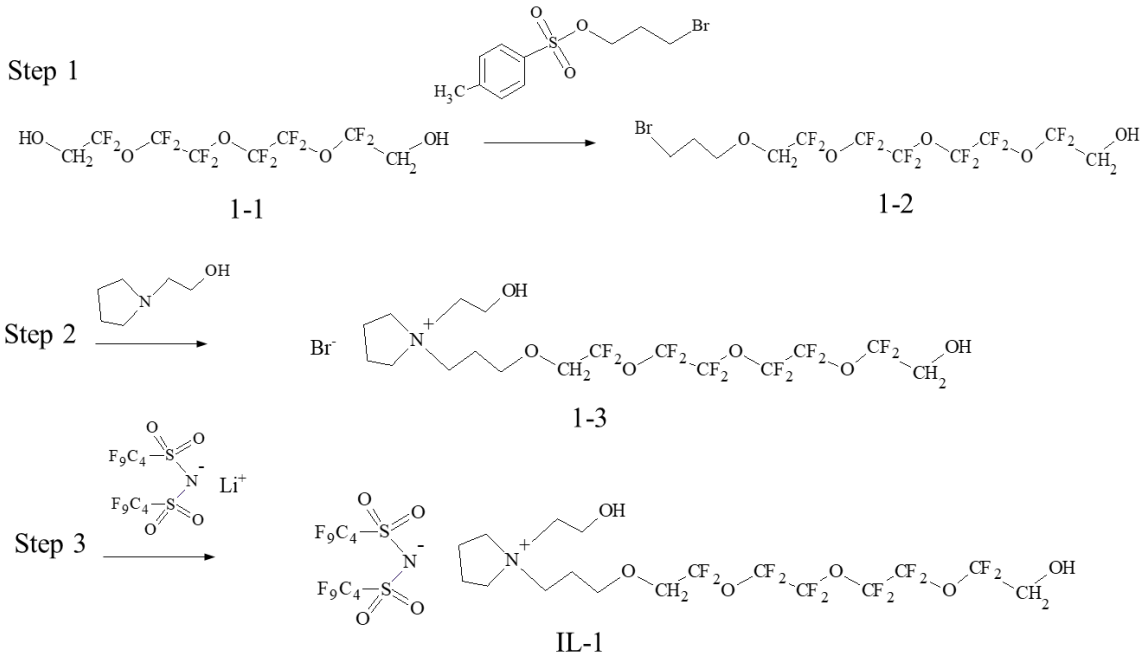

Fig. 3-3 Synthesis of IL-1

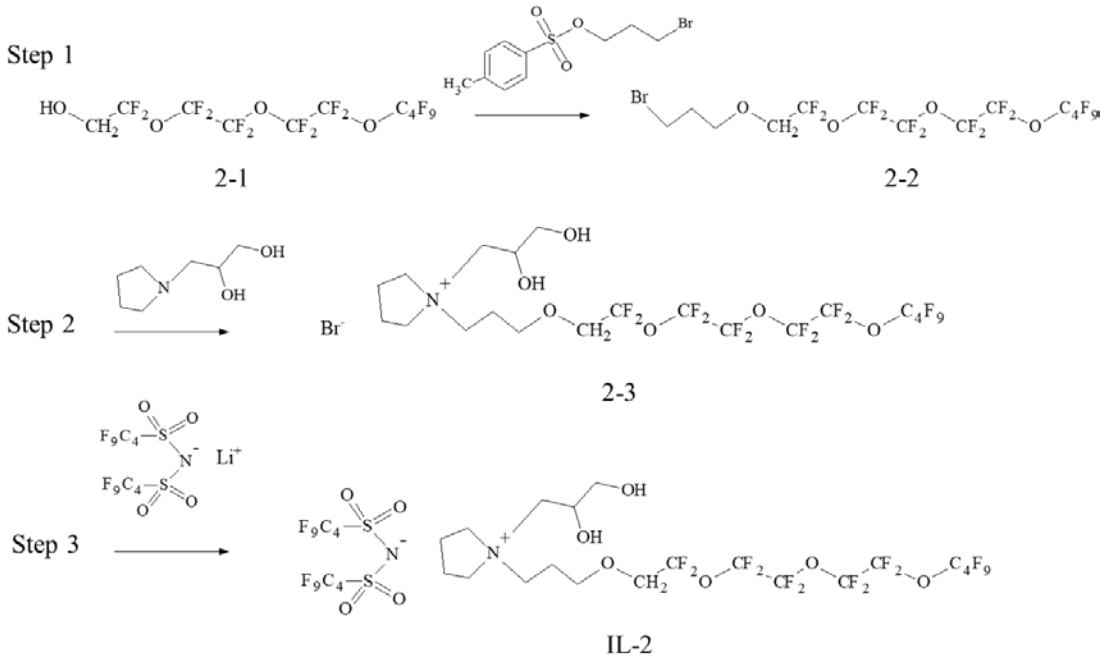

Fig. 3-4 Synthesis of IL-2

The chemical structure and purity of Br-terminated perfluoroethers were checked by proton nuclear magnetic resonance and liquid chromatography coupled with mass spectroscopy (LC/MS). In step 2, the Br-terminated

perfluoroether chain was introduced to the nitrogen atom of a pyrrolidine compound. The chemical structure and purity of the pyrrolidinium bromide salt were confirmed by LC/MS. In step 3, the anion of the pyrrolidinium bromide salt was exchanged with that of the bis(nonafluorobutansulfonyl)imide lithium salt (Mitsubishi Materials Electronic Chemicals Co., Ltd.) in an aqueous system, yielding IL-1 or IL-2. In the salt exchange reaction, only the ionic liquid participated because LiBr was soluble in water. These ILs were collected and washed by water several times to remove ionic contaminants, and the total quantity of ion contamination in the product was verified by ion chromatography to be less than 10 ppm. The purity of these ionic liquid was examined by LC/MS. No peaks other than those of the IL anion and cation were detected.

2.3 Sample preparation

Each lubricant film was coated on magnetic disks by dip coating. The lubricants were dissolved in Vertrel XF, and the lubricant film thickness varied with the lubricant concentration in the solution. The disk was immersed in a solution of lubricant for 180 s, and the pull up speed was 1 mm/s. Ultraviolet irradiation and heat treatment were not performed after the lubricant was applied on the disk. The lubricant film thickness was measured using a scanning ellipsometer (FiveLab Co., Ltd., MARY-102). Various disk sample thicknesses were prepared for each lubricant. The thickness profiles of IL-1, IL-2, and Z-Dol 2000 are shown in Fig. 3-5.

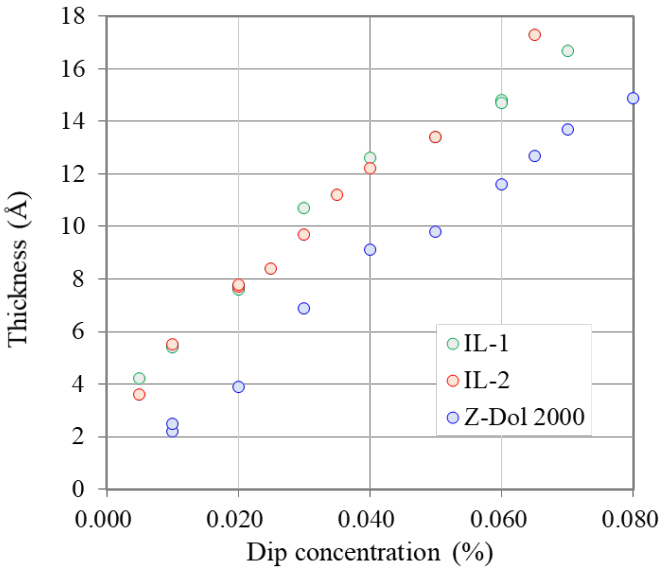

Fig. 3-5 Thickness profiles of IL-1, IL-2, and Z-Dol 2000

3. Results

3.1 Terrace flow

The spreading profiles for the ILs and Z-Dol with three different MWs are shown in Fig. 3-6. The profiles exhibit a shoulder corresponding to a monolayer thickness. The monolayer thicknesses of Z-Dol 1500, 2000, and 4000 are found to be 13, 18, and 25 Å, respectively. The monolayer thickness of Z-Dol decreases with the MW. It was

mentioned in the previous chapter that the monolayer thickness of Z-Tetraol 2000s (MW: 2300) was 17 Å, which was extremely close to that of Z-Dol 2000 because they had comparable MWs. For Z-Dol and Z-Tetraol, the PFPE backbone (with the monolayer thickness scales and the radius of gyration) is attached to the disk surface at both terminal ends. For IL-1 and IL-2, the monolayer thicknesses are 6 and 12 Å, respectively. The different monolayer thicknesses indicate that the molecular conformations of IL-1 and IL-2 vary with the position of the OH groups.

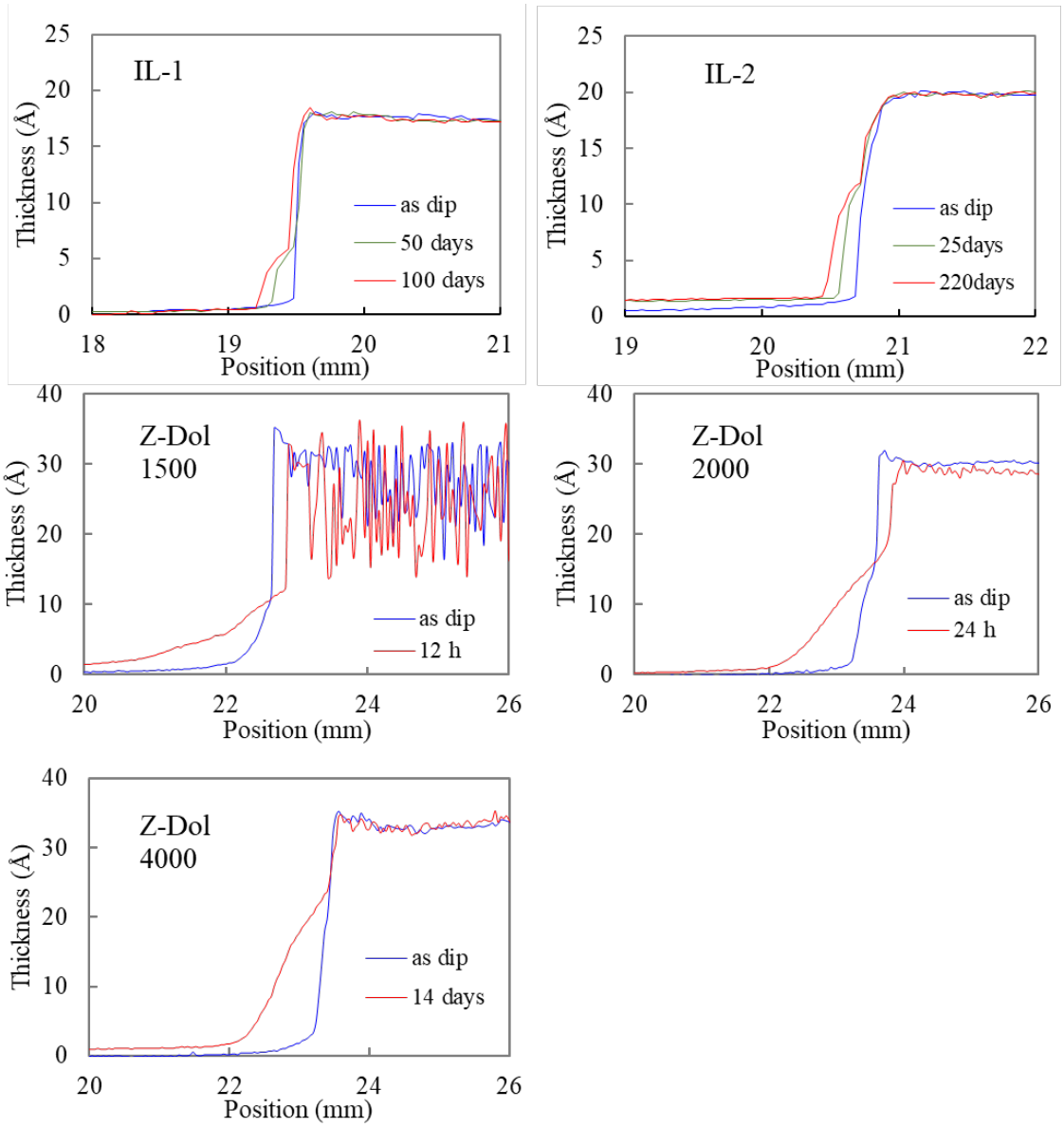

Fig. 3-6 Spreading profile of each lubricant measured using scanning ellipsometry at room temperature: IL-1, IL-2, Z-Dol 1500, Z-Dol 2000, and Z-Dol 4000

The thickness of each lubricant as a function of the square root of MW is shown in Fig. 3-7. The monolayer thickness of Z-Dol is proportional to the square root of MW, and the data point for IL-2 in the figure is consistent with the extrapolated Z-Dol value. In contrast, the data point of IL-1 is below the extrapolated value. The monolayer thickness of IL-1 conforms with the cross-sectional diameter of the PFPE backbone, which is approximately 7 Å, thus, the

conformation IL-1 is flat, as shown in Fig. 3-1, but that of IL-2 is not. Several physical chemists have directly performed observations on the molecular orientation of ILs at an interface via the spectroscopic method. Maier et al. conducted angle-resolved X-ray photoelectron spectroscopy for a series of ILs with octylmethylimidazolium as cation but with a different size of anion. They proposed a layering model in which the ionic part of the cation and anion were located near the surface of the silicon substrate as an ionic sublayer with an aliphatic carbon overlayer consisting of octyl chains formed on the ionic sublayer [56]. Baldelli et al. examined pyrrolidinium ILs, which were comparable to those in this study. The ILs possessed a long alkyl chain instead of a perfluoroether attached to the nitrogen atom of the pyrrolidinium ring. They concluded that the long alkyl chain pointed upward from the surface, and the pyrrolidinium ring was parallel to the surface on the interface [57]. Considering these results together with the location of the two OH groups placed near the pyrrolidinium ring, the perfluoroether chain of IL-2 may also point upward from the surface, and the pyrrolidinium ring may be located near the disk surface by anchoring with the two OH groups, as shown in Fig. 3-1.

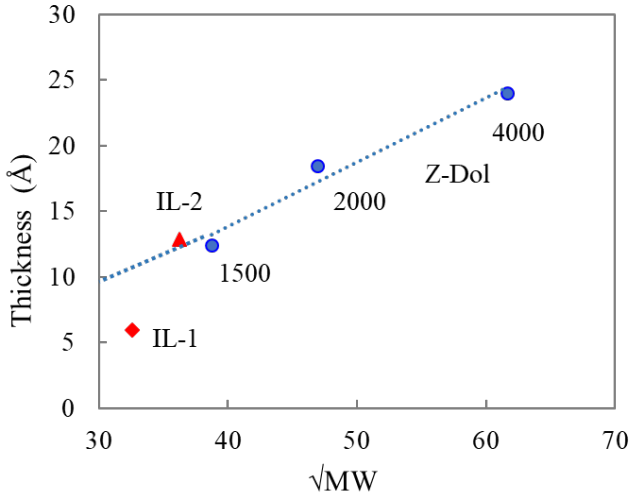

Fig. 3-7 Molecular weight of lubricants derived from spreading profiles; horizontal axis represents square root of molecular weight (MW)

Figure 3-6 show that the spreading rate decrease in the following order: Z-Dol 1500 > Z-Dol 2000 > Z-Dol 4000 > IL-1, IL-2. For PFPE, a previous paper clearly indicated that the spreading rate was correlated to mobility, surface energy, and film thickness [45]. The mobility was related to the adsorption force on the disk surface, MW, and molecular polarity. According to [16], the spreading rate of Z-TMD (eight OH groups) was considerably smaller than those of Z-Dols. Because each Z-Dol had two OH groups, the spreading rate of Z-Dols was simply correlated to the MW, i.e., the spreading rate decreased with increasing MW. In contrast, the spreading rate of ILs was 2–3 orders of magnitude smaller than those of Z-Dols although the MWs of ILs were relatively small. Ueno et al. indicated that the viscosities of nanoconfined ILs were 1–3 orders of magnitude higher than those of the bulk IL because of their strong layering force [53]. This is possibly the reason for the low spreading rate of ILs.

3.2 Surface energy

Molecular orientation can be distinguished based on the polar surface energy. This may be obtained by contact angle measurement because the polar surface energy is determined by the outermost atomic group of lubricant layers. If the outermost lubricant layer is mainly occupied by CF_3 or CF_2, then the polar surface energy is low, if it is occupied by a polar group, then the polar surface energy increases. For PFPE lubricants, distinct oscillations were observed in γ_p as a function of film thickness, indicating that the molecular layering of the PFPEs was induced by the polar interactions with the underlayer [12,13,22]. Figure 3-8 shows the polar surface energy as a function of the film thickness for IL-1, IL-2, and Z-Dol 2000. The polar surface energy decreases in the following order: IL-1 > IL-2 > Z-Dol 2000. The chemical polarity increases in the order CF_3 or CF_2 < OH < ion pair. Among the three lubricants, Z-Dol 2000 has the lowest polar surface energy because it does not have an ion pair in its chemical structure; the polar surface energy of IL-1 is higher than that of IL-2. As shown by the molecular conformation in Fig. 3-1, when the water droplet is in contact with the top surface of the lubricant layer, the perfluoroether chain of IL-1 lies on the disk surface, and the ion pair is not covered by the perfluoroether chain, resulting in high polar surface energy. In contrast, for IL-2, the perfluoroether chain pointing upward from the surface prevents the water molecules from accessing its inner ion pair.

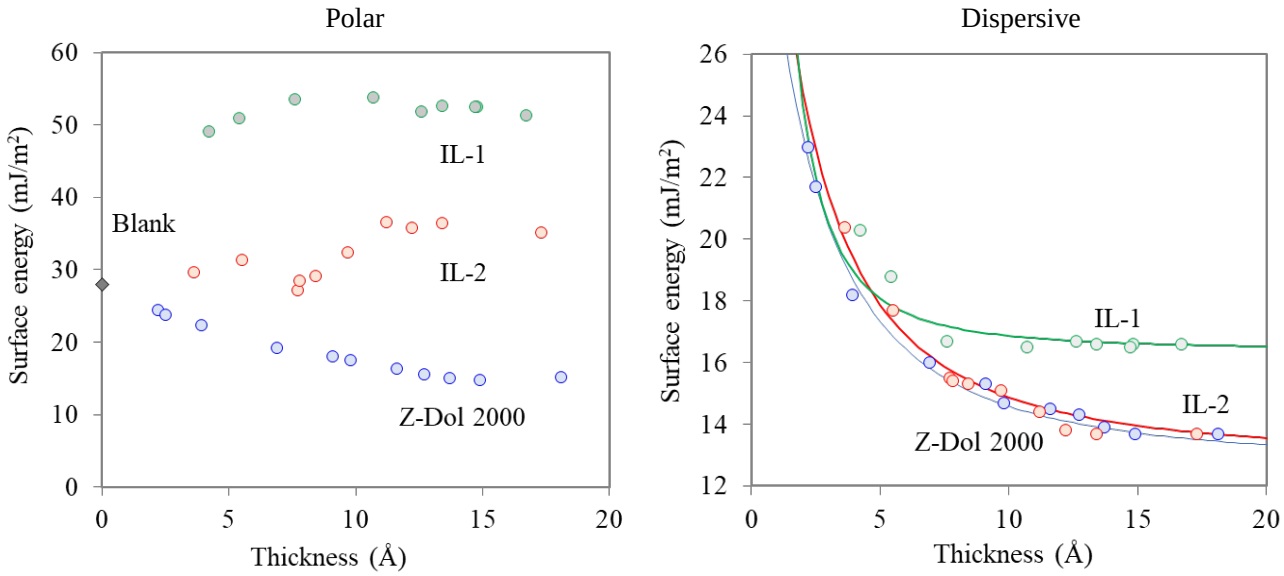

Fig. 3-8 Polar and Dispersive surface energy as a function of lubricant thickness

Fig. 3-8 shows the dispersive surface energy as a function of lubricant thickness. For a non-lubricated (blank) disk, the dispersive component of the surface energy is 38 mJ/m^2, which is significant. The dispersive component decreases monotonically in each lubricant as the lubricant film thickness increases and approaches a saturated value when the disk surface is fully covered by the lubricant. The experimental data are fitted by the Hamker equation. The saturated thickness values are 8, 14, and 18 Å for IL-1, IL-2, and Z-Dol 2000, respectively; the measured saturated dispersive energy values were 16.5, 13.8, and 13.7 mJ/m^2, respectively.

3.3 Adhesion force measurement

The microscopic adhesion force is a critical parameter for magnetic disk lubrication. A low adhesion force is required

for achieving a low-head flight. The adhesion measurements are presented in Fig. 3-9. The adhesion force is defined as the minimum value in the pull-out region. Figure 3-10 shows the adhesion force as a function of the lubricant thickness for IL-1, IL-2, and Z-Dol 2000. For Z-Dol 2000, the adhesion force decreases with increasing lubricant thickness. In general, the microscopic adhesion force emanates from the interaction between two bodies and correlates with the surface energy [59]. For a non-lubricated disk, the surface energy is large. With increasing lubricant thickness, the surface energy and corresponding adhesion force both decrease. Therefore, the measurement results for Z-Dol 2000 obtained in this study are anticipated. In contrast, the adhesion behaviors of the ILs are unique in that the adhesion force appears to be independent of the lubricant thickness. The adhesion force decreases in the following order Z-Dol 2000 > IL-2 > IL-1 at approximately 10 Å, whereas the surface energy values of the three lubricant films decrease in the order IL-1 > IL-2 > Z-Dol 2000.

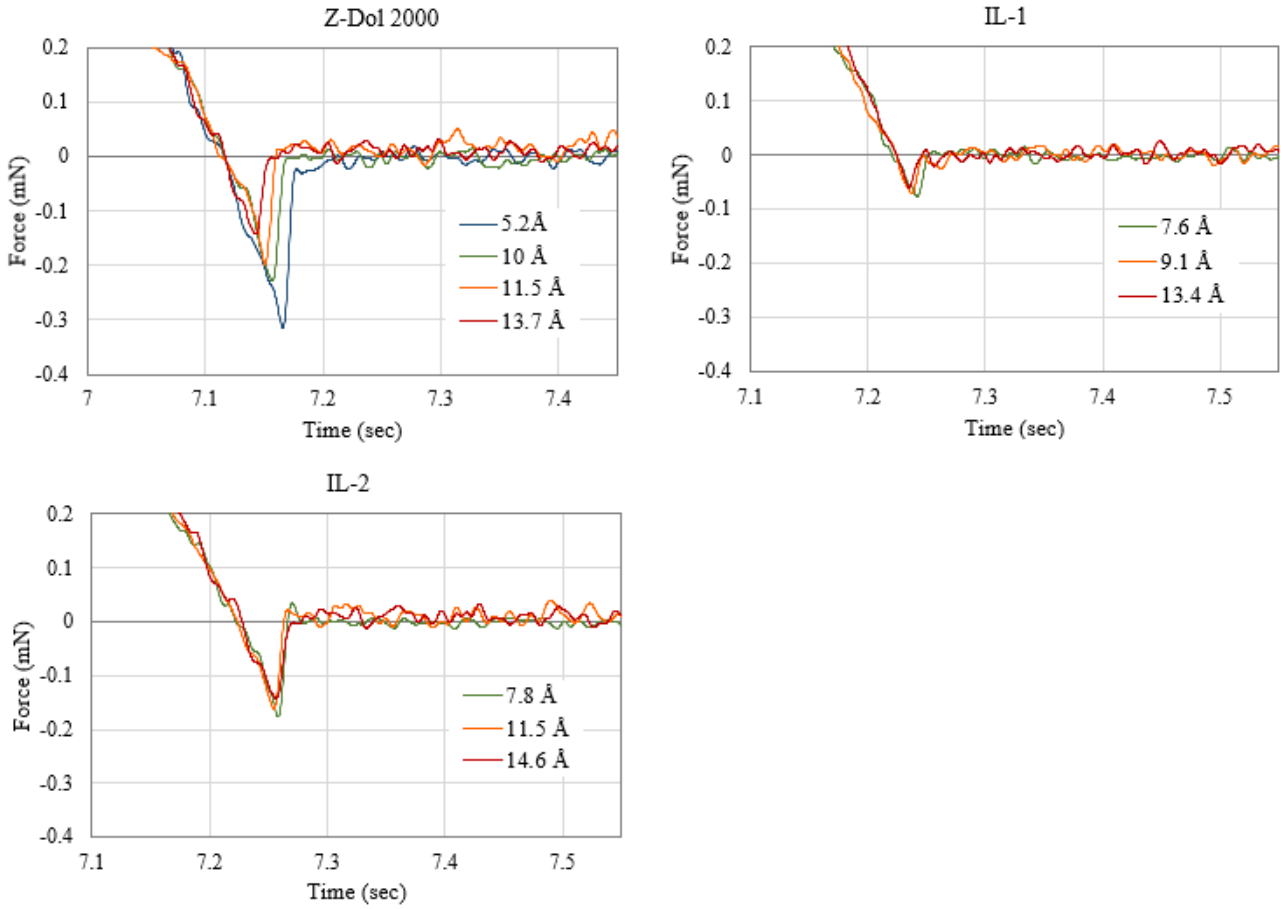

Fig. 3-9 Adhesion measurement results for IL-1, IL-2, and Z-Dol 2000 obtained by pin-on-disk microtribotester

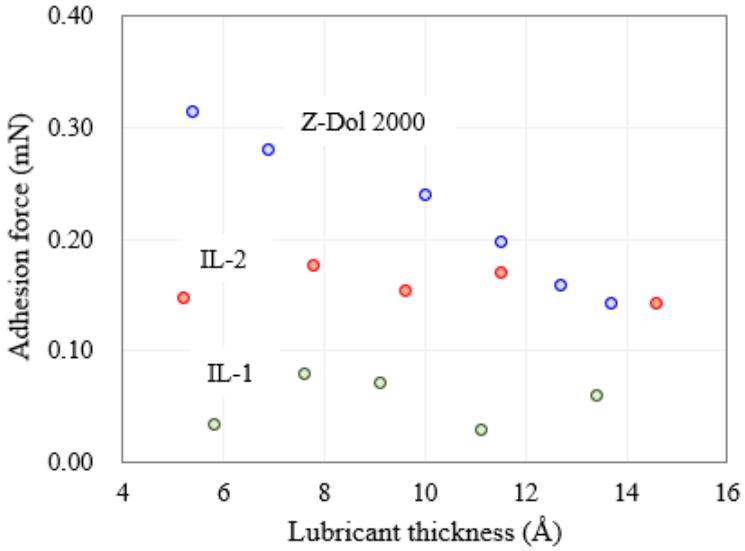

Fig. 3-10 Adhesion force as a function of lubricant film thickness

3.4 Thermal stability

To evaluate the bulk thermal stability of the lubricants, thermogravimetric measurements are performed on the lubricants used in this study, with the temperature at the 10% weight loss defined as T_{d10}. Figure 3-11 shows T_{d10} as a function of MW. For Z-Dols, T_{d10} decreases with decreasing MW. A comparison of Z-Dol 2000 with Z-Tetraol 2000s shows that T_{d10} of Z-Tetraol is higher than that of Z-Dol 2000 by 60 °C owing to the additional hydrogen bonding within the lubricant. The T_{d10} value of IL-1 or IL-2 is higher for a relatively small MW, which is an IL characteristic resulting from the electrostatic interaction within the material.

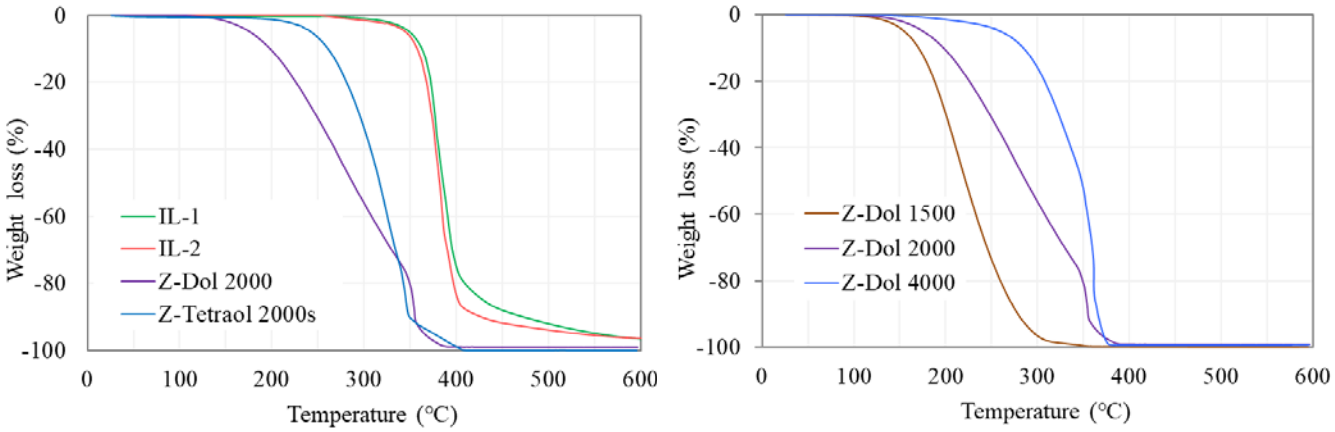

Fig. 3-11 Thermogravimetric analysis measurement results

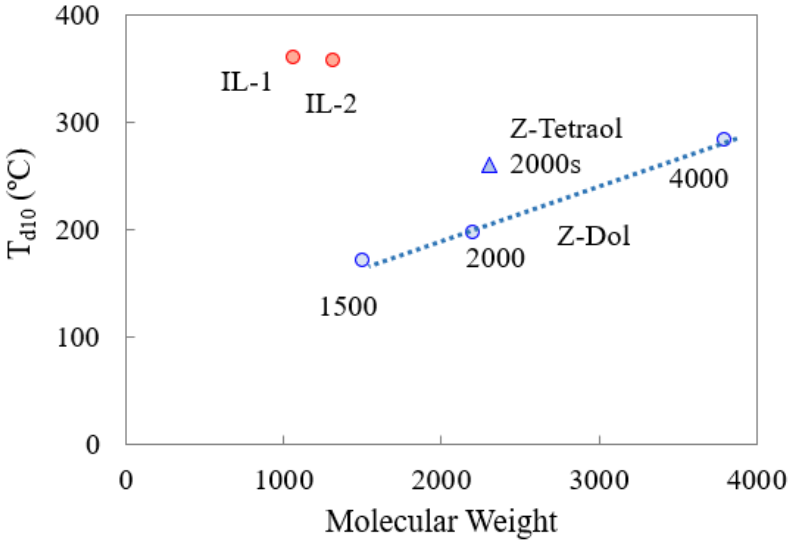

Fig. 3-12 Correlation between T_{d10} and MW; T_{d10} is temperature at 10% weight loss

Figure 3-13 shows the thermal stability of ultrathin films. Disks with a film thickness of approximately 10 Å are subjected to a 12 h heat treatment. The thickness loss is in the order IL-1 or IL-2 < Z-Tetraol 2000s < Z-Dol 2000 under all heating conditions, thus conforming with the bulk thermal stability obtained during the thermogravimetric measurement. Lubricants with high T_{d10} values as bulk liquids experience small thickness losses as thin films. In other words, the ILs are thermally stable not only in bulk, but also as ultrathin films. Figure 3-14 shows the thickness loss (as a percentage) as a function of the heating time at 60, 130 and 160 °C. For 130 and 160 °C, Z-Dol 2000 and Z-Tetraol 2000s approach a constant value of 2 h after the heating starts. Normally, among the PFPE lubricants, only the mobile lubricant evaporates, and the bonding reaction is enhanced by heating. Table 3-1 summarizes the bond ratios before and after the heat treatment and the corresponding thickness losses of 160 °C.

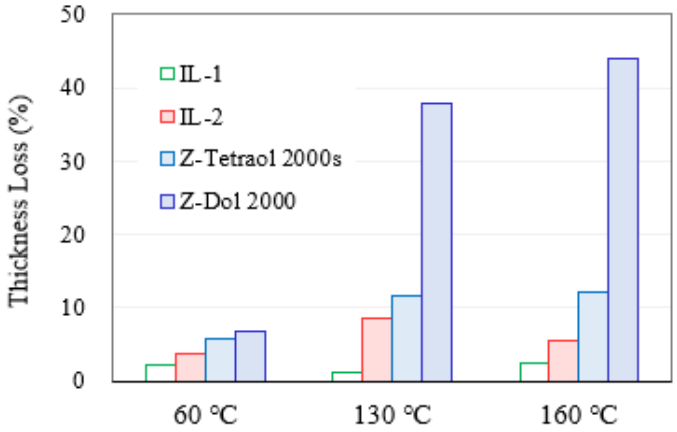

Fig. 3-13 Thickness loss after 12 h of heat treatment at 60, 130, and 160 ºC

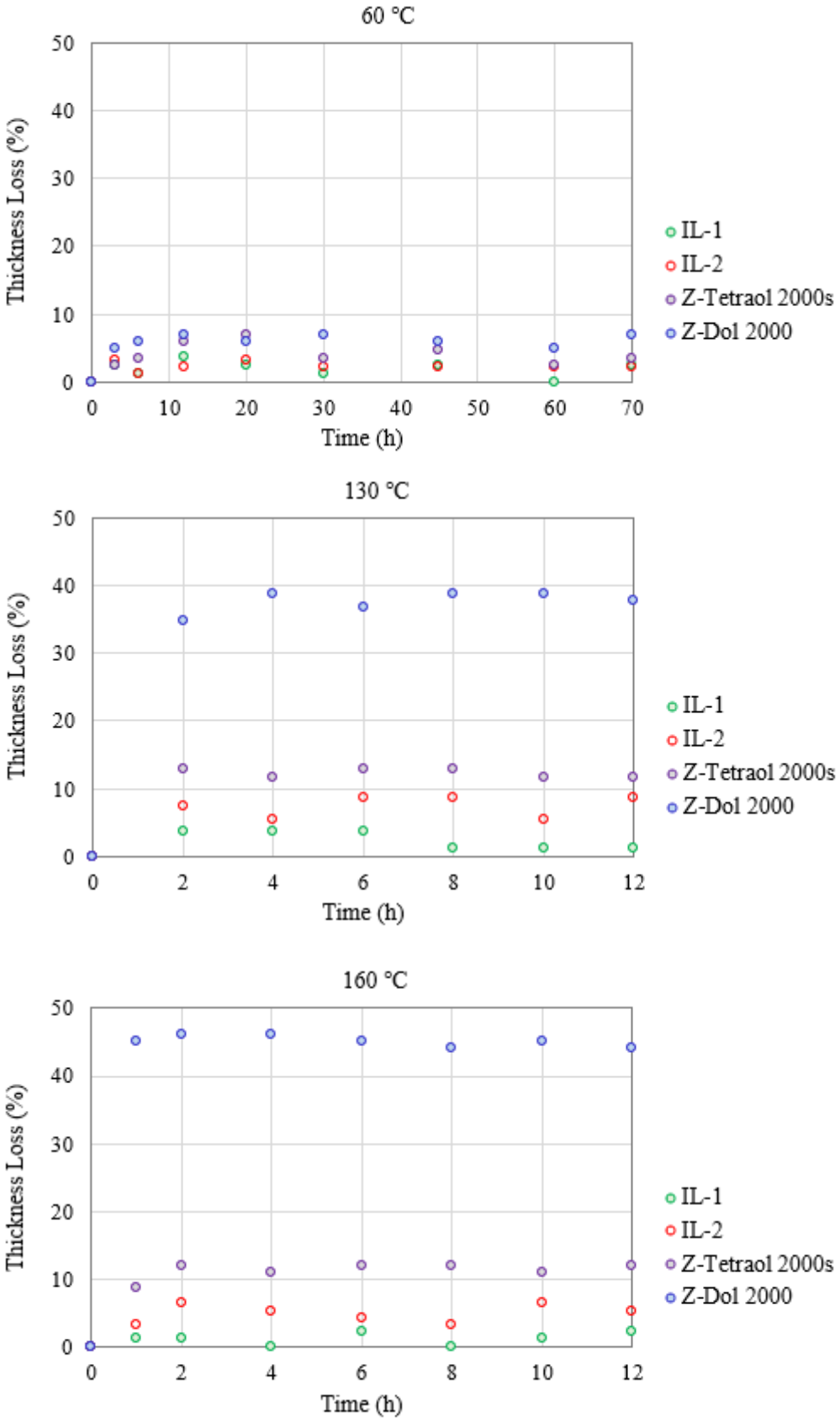

Fig. 3-14 Thickness loss as a function of heating time at 60, 130 and 160 ºC

Table 3-1 Summary of heat treatment test results (at 160 °C for 12 h)

Lubricant	Before heat treatment		After heat treatment		
	Lubricant thickness (Å)	Bond ratio (%)	Thickness Loss (%)	Bond Ratio (%)	Mobile Ratio (%)
IL-1	8.2	19	2.4	59	41
IL-2	9.3	11	5.4	56	44
Z-Tetraol 2000s	9.1	61	12.1	85	15
Z-Dol 2000	10.0	23	44.0	49	51

For each lubricant, the bond ratio increases from before to after heat treatment. The quantity of mobile lubricant is the difference between 100% and bond ratio (as a percentage), as shown in the rightmost column. For Z-Dol 2000 and Z-Tetraol 2000s, the ratio of mobile lubricant is consistent with the thickness loss. In contrast, the thickness losses of IL-1 and IL-2 are small despite the larger quantity of mobile lubricant. These results indicate that the thermal stability of the IL ultrathin film is high and independent of the bond ratio and MW.

4. Discussion

The monolayer thickness can be reduced by the IL-1 without the evaporation problem. The monolayer thickness of IL is confirmed by the terrace flow method, and the ILs exhibit good thermal stability on the TGA as well as the ultrathin film. To explain the behavior of ILs on coverage and adhesion, it is necessary to determine the underlying mechanism. The manner of bonding on the ILs is a key characteristic. Basically, the thickness loss increases with the increase in mobile ratio because mobile lubricants evaporate readily.

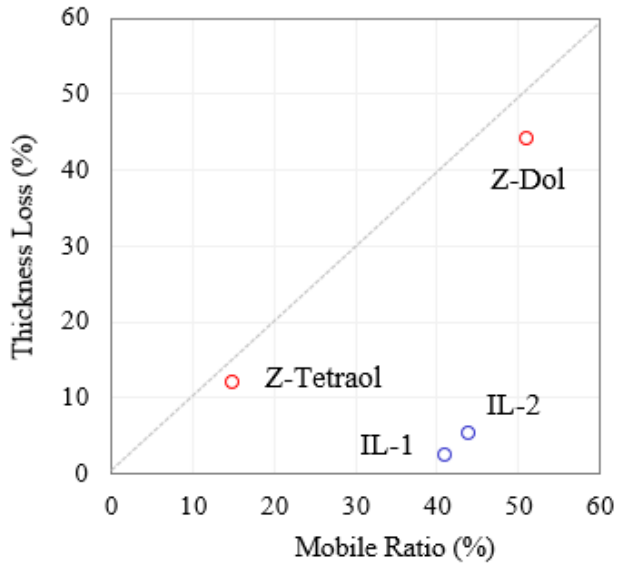

Fig. 3-15 Correlation between thickness loss and bond ratio for 160 °C 12 h

Fig. 3-15 shows the foregoing correlation between the mobile ratio and thickness loss. The thickness losses of PFPEs

is alomost the same as the mobile ratio, whereas the ILs exhibits small thickness losses regardless of the mobile ratio. These results suggest the existence of an interaction between the ion pair of the ILs and disk surface, i.e., the ILs adsorb to the disk surface via the ion pair. In the previous chapter, the monolayer thickness of the IL derived from the terrace flow measurement is not identical to the thickness corresponding to 100% of the coverage ratio. It is hypothesized that this difference in the monolayer thickness may be attributed to the inclination angle of the perfluoroether chain and the packing density on the surface. This hypothesis may be verified through IL-1: the IL-1 perfluoroether chain lies parallel to the disk surface and is anchored via its terminal OH group. Figure 3-16 shows the coverage ratio as a function of lubricant thickness.

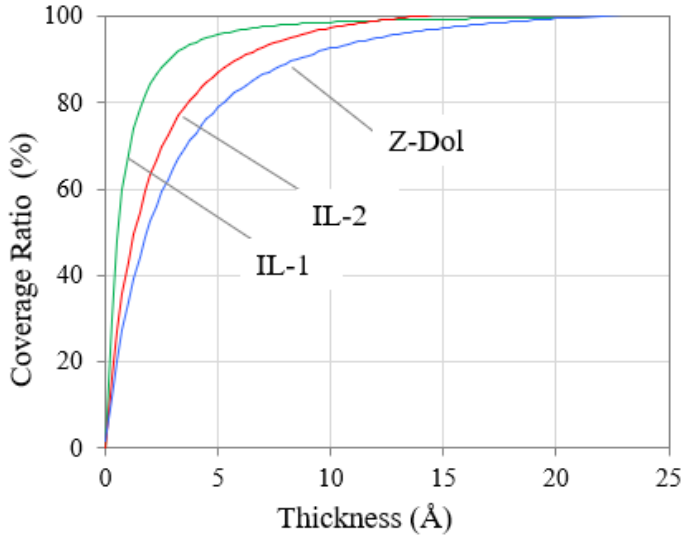

Fig. 3-16 Coverage ratio as a function of lubricant thickness
(IL-1, IL-2, and Z-Dol 2000)

The thickness values corresponding to the 100% coverage ratio are 10, 15, and 18 Å for IL-1, IL-2, and Z-Dol, respectively. The 100% coverage thickness of IL-1 is smaller than those of the other lubricants, corresponding to the monolayer thickness value derived from the terrace flow measurement. As shown in Fig. 3-8, the saturated dispersive energy of IL-1 is higher than that of the other lubricants, suggesting a low packing density. A hexadecane droplet comes into contact with the surface of the carbon overcoat because of the low packing density. Furthermore, hydrocarbon unit of IL-1 is facing up because the perfluoroether laying down. The carbon surface and hydrocarbon unit have strong affinity to hexadecane, resulting in low contact angle of hexadecane. In contrast, the perfluoroether chain of IL-2 is pointing upward, exhibiting a relatively strong oil repellency because of CF_3 and CF_2. A comparison of the two ILs having two different inclination angles shows that the ultrathin surface properties vary, providing direct evidence for the proposed model shown in Fig. 2-22.

The adhesion force is also related to the molecular configuration. The findings presented in the previous chapter include the following: the adhesion force of ILs is weaker than that of Z-Tetraol and is not correlated with the surface energy originating from van der Waals interactions. IL-1 has a weaker adhesion force than IL-2, indicating that the origin of the low adhesion force is the ion pair located at the top part of the lubricant layer. The ion pair is extremely concentrated that the electric double-layer repulsive force performs work on the pin. The attraction force work between the carbon layer and the pin is stronger than those of between the perfluoroether and the pin. The total

adhesive force is determined by balancing these attractive forces and the repulsive force of IL. As shown in Fig. 3-18, the repulsive force may be affected by the inclination angle.

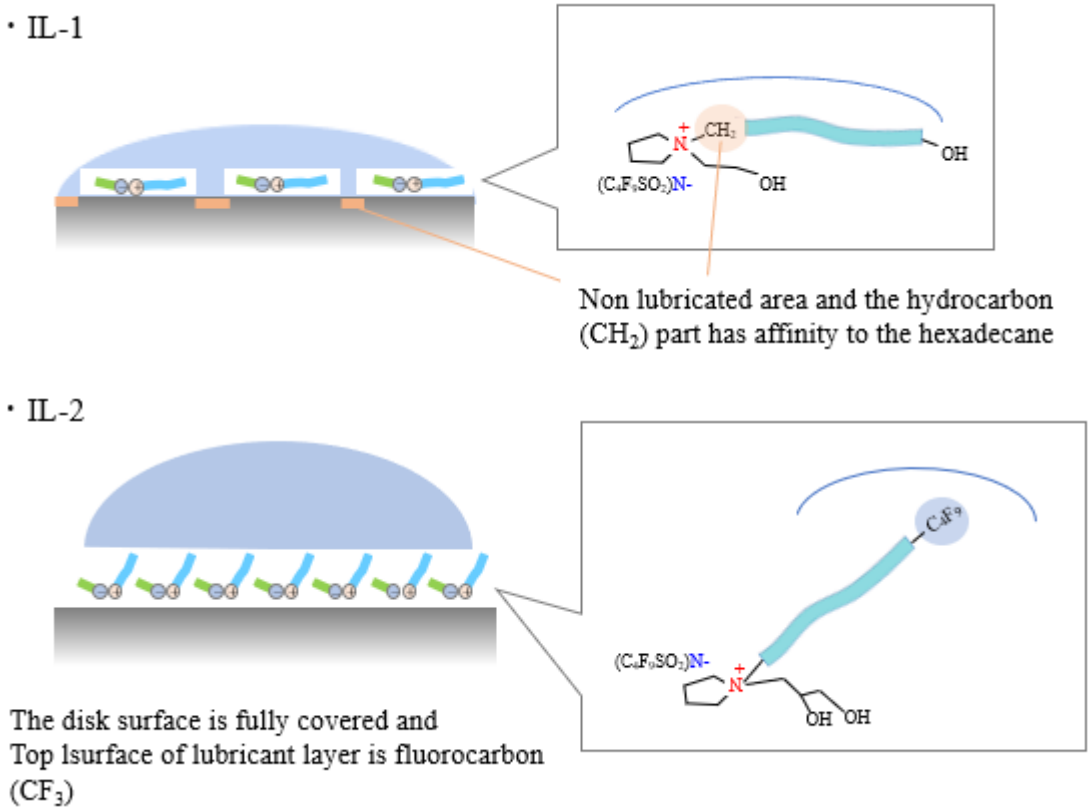

Fig. 3-17 Schematic of interaction between hexadecane and IL

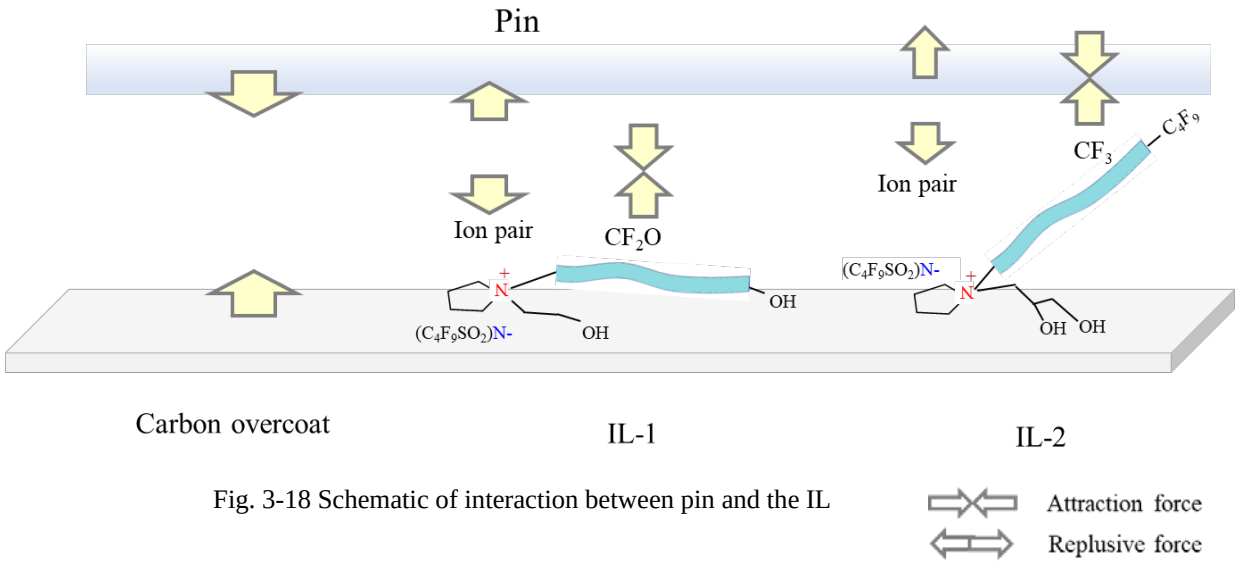

Fig. 3-18 Schematic of interaction between pin and the IL

For IL-1, the repulsive force increases because the ion pair comes into close contact with the pin although the attractive force is high because of the relatively low coverage ratio. In contrast, for IL-2 the repulsive force decreases

when the ion pair is covered by the perfluoroether. The weaker adhesion force of IL-1 than that of IL-2 because of the small inclination angle of IL-1 is a direct evidence for the foregoing hypothesis.

4. Conclusion

In this study, the ultrathin film properties of newly designed IL lubricants were compared with those of conventional PFPEs. The design concepts include the following: the new ILs have small MWs, and the optimized placement of OH groups increases their confinement on the disk surface. These concepts have been verified experimentally. The following conclusions were obtained:

(1) The monolayer thickness values were 6 and 12 Å for IL-1 and IL-2, respectively, which were smaller than those of Z-Tetraol 2000s (18 Å). Considering the position of the OH groups, the perfluoroether chain of IL-1 is attached to the disk surface with a terminal OH group, and the perfluoroehter chain of IL-2 points upward from the surface. These assumptions for the molecular conformations on the disk surface are supported by the obtained surface energy data (polar and dispersive terms).

(2) The adhesion force was measured using a pin-on-disk microtribotester. This force is one of the key parameters for achieving a low slider head flight. The adhesion force decreased in the order Z-Dol 2000 > IL-2 > IL-1. The adhesion force varies for different molecular conformations of IL on the disk surface, and the adhesion force is determined by balancing the electrostatic repulsion and van der Waals attraction. When the ion pair is located at the top of the lubricant surface, the repulsion increases, resulting in a low adhesion force.

(3) According to heat treatment results at 160 °C, the upper limit of evaporation loss was dependent on the bond ratio of PFPEs, the PFPE bonded lubricants were not observed to evaporate significantly. A high bond thickness is necessary for low evaporation loss. In contrast, the bond ratio of ILs was low even after heating, however, these ILs exhibited low evaporation losses owing to the ionic interactions within the materials. These results indicate that the ionic interaction is involved in the adsorption on the disk surface.

Novel IL lubricants were developed with the aim of further reducing the HMS. Several promising results were obtained because of the unique characteristics of ILs, these results have not been obtained for conventional PFPEs. However, this study revealed that the lubricants had low bond ratios and poor hydrophobicity. According to the evaluation of the thermal stability stated above, the low bond ratios did not seem to be critical. The effect of high temperature and high humidity on the IL was not examined in this study. In the case of poor hydrophobicity, lubricant dewetting, corrosion and microtribological properties are problematic. In contrast, a change in the pervading air inside the HDD is undergoing development (i.e., helium-filled HDD), hence, the actual criteria for HDDs can potentially change. With these trends in the HDD technology, further research and development are necessary to ensure the reliability of IL-lubricated hard disk drives.

4. Application of IL for HAMR

4.1. Background and objective of this study

HAMR is among the candidates for next-generation magnetic recording systems. However, this technology introduces the lubricant depletion problem owing to lubricant evaporation and thermal decomposition because the laser is locally focused on the top surface of the magnetic disk media. The depletion characteristics of perfluoropolyether (PFPE)-type lubricants have been investigated under various laser conditions, such as laser power, laser irradiation duration, and on/off laser irradiation duration [60–65]. However, a fundamental solution to this depletion problem is to develop thermally stable lubricants as alternatives to PFPE. The IL is an attractive material because of its high thermal stability. Based on thermogravimetric analyses (TGA), ILs have superior thermal stability when exposed to elevated temperatures. Despite the superior bulk properties of IL, however, the feasibility of applying IL lubricants to the HAMR system should be investigated. The thermal stability of ultrathin lubricant films on magnetic disks cannot be predicted from bulk TGA properties because of the interaction between the lubricant and disk surface. In the application of heat, the laser is focused on the disk surface in the actual HAMR system via near-field irradiation for a few nanoseconds. However, the scale of the rate of increase of the TGA temperature is minimal; the rate is 10^{10} times slower than that in actual HAMR systems. In this study, the lubricant depletion on magnetic disks is measured using the far-field laser irradiation on a rotating disk and compared between the newly developed IL-type lubricant and conventional PFPE-type lubricants.

4.2. Lubricant

In this study, a new material, IL-3, is synthesized, and its chemical structure is shown in Fig. 4-1.

IL-3

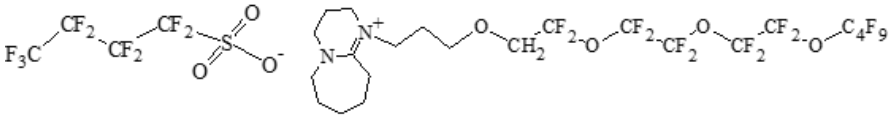

Z-Tetraol 2000s

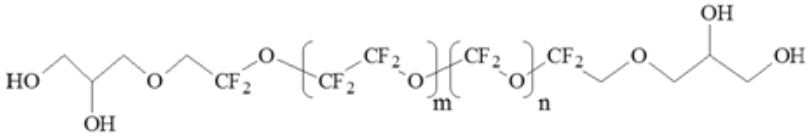

PFPE molecular weight: approximately 2300

Z-Dol 2000

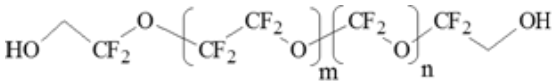

PFPE molecular weight: approximately 1900

Z-Dol 4000

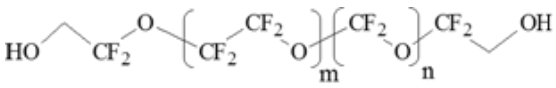

PFPE molecular weight: approximately 4200

Fig. 4-1 Chemical structures in this study

For cation moiety, the perfluoroether group was introduced to the 1,8-diazabicyclo[5.4.0]undec-7-ene (DBU) ring in the nitrogen atom; the anion was nonafluorobutanesulfonate. The MWs of the anion and cation were 299 and 741, respectively, for a total MW of 1040. The synthesis is described in detail in [67]. The chemical structure and purity were verified by liquid and ion chromatographies. Z-Tetraol 2000s (Solvay), Z-Dol 2000 (Solvay), and Z-Dol 4000 (Solvay) were used. According to the F-NMR results of the PFPE backbone, the MWs of Z-Tetraol 2000s, Z-Dol 2000, and Z-Dol 4000 were approximately 2300, 1900, and 4200, respectively. All PFPEs and the IL are in the liquid state at room temperature.

4.3. Dip coating and lubricant thickness measurement

Each lubricant film was coated on the magnetic disk by dip coating. The film thickness varied depending on the lubricant concentration in the solution. The disk was immersed in a solution of the lubricant dissolved in Vertrel XF (Dupon-Mitsui Fluorochemicals Co., Ltd., Vertrel XF) for 180 s and pulled up at a speed of 1 mm/s. The lubricant film thickness was measured using a scanning ellipsometer (FiveLab Co., Ltd., MARY-102).

4.4. Bonding Process

Ultraviolet and heat treatments are commonly used for enhancing the bond ratio in the magnetic disk media. A low-pressure mercury lamp with wavelengths of 185 and 254 nm was used as the UV light source. The UV irradiation duration was 30 s, and the UV intensities were 1 and 5 mW at 185 and 254 nm, respectively. The UV chamber was purged using nitrogen gas to avoid ozone generation. The heat treatment was at a temperature of 100 °C for 1 h.

4.5. Bond ratio ladder sample preparation

The bond ratio of an ultrathin lubricant film depends on the bonding process, such as UV treatment, heat treatment, and combined heat and UV treatments. For the PFPE, the number of OH groups also affect the bond ratio because the OH group adsorbs on the carbon surface.

Table 4-1 Disk sample condition and bond ratio for lubricant depletion measurement

Exp.	Lubricant	Bonding Process	Bond Ratio (%)
(1)	Z-Tetraol 2000	UV	96
(2)	Z-Tetraol 2000	-	82
(3)	Z-Dol 2000	UV	62
(4)	Z-Dol 2000	-	44
(5)	Z-Dol 4000	-	42
(6)	IL-3	Heat + UV	71
(7)	IL-3	UV	59
(8)	IL-3	-	55

By considering the bonding process and lubricant chemical structure, the bond ratio ladder sample for PFPEs was prepared; this ladder and IL-3 are listed in Table 4-1. The lubricant thickness was adjusted to approximately 11 Å. The residual thickness after Vertrel-XF rinsing was considered as bond thickness. The disk was immersed in Vertrel-XF for 180 s, and the pull up speed was 1 mm/s. The bond ratio was defined as the ratio of thickness after rinsing to that before rinsing. The thickness of each lubricant was adjusted to approximately 11 Å. Z-Dol 4000 was used to examine the effect of MW on lubricant depletion.

4.6. Lubricant flow rate measurement

The lubricant was applied only to a part of the disk surface to observe the spread of the front over time. UV irradiation and heat treatment were not performed after applying the lubricant onto the disk. The thickness profiles of the films were measured using a scanning ellipsometer. The thickness profile measurements were made immediately after the lubricant film was applied. After a sufficiently long period had elapsed under ambient conditions, the lubricant film spread [45]. The lubricant flow rate was calculated by dividing the spread distance (with a lubricant thickness of 11 Å) by time.

4.7. Far-field Laser Irradiation System

A schematic of the tester is shown in Fig. 4-2 (a). The magnetic disk was mounted on the spindle, and a laser light (λ = 830 nm) was focused on the disk surface through an objective lens (numerical aperture (NA) = 0.5).

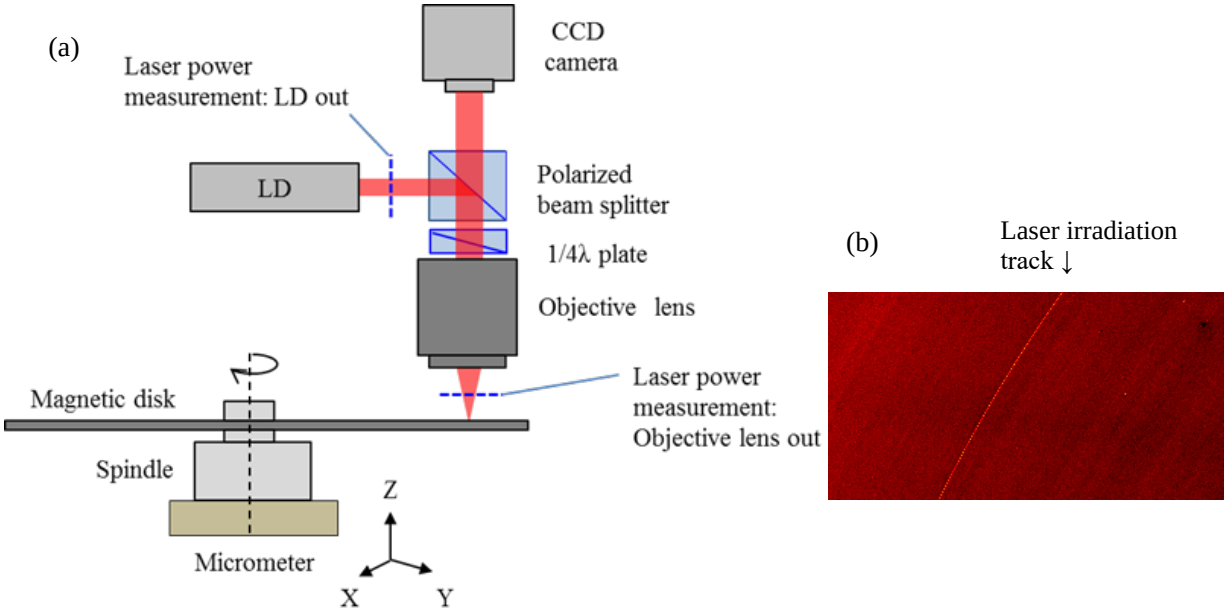

Fig. 4-2 (a) Schematic of far-field laser irradiation system; (b) OSA image after laser irradiation

The diffraction limit for the full-width at half-maximum optical spot (d) has a 1.0 μm radius; it was calculated by d=0.61 λ /NA. Table 4-2 lists the measured laser power at laser diode (LD) out and objective lens out. The coupling efficiency of this optical system, defined as the ratio of laser power at objective lens out to LD out, was approximately

29%. The reflected light from the disk surface was monitored using a CCD camera. The spot size of the reflected light on the CCD monitor was set to be minimum using the Z axis micrometer to exactly align the laser focal point at the top surface of the disk. The laser focus point alignment in the vertical direction is critical because it is directly related to the measurement accuracy. For the horizontal direction, the laser focus point was positioned at a radius of 25,000 μm, and the rotational speed of the disk was fixed at 500 rpm, corresponding to a linear velocity of 1,300 mm/s. In a previous study in [65], the temperature at the laser focus point was measured using a thermo-label, i.e., a temperature indicator that changed color when the temperature reached a preset threshold. The laser currents of 120, 130, and 140 mA correspond to local spot temperatures of 211, 241, and 272 °C, respectively. The irradiation time for a rotation was calculated by the laser spot diameter and the linear velocity of this experimental setup. The calculated irradiation time was 1.5 μs, and its duty was 0.0013%. The 1.5 μs irradiation time was considerably longer than that of the actual HAMR (only a few nanoseconds). Nevertheless, the result of the aforementioned study compared with that of the TGA was considerably closer to actual the HAMR condition.

Table 4-2 Corresponding laser power and coupling efficiency for various laser currents (mA)

Laser Current (mA)	Laser power (mW)		Coupling efficiency (%)
	LD out	Objective lens out	
117.5	66.8	19.1	28.6
120	69.3	20.4	29.4
130	78.3	22.5	28.7
140	83.6	24.6	29.4

As shown in Fig. 4-2 (b), the lubricant depletion caused by laser heating is visible using an optical surface analyzer (OSA) (KLA Corporation, Candela5100). The OSA enables the collection of reflectivity change data over the disk with high spatial resolution. The thickness profile is calculated based on the measured OSA reflectivity change after the difference in the OSA reflectivity is calibrated using the absolute lubricant film thickness on a half-dipped disk.

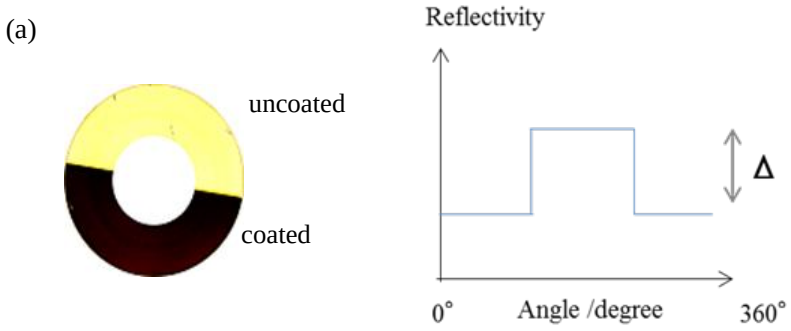

(b)

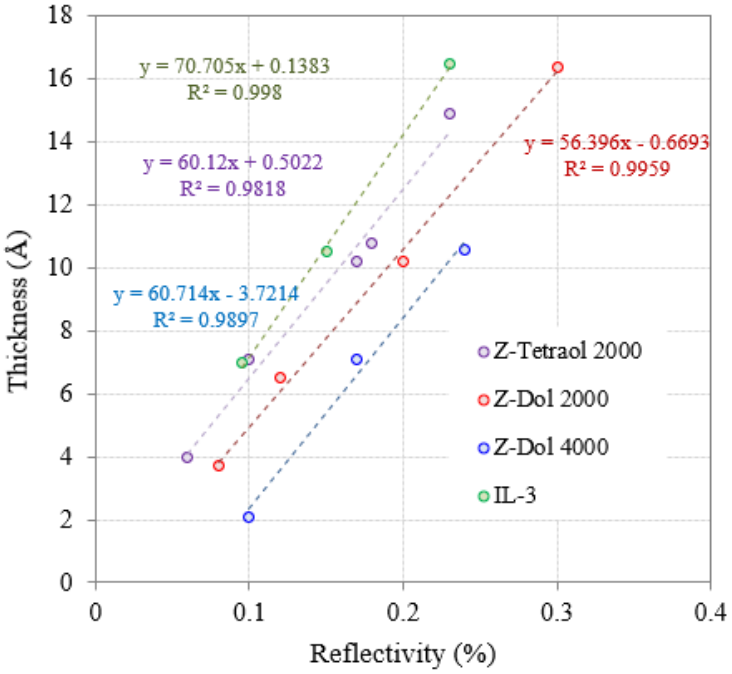

Fig. 4-3 (a) OSA image of half-dipped disk and illustrated angular average chart;
(b) OSA reflectivity change–absolute thickness calibration for each lubricant

The OSA reflectivity difference is the difference between the reflectivity of coated and uncoated surfaces based on the angular average reflectivity chart (Fig. 4-3 (a)). In this study, the absolute lubricant film thickness was measured by an ellipsometer. For the correlation between the absolute lubricant film thickness and OSA reflectivity difference, both the OSA and ellipsometry measurements were conducted for the thickness ladder of the half-dipped disk. Figure 4-3 (b) shows the OSA reflectivity difference–absolute thickness calibration for each lubricant. The OSA measurement was conducted on the disk within 3 min after laser irradiation. Within this period, the lubricant reflows did not affect the depletion profile considering the flow rate of each lubricant film. A digital average lubricant thickness chart was generated by the software bundled with Candela 5100. The Δ thickness profile is the difference between the thicknesses before and after laser irradiation. As shown in Fig. 4-4, the negative values in the Δ thickness profile indicate lubricant depletion, whereas positive values indicate lubricant accumulation.

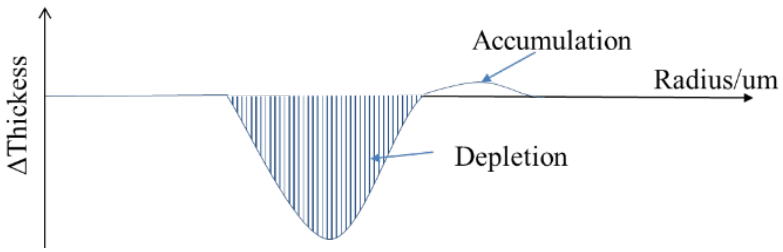

Fig. 4-4 Illustration of lubricant depletion calculation

The quantity of depletion was calculated using the OSA spatial resolution (μm) in the radial direction times the

summation of each depletion (Å) at the region where the sign was negative. In this study, the OSA spatial resolution in the radial direction was 0.3 μm. Therefore, the lubricant depletion was defined as the cross-sectional depletion area across the laser-heated track.

4.8. Lower Limitation of Lubricant Depletion Measurement

Tagawa et al. reported that the reflectivity of the carbon layer changed because of the rapid laser heating, resulting in the damage to the carbon layer [65]. This reflectivity change in the carbon layer affects the lubricant depletion measurement because the changes cannot be distinguished in the optical reflectivity. The reflectivity changes in the non-lubricated disk after 2 h of laser irradiation increased with the increasing laser current. To examine the effect of the reflectivity change in the carbon layer on the lubricant depletion measurement, the reflectivity change in the carbon layer is converted to lubricant thickness change using the OSA reflectivity difference–thickness calibration equation of Z-Dol 2000.

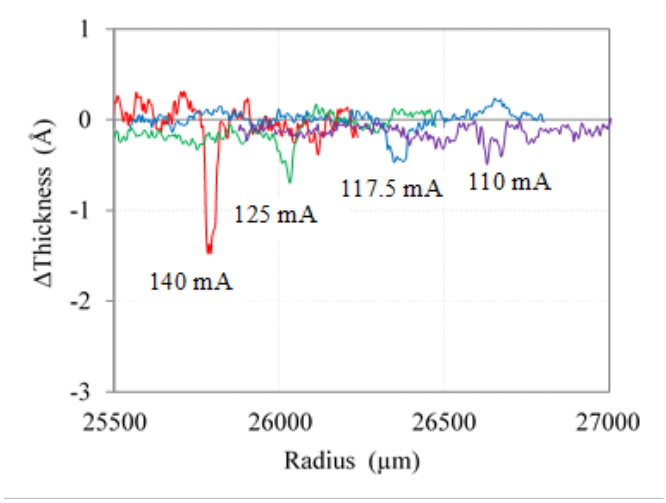

Fig. 4-5 OSA reflectivity changes converted to lubricant thickness using calibration equation of Z-Dol 2000

Table 4-3 Corresponding depletion quantity of non-lubricated disk for various laser current (mA)

Laser Current (mA)	Depletion Quantity (μm×Å)
110	1.7
117.5	2.0
125	2.1
140	3.6
	3.4

Figure 4-5 shows the converted thickness profile of the non-lubricated disk for various laser currents. Table 4-3 lists the corresponding lubricant depletion quantities for the carbon layer reflectivity change at each laser current. Below these levels, the actual lubricant depletion measurement for the lubricated disk is affected by the carbon layer reflectivity change, resulting in a lower limit of the lubricant depletion measurement.

3. Results

3.1 TG/DTA

Figure 4-6 shows the TG/DTA results as a function of temperature. The thermal stability increases in the order of Z-Dol 2000, Z-Tetraol 2000s, Z-Dol 4000, and IL-3. For the PFPE-type lubricants, the thermal stability depends on their MW and number of OH groups resulting from hydrogen bonding. The temperatures corresponding to the weight loss of Z-Tetraol 2000s, Z-Dol 2000, and Z-Dol 4000 are 150, 230, and 230 °C, respectively. The exothermic peak at approximately 360 °C indicates thermal decomposition. The exothermic peak intensity of DTA depends on the residual weight quantities at their peak temperatures. The weight loss was gradual with the increase in temperature

until 360 °C owing to evaporation. Compared with PFPEs, the IL-3 material exhibited superior bulk thermal stability. The exothermic peak of IL-3 is 430 °C, which is the thermal decomposition temperature of IL-3. For the actual HAMR, the top surface of the magnetic disk was heated up to 600 °C over an exposure time of a few nanoseconds [27,28]. The heat stress on the lubricant molecules could not be discussed simply based on TG measurement results because the manner of applying heat to the lubricant in the HAMR considerably differs from that in the TG measurement.

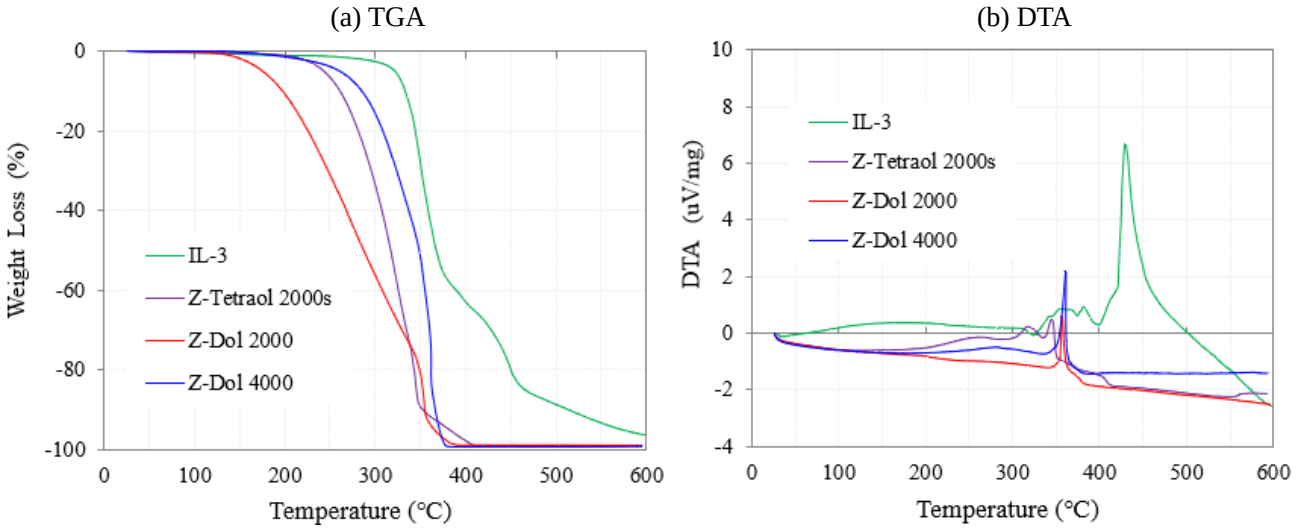

Fig. 4-6 (a) TG and (b) DTA as functions of temperature for PFPEs and IL

3.2 Lubricant flow rate

Table 4-4 lists the flow rates of lubricant films over a 1 h period. The flow rate decreases in the order Z-Dol 2000 > Z-Dol 4000 > Z-Tetraol 2000s > IL-3. The flow rates of PFPE lubricants decrease with higher MW and bond ratio. The flow rate of IL-3 is considerably smaller than those of the PFPE lubricants owing to the ionic interactions among molecules.

Table 4-4 Flow rate of lubricants in this study

Lubricant	Z-Tetraol 2000s	Z-Dol 2000	Z-Dol 4000	IL-3
Flow rate (μm/h)	6.6×10^{-1}	2.3×10	1.4×10	1.9×10^{-2}

3.3 Lubricant Depletion as Ultrathin Film

Figure 4-7 shows the thickness profiles at the laser irradiation of 140 mA. For Z-Dol 2000 without UV irradiation, lubricant accumulation was observed at the outer side of depletion to the spindle center. The depletion of Z-Tetraol 2000s was smaller than that of Z-Dol 2000, indicating that the bond ratio is critical to lubricant depletion because of the same MW backbone.

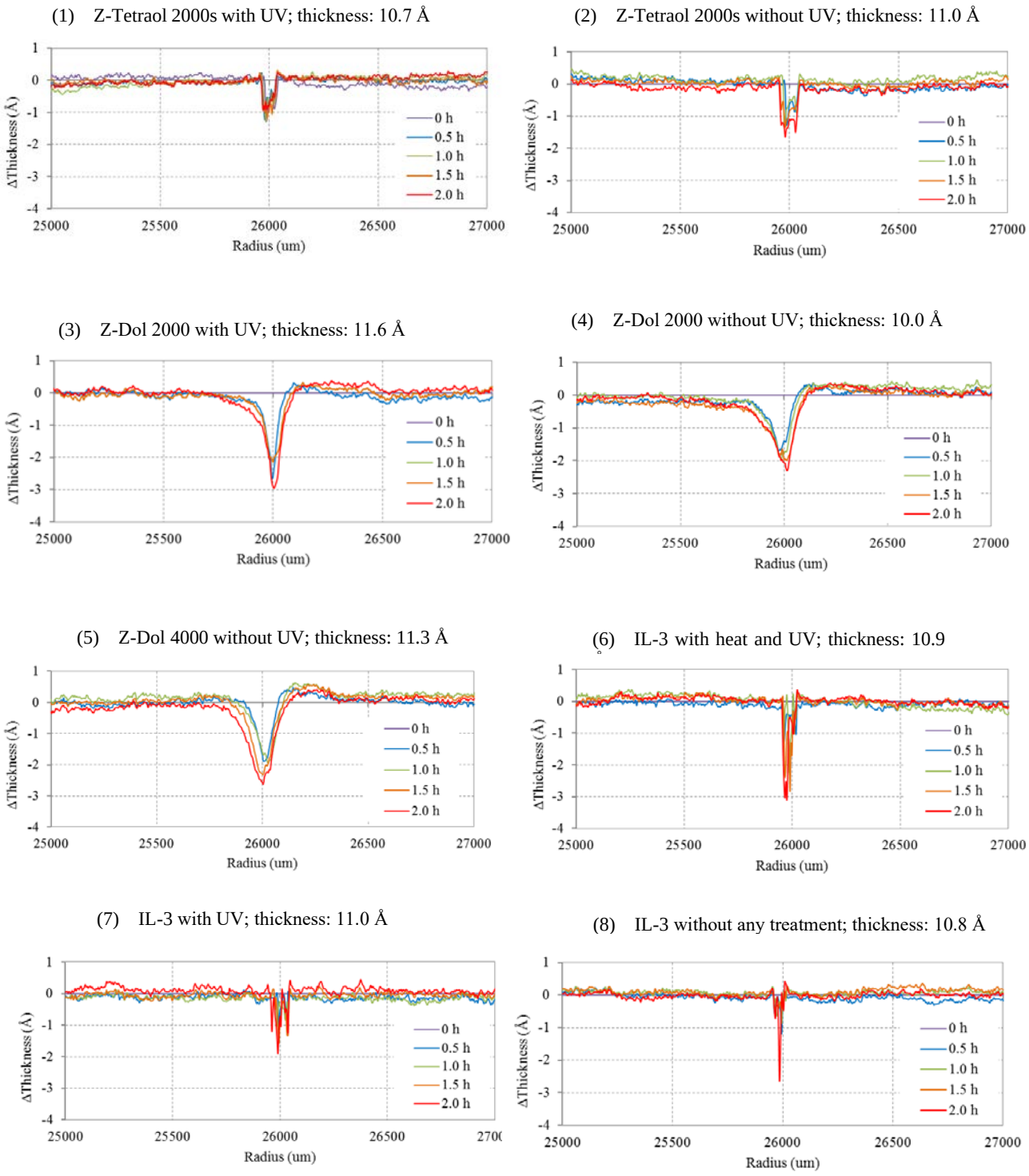

Fig. 4-7 Thickness profiles at 140-mA laser irradiation

Figure 4-8 shows the thickness profiles resulting from the 117.5 mA laser irradiation of Z-Dol 2000 or Z-Dol 4000 without UV; the lubricant depletion is smaller than that when the laser is at 140 mA because the laser power in the former is lower than that in the latter.

(4) Z-Dol 2000 without UV; thickness: 10.0 Å

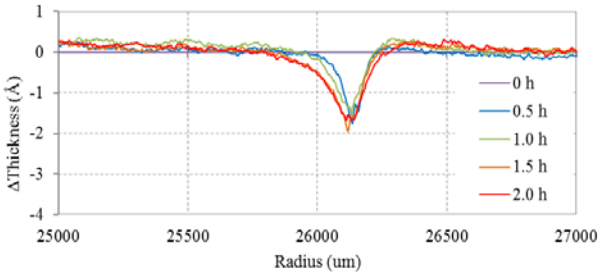

(5) Z-Dol 4000 without UV; thickness: 10.0 Å

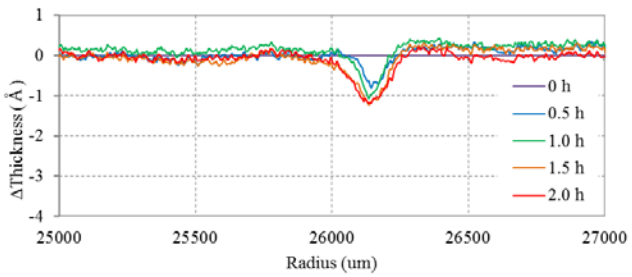

Fig. 4-8 Thickness profiles under 117.5-mA laser irradiation

4. Discussion

4.1 Correlation between lubricant depletion and bond ratio

Figure 4-9 shows the dependence of the lubricant depletion quantity on the bond ratio of PFPEs and IL-3. For the PFPEs, the depletion quantity decreases proportionally with the increasing bond ratio to the surface. These results suggest that bonded lubricant is durable, and the mobile lubricant is affected by laser irradiation. In contrast, IL-3 exhibits a small depletion despite the low bond ratio. As shown in the TGA measurement results, the IL-3 molecules interact electrostatically, resulting in high thermal stability. The origin of ionic interaction is the attraction force between the negative and positive charges. This ionic interaction is weaker than the chemical bond, however, it is sufficiently strong to maintain stability.

For both IL-3 and Z-Tetraol 2000s with UV, the depletion quantity was comparable with the reflectivity change in the non-lubricated disk after 2 h of laser irradiation (dotted line in Fig. 4-9), as discussed above. Thus, the most superior lubricant cannot be determined because the reflectivity change is extremely small.

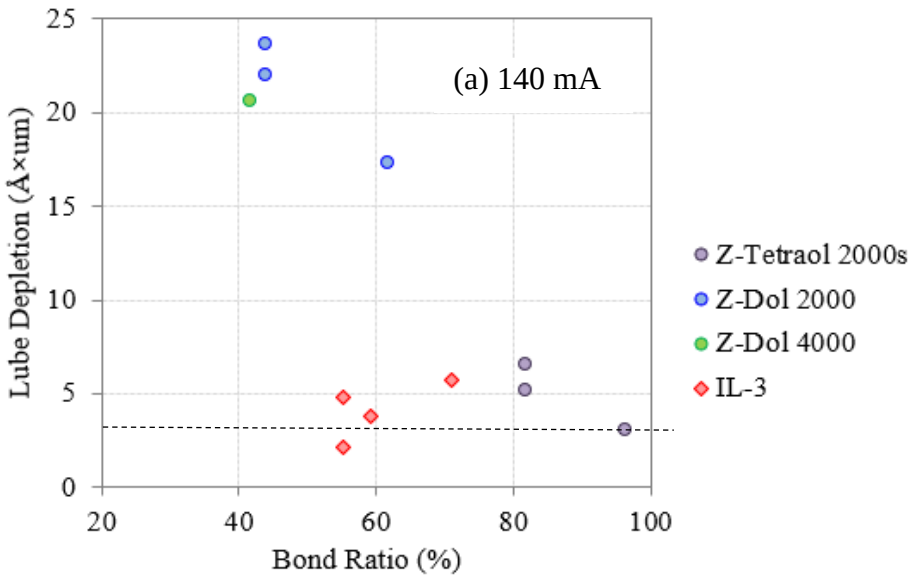

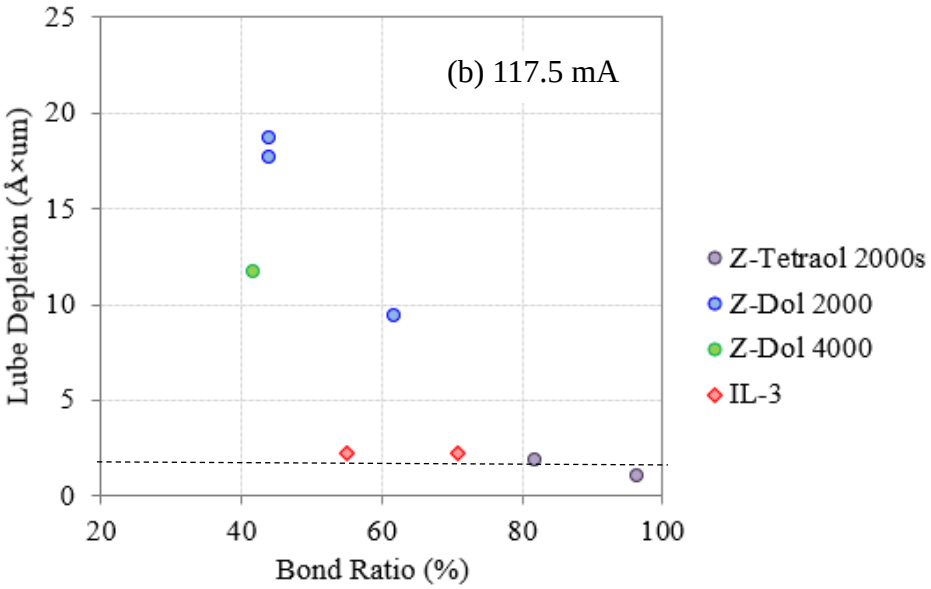

Fig. 4-9 Dependence of lubricant depletion quantity on bond ratio at 140-mA (a) and 117.5-mA (b) irradiation. Dotted line: corresponding depletion of non-lubricated disk caused by 2-h laser irradiation

As shown in Fig. 4-9, the dependency trend on the bond ratio at 117.5 mA laser irradiation was the same as that at 140 mA, except for Z-Dol 4000. Compared with Z-Dol 2000, Z-Dol 4000 exhibits a drastic decrease in lubricant depletion corresponding to the laser irradiation from 140 mA to 117.5 mA. This behavior suggests that the predominant mechanism of lubricant depletion at 117.5 mA is evaporation because Z-Dol 4000 has a greater bulk thermal stability than Z-Dol 2000 owing to its higher molecular weight. In contrast, at 140 mA, the depletion of PFPEs decreases proportionally with the increasing bond ratio. Considering that the dissociation energy of each chemical bond, such as C–C, C–O, and C–F, is higher than the photoelectron energy of the 830 nm laser wavelength: 1.49 eV which is calculated by $E=h\times c/\lambda$, and the thermal decomposition temperature of IL-3 is 430 °C is higher than the temperature of laser irradiation (272 °C at 140 mA), the lubricant depletion mechanism at 140 mA is assumed to be laser ablation. This is an explosive phenomenon owing to the high laser flux [68]. The local temperature increases or bond breaking by electronic excitation owing to the multiphoton absorption has a dominant role in laser ablation.

4.2 Lubricant Flow Back to Depletion Area

Figure 4-10 shows the thickness profile immediately after 2 h of 140-mA laser irradiation (red) and 24 h of storage in ambient environment after laser irradiation (blue). For Z-Dol 2000, without UV and at a 10.0 Å thickness, the depletion track caused by the laser irradiation disappeared after 24 h. This is because at this disk condition, the bond ratio is 44%, and the flowable layer (called mobile lubricant) is 56%. According to the flow rate measurement results, the distance traveled by Z-Dol 2000 in 24 h is 552 μm, which is comparable to the radius of the top surface of depletion (approximately 400 μm). Thus, the laser irradiation track disappears because the mobile lubricants flow

back to the depletion area. Ma et al. also observed the same phenomena using a considerably similar laser irradiation system [63].

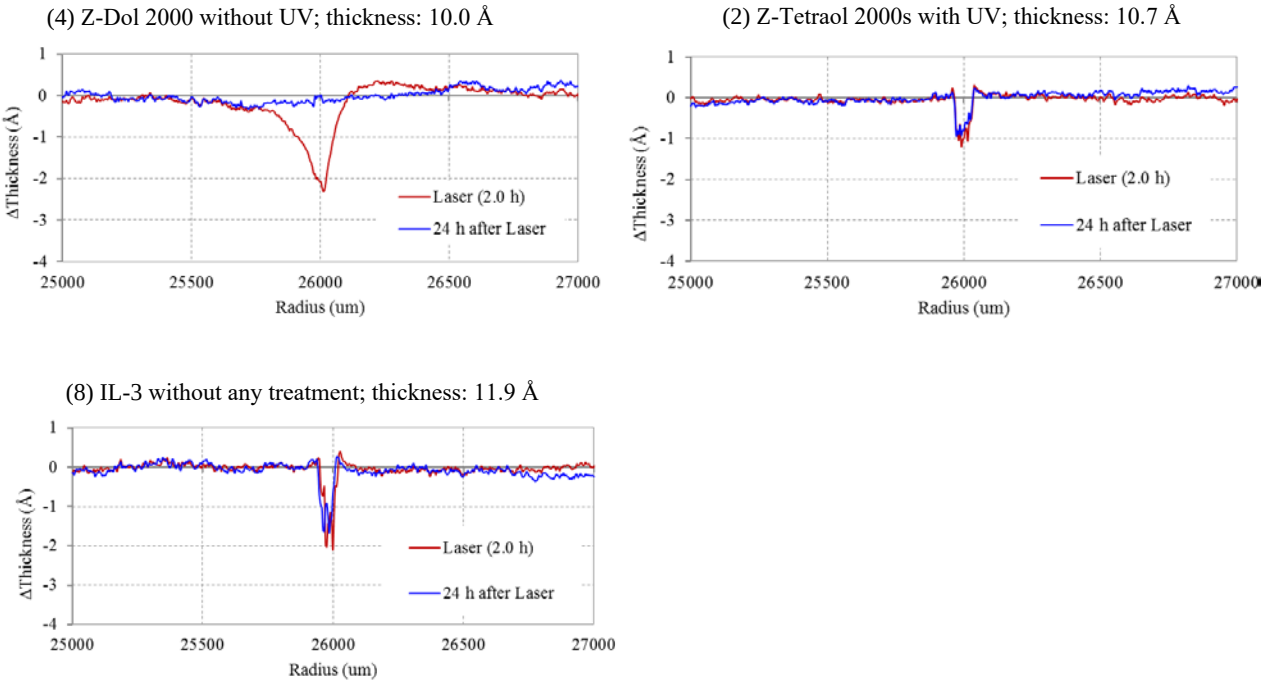

Fig. 4-10 Thickness profile immediately after or 24 h of 2-h laser irradiation

There was no change in the depletion profile of IL or Z-Tetraol 2000s irradiated with UV during the 24 h storage of these lubricants. The distance traveled by Z-Tetraol 2000s in 24 h is 16 μm, however, the reflow phenomena cannot be observed. Considering the foregoing as well as the considerably small depletion quantities, which are comparable to the reflectivity change in the carbon layer, the reason for thickness depletion is the reflectivity change in the carbon layer under these two conditions (IL-3 or Z-Tetraol 2000s with UV).

4. Conclusion

In this study, new thermally stable IL-type lubricants have been developed to solve the problem related to HAMR systems. Ultrathin lubricant film depletion for the IL-type and PFPE-type lubricants was quantitatively evaluated using the far-field laser irradiation system. The results for IL-3 can be summarized as follows.

(1) At 140 mA, the PFPE-type lubricant film depletion decreased proportionally with increasing bond ratio. The IL-type lubricant depletion was small and did not depend on bond ratio.

(2) The lubricant depletion quantified at 117.5 mA was smaller than that at 140 mA because of the lower laser power. Although the depletions of Z-Dol 4000 and Z-Dol 2000 were the same at 140 mA, Z-Dol 4000 exhibited a drastic decrease at 117.5 mA owing to higher MW.

(3) The depletion mechanism at 117.5 mA was predominantly evaporation based on (2). The mechanism at 140 mA may be laser ablation because the depletion quantity depended on the bond ratio.

(4) According to the OSA, for Z-Dol 2000 without UV, the lubricant flowed back to the depletion area. The depletion profile of IL or Z-Tetraol 2000s after UV irradiation did not change after 24 h of storage because the depletion quantities were extremely smaller than the reflectivity change in the non-lubricated disk.

In this study, the ILs were compared with the PFPE with the highest bond ratio. However, the more superior lubricant type between the two cannot be ascertained based solely on the depletion measurement by the OSA reflectivity change. Other analysis methodologies of laser irradiation track are required. These include atomic force microscopic friction measurement, Auger electron spectroscopy, and time-of-flight secondary ion mass spectroscopy, which have high spatial resolutions.

5. Conclusion and Outlook

The objective of this study is to prepare a new type of IL lubricant for wide use in the hard disk industry. For this objective, ILs were synthesized, and their basic properties were investigated relative to HDI performance. Collaboration with several companies in this industry was forged, and considerable amounts of feedback were received from these entities. The author cannot disclose the HDI evaluation results from the HDD company because the evaluation data are included in the non-disclosure agreement. The HDI evaluation data depend on the disk media and processes, such as dip coating, tape vanish, and UV condition. If the same type of sample is provided to two different HDD companies, different results are supposed to be obtained. In contrast, numerous investigations have reported on the correlation between the basic properties of PFPE and HDI performance. It is known that how those basic properties work for HDI performance. Similarly, the author attempted to predict the HDI performance according to the data on the basic properties of ILs compared with those of Z-Tetraol 2000s (Table 5-1).

Table 5-1 Comparison between IL and PFPE on thin film properties at approximately 10 Å

		Unit	PFPEs		ILs			
			Z-Tetraol 2000s	Z-Dol 2000	IL	IL-1	IL-2	IL-3
Chem	Molecular Weight	-	2300	2200	1284	1066	1314	1040
	Number of OH group	-	4	2	1	2	2	0
Bulk	TGA (10% weight loss)	°C	261	198	349	361	358	334
Thin Film at 10 Å	Bond Ratio*1	%	82	49	36	59	56	55
	Polar surface energy	mJ/m^2	14.5	17.5	31.3	53.8	32.5	-
	Dispersive Surface Energy	mJ/m^2	15.5	14.7	15.6	16.5	15.1	-
	Monolayer thickness	Å	18	17	12	6	13	-
	Mobility*2	μm/h	0.7	20	0.13	0.10	0.03	0.02
	Coverage Ratio	%	91	93	92	99	95	-
	Adhesion Force	mN	0.24	0.24	0.11	0.07	0.15	-
	Friction Force	mN	0.49	-	0.40	-	-	-
	Thickness Loss (160 °C 12 h)	%	12	44	-	2	5	-
	Laser Depletion (140mA)	Å×μm	5.2	23.7	-	-	-	4.8

*1: Bond ratio considerably depends on the type of magnetic disk and its freshness; techniques for enhancing the bond ratio exist. No treatments for IL and IL-3; Heat treatment for IL-1 and IL-2. Z-Tetraol and Z-Dol.
*2: Mobility data are derived from the terrace flow measurement.

Figure 5-1 is the rader chart displaying multivariate data of Table 5-1. For each properties, the direction of the axis is determined individually as enhancing HDI performance, i.e., touchdown performance become better as monolayer thickness decrease, low bond ratio and high coverage ratio is advantagerous for better head wear performance. Thus the wider area of the rader chart indicate the better lubricant performance of magnetic disk shall be attained. ILs exhibit better thickness stability despite of low bond ratio and smaller monolayer thickness.

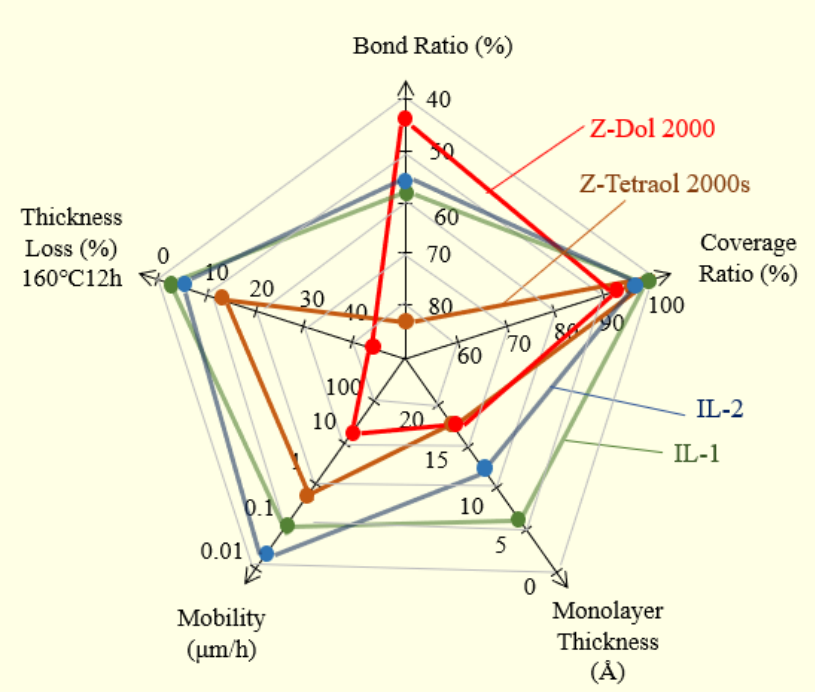

Fig. 5-1 Radar chart of the lubricant properties for IL as the comparison with Z-Tetraol and Z-Dol

The conclusions regarding IL can be summarized as follows.

(1) Design concept of ILs: The design concept was experimentally confirmed. As the demand for a narrower HMS increases, thinner lubricants are desired. In this study, the monolayer thicknesses were 6 and 12 Å for IL-1 and IL-2, respectively. These thickness values are smaller than that of Z-Tetraol 2000s (18 Å). By designing the position of the OH groups, the perfluoroether chain of IL-1 is tethered to the disk surface with a terminal OH group at each end, the perfluoroehter chain of IL-2 points upward from the surface. The small monolayer thickness is considerably advantageous, allowing the ILs to achieve a superior touchdown performance. At the same time, the IL exhibits small amounts of depletion under laser irradiation and acceptable thickness stability when exposed to 130 °C or 160 °C of heating because of ionic interactions. This thermal stability is required for HAMR lubricants as shown in Fig. 5-1.

(2) New IL bonding approach: Generally, lubricants with a low bond ratio exhibit a good head wear owing to the large amount of mobile lubricant; however, this mobile lubricant causes poor thermal stability and lubricant pick-up. This is a trade-off problem in HDI performance. The ILs exhibit a small bond ratio but high thermal stability. Its mobility is also small, as confirmed by the terrace flow. These IL results indicate that high thermal stability and low mobility have been attained simultaneously despite the low bond ratio. The ILs adsorb on the disk surface via the ionic pair. This is a new insight with regard to the manner of bonding, which can lead to the simultaneous satisfaction of the specifications on head wear and thermal stability. This IL performance cannot be attained by the chemical

bonding of the PFPE lubricant.

(3) Adhesion force: The adhesion force of IL is lower than that of the PFPE despite its high surface energy. The small adhesion force is a key parameter for stable head flying in the HDD. It is experimentally confirmed that the adhesion force depends on the molecular orientation, and a low adhesion force is necessary for the stable head flying of HDD. Moreover, a stiction issue of other micro-machines is effectively resolved by these IL type lubricant with such a property.

(4) Corrosive property: The polar surface energy of ILs is high, but its dispersive surface energy is comparable to that of the PFPE, indicating that the disk surface is sufficiently covered by the lubricant. When the surface energy is high for PFPEs, the disk surface is not covered by the lubricant, causing a corrosion problem. The high surface energy of ILs (polar) is different from the phenomenon that is observed in PFPEs (dispersive). Moreover, corrosion is the consequence of the combination of the carbon overcoat and lubricant. Further investigations are necessary for the corrosion problem.

As stated above, the bonding of IL differs from that of the conventional lubricant, and the IL's molecular orientation can be controlled because of its high ordering ability. By designing the molecular structure of the IL, this material can simultaneously satisfy several specifications. Because the HDI condition becomes more severe than that of the HAMR, the aforementioned IL characteristics are critical to the formulation of lubricants for the HAMR.

6. Acknowledgement

I would like to thank Mr. Nobuo Tano for assisting in the synthesis of the ILs. We frequently discussed the molecular design of ILs based on the results of the HDI evaluation, our discussion revolved on ideas regarding ILs. Our ILs are original chemical compounds, hence, details regarding their synthesis are not available. He established the original synthesis recipe and skillfully prepared the actual samples. At the first stage of development, the chemical structure of ILs were relatively simple. As the development progressed, we were able to determine the correlation between the chemical group and specific HDI performance. The corresponding chemical groups are supposed to be in one molecule, leading to a complex chemical structure of the IL. As stated in the experiment section of Chapter 3, three steps are necessary for synthesizing IL-1 and IL-2, which are extremely complex and have multiple functions. Accordingly, numerous researchers worldwide have investigated ILs. However, I believe that no one can make such ILs with a complex chemical structure. As one of the motivations for publishing this paper, I would like to introduce these ILs to the world.

I would like to thank Prof. Tani. Before I joined Prof. Tani's laboratory, I read his papers to understand how the PFPE-type lubricants function on the magnetic disk surface and to identify the key parameters involved in this field. His papers demonstrated the "beauty" of the graphs, which are indicative of the underlying mechanism of micro-tribology; I profoundly appreciated his work. While working in his laboratory, I was delighted using the measurement apparatus that he devised, especially the scanning ellipsometry, which enabled the accurate measurement of lubricant thickness. Lubricant thickness is a critical parameter of bond ratio, film stability, and terrace flow profile. Because our IL properties are unique compared to those of the PFPEs, I enjoyed gathering the experiment data on the new ILs and these basic data are necessary for the fundamental understanding of HDIs. Our Ionic liquids are state-of-the-art materials as synthesized by Mr. Tano , and in Kansai University, the instruments for working on ILs are also state-of-the-art. During my stay at Kansai University, I was always afforded the opportunity to discuss the molecular design of ILs with Prof. Tani. I always shared those discussions with my team as feedback in developing our lubricant. After I left his laboratory, he allowed me to have the opportunity to pursue my Ph.D. He continued to support me and spent considerable time to examine the manuscript despite of his busy schedule. No words can express my gratitude.

I would like to express my gratitude to Prof. Tagawa and Prof. Shinguhara who to took time to examine my work. I had meaningful discussions with them, and those discussions were invaluable to this thesis.

I would like to thank all the people who have assisted in developing our ILs, including my colleague and our client. They devoted considerable efforts for evaluating our ILs. All this work would not have been possible without their support.

7. References

Business Perspective for HDD

[1] An IDC White Paper – #US44413318, “The Digitization of the World from Edge to Core,” Nov. 2018

[2] Marchon, B., Pitchford, T., Hsia, Y.T, and Gangopadhyay, S., “The Head-Disk Interface Roadmap to an Areal Density of 4 Tbit/in^2,” *Adv. Tribol.*, Article ID 521086, 2013

PFPE as Lubricant for Magnetic Media

[3] Bhushan, B. “Tribology and Mechanics of Magnetic Storage Devices,” Second edition *Springe*r, IEEE press ISBN 0-7803-3406-X

UV Treatment

[4] Vurens, G.H., Gudeman, C.S., Lin, L.J., and Foster, J.S., “Mechanism of Ultraviolet and Electron Bonding of Perfluoropolyethers,” *Langmuir*, 8, 1165–1169, 1992

[5] Zhang, H., Mitsuya, Y., Imamura, M., Fukuoka, N., and Fukuzawa K., “Effect of Ultraviolet Irradiation on the Interactions between Perfluoropolyether Lubricant and Magnetic Disk Surfaces,” *Tribo.Lett.*, 20, pp. 191–199, 2005

[6] Guo, X.C. and Waltman, R.J., “Mechanism of Ultraviolet Bonding of Perfluoropolyethers Revisited” *Langmuir*, 23, 8, 4293–4295, 2007

[7] Tani, H., Kitagawa, H., and Tagawa, N., “Bonding Mechanism of Perfluoropolyether Lubricant Film with Functional Endgroup on Magnetic Disks by Ultaviolet Irradiation,” *Tribol. Lett.* 45, 117–122, 2012

Key Parameters of PFPE for Touchdown Clearance Performance

[8] Waltman, R.J. and Deng, H., “Low Molecular Weight Z-Tetraol Boundary Lubricant Films in Hard Disk Drives,” *Adv. Tribol*., Article ID 964089, 2012

[9] Khurshudov, A. and Waltman, R. J., “The Contribution of Thin PFPE Lubricants to Slider–Disk Spacing,” *Tribol. Lett.*, 11, 3–4, 143–149, 2001

[10] Waltman, R.J. and Khurshudov, A.G., “The Contribution of Thin PFPE lubricants to Slider–Sisk Spacing. 2. Effect of film thickness and lubricant end groups,” *Tribol. Lett.*, 13, 3, 197–202, 2002

[11] Waltman, R.J., Raman, V., and Burns, J., “The Contribution of Thin PFPE Lubricants to Slider–Disk Spacing. 3. Effect of main chain flexibility,” *Tribol. Lett.*, 17, 2, 239–244, 2004.

[12] Waltman, R.J., “The Adsorbed Film Structure of End-Functionalized Poly(Perfluoro-n-Propylene Oxide),” *Tribol. Online*, 9, 3, 113–120, 2014.

Multidentate-type PFPE Lubricant

[13] Waltman, R.J., “Boundary Lubricant Film Properties versus Molecular Polarity of Perfluoropolyethers Containing a Pendant Chain,” *Tribol. Online*, 7, 1, 41–45, 2012

[14] Marchon, B., Guo, X.C., Karis, T., Deng, H., Dai, Q., Burns, J., and Waltman, R., “Fomblin Multidentate Lubricants for Ultra-Low Magnetic Spacing,” *IEEE Trans. Magn.*, 42, 10, 2504–2506, Oct. 2006

[15] Guo, X.C., Knigge, B., Marchon, B., Waltman, R.K., Carter, M., and Burns, J., “Multidentate Functionalized Lubricant for Ultralow Head/Disk Spacing in a Disk Drive” *J. Appl. Phys.*, 100, 044306, 2006

[16] Waltman, R. J., Deng, H., Wang, G. J., Zhu, H. and Tyndall, G. J. “The Effect of PFPE Film Thickness And Molecular Polarity on the Pick-up of Disk Lubricant by a Low-flying Slider,” *Tribol. Lett.*, 39, 211–219, 2010

[17] Guo, X.C., Marchon, B., Wang, R.H., Mate, C.M., Dai, Q., Waltman, R.J., Deng, H., Pocker, D., Xiao, Q.F., Saito, Y., and Ohtani, T., “A Multidentate Lubricant for use in Hard Disk Drives at Sub-Nanometer Thickness,” *J. Appl. Phys*. 111, 024503, 2012.

[18] Tani. H., Shimizu, T., Kobayashi, N., Taniike, Y., Mori, K., and Tagawa, N., “Study of Molecular Conformation of PFPE Lubricants with Multidentate Functional Groups on Magnetic Disk Surface by Experiments and Molecular Dynamics Simulations.” *IEEE Trans. Magn.* 46, 6,1420–1423, 2010

Thickness Measurement

[19] Linder, R.E. and Mee, P.B., “ESCA Determination of Fluorocarbon Lubricant Film Thickness on Magnetic Disk Media.” *IEEE Trans. Magn.* MAG-18, 6, 1073–1076, Nov. 1982

[20] M. Hoshino and Y. Kimachi, “XPS Measurement of Lubricant Layer Thickness on Magnetic Recording Disks,” *J. Elect. Spect. Related Phenom.*, 81, 1996, 79–85

[21] Tang, H., Ma, X., Barth, G., Liu, J., Stirniman, M., and Gui J., “ESCA-Thickness Metrology and Head-Medium Spacing Impact of Disk Lubricant,” *IEEE Trans.Magn*., 41, 2, 2504–2506, Feb 2005

Basic Theory of Surface Energy

[22] Tyndall, G.W., Leezenberg, P.B., Waltman, R.J., and Castenada, J., “Interfacial Interactions of Perfluoropolymer Lubricants with Magnetic Recording Media,” *Tribol. Lett*., 4, 2, 103−108, 1998

Contamination

[23] Sonoda, K., “Flying Instability due to Organic Compounds in Hard Disk Drive,” *Adv. Tribol*, Article ID 170189, 2012

[24] Seo, Y.W., Ovcharenko, A., Bilich, D., and Talke, F.E., “Experimental Investigation of Hydrocarbon Contamination at the Head–Disk Interface,” *Tribol. Lett.* 65, Article number 54, 2017

[25] Tani, H., Uesaraie, Y., Lu, R., Koganezawa, S., Tagawa, N., “Smear Growth on Head Slider Surface from Siloxane Outgas on Heat-assisted magnetic recording,” *Microsys. Tech*. 24, 4641–4648, 2018

[26] Kiely, J.D., Jones, P.M., Yang, Y., Brand, J.L., Anaya-Dufresne, M., Fletcher, P.C., Zavaliche, F., Toivola, Y., Duda, J. C., and Johnson, M.T., “Write-Induced Head Contamination in Heat-Assisted Magnetic Recording,” *IEEE Trans. Magn*., 53, 2, Article number 3300307, Feb. 2017

HAMR as Next-Generation Recording System

[27] Kryder, M.H., Gage, E.C., McDaniel, T.W., Challener, W.A., Rottmayer, R.E., Ju, G.P., Hsia, Y.T., and Erden, M.F. “Heat-Assisted Magnetic Recording,” *Proc. IEEE*, 96, 1810−1835, 2008

[28] Marchon, B., Guo, X.C, Pathern, B.K., Rose, F., Dai, Q., Feliss, N., Schreck, E., Reiner, J., Mosendz, O., Takano, K., Do, H., Burns J., and Saito Y., "Head-Disk Interface Materials Issues in Heat-Assisted Magnetic Recording," *IEEE Trans. Magn.*, 50, 3 Mar., Article ID 3300607, 2014

Thermal Stability of Ionic Liquid

[29] Miran, M.S., Kinoshita, H., Yasuda, T., Susan, M. A. H., and Watanabe, M., "Physicochemical Properties Determined by for Protic Ionic Liquids Based on an Organic Super-Strong Base with Various Bronsted Acids," *Phys. Chem. Chem. Phys*., 14, 15, 5178–5186, 2012

[30] Yoshizawa, M., Xu, W., Angell, C.A., "Ionic liquids by Proton Transfer: Vapor Pressure, Conductivity, the Relevance of Aqueous Solutions," *J. Am. Chem. Soc.*, 125, 50, 15411–15419, 2003

[31] Luo, H., Baker, G.A., Lee, J.S., Pagni, R.M., and Dai, S., "Ultrastable Superbase-Derived Protic Ionic Liquid," *J. Phys. Chem B*, 113, 13, 4181–4183, 2009

Previous Investigation of Ionic Liquid on Lubricant for Magnetic Disk Media

[32] Ye, C., Liu, W., Chen, Y., Yu, L., "Room-Temperature Ionic Liquids: A Novel Versatile Lubricant," *Chem. Commun.*, 2244–2245, 2001

[33] Kondo, H., Seki, A., Watanabe, H., and Seto, J., "Frictional Properties of Novel Lubricants for Magnetic Thin Film Media," *IEEE Trans. Magn.*, 26, 5, 1990, 2691–2693

[34] Kondo, H., Seki, A., and Kita, A., "Comparison of an Amide and Amine Salt as Friction Modifiers for a Magnetic Thin Film Medium," *Trib. Transac.*, 37, 1, 99–105, 1994

[35] Kondo, H., "Protic Ionic Liquids with Ammonium Salts as Lubricants for Magnetic Thin Film Media," *Tribol. Lett.*, 31, 3, 211–218, 2008

[36] Gong, X., Kozbial, A., Rose, F., and Li, L., "Effect of $\pi-\pi+$ Stacking on the Layering of Ionic Liquids Confined to an Amorphous Carbon Surface," *ACS Appl. Mater. Interfaces*, 7, 13, 7078–7081, 2015

[37] Gong, X., West, B., Taylor, A., and Li, L., "Room-Temperature Ionic Liquids (RTILs): Media Lubricants for Heat Assisted Magnetic Recording (HAMR)," *IEEE Trans. Magn.*, DOI: 10.1109/TMAG.2015.2438253, 2015

[38] Gong, X., West, B., Taylor, A., and Li, L., "Study on Nanometer-Thick Room-Temperature Ionic Liquids (RTILs) for Application as the Media Lubricant in Heat-Assisted Magnetic Recording (HAMR)" *Ind. Eng. Chem. Res.* 55, 20, 6391–6397, 2016

[39] Kondo, H., Ito, M., Hatsuda, K., Yun, K.Y., and Watanabe M., "Novel Ionic Lubricants for Magnetic Thin Film Media," *IEEE Trans. Magn.*, 49, 7, 3756–3759, 2013

[40] Kondo, H., Hatsuda, K., Tano, N., Ito, M., Yun, K.Y., and Watanabe, M., "Novel Ionic Lubricants for Magnetic Thin Film Media," *IEEE Trans. Magn.*, 50, Article ID 3302504, 2014

[41] Kondo, H., Hatsuda, K., Tano, N., Baghel, P., and Noguchi, T., "Thin Film Properties of Ammonium Sulfonate Ionic Liquids Having a Long Alkyl Chain," *Bull. Chem. Soc. Jpn.* 90, 2, 188–194, 2016

[42] Tani, H., Lu, R., Koganezawa, S., and Tagawa, N., "Adsorption Properties of an Ultrathin PFPE Lubricant With Ionic End-Groups for DLC Surfaces," IEEE Trans. on Magn., 54, 2, Article number 3300106, Feb. 2018

[43] Wang, B., Moran, C., Lin, D., Tang, H., Gage, E., and Li, L., "Nanometer-thick Fluorinated Ionic Liquid Films as

Lubricants in Data-Storage Devices," *ACS Appl. Nano. Mater.*, 14, 155–162, 2019

Lubricant Synthesis of Chapter2

[44] Japan patent: P2018-1780792

Terrace Flow Method

[45] Tyndall, G.W., Karis, T.E., and Jhon, M.S., "Spreading Profiles of Molecularly Thin Perfluoropolyether Films," *Tribol. Trans.* 42, 3, 463470, 1999

Pin-on-Disk microtribometer

[46] Tani, H. and Tagawa, N., "Adhesion and Friction Properties of Molecularly Thin Perfluoropolyether Liquid Films on Solid Surface," *Langmuir*, 28, 8, 3814-3820, 2012

[47] Tani, H., Mitsutome, T., and Tagawa, N., "Adhesion and Friction Behavior of Magnetic Disks with Ultrathin Perfluoropolyether Lubricant Films having Different End-Groups Measured Using Pin-On-Disk Test," *IEEE Trans. Magn.*, 49, 6, 2638–2644, 2013

FT/IR RAS

[48] Kondo, H. and Iimura, K., "Effect of Partially Fluorinated Alkyl Chain on Friction and Surface Energy," *Bull. Chem. Soc. Jpn.*, 87, 4, 564–569, 2014

[49] Ren, Y., Iimura, K., and Kato, T., "Polarized Infrared Study on the Structure of Two-Dimensional Nanoclusters of Partially Fluorinated Long-Chain Fatty Acid Salts at Ambient and Elevated Temperatures," *J. Chem. Phys.*, 113, 3, 1162–1169, 2000

[50] Chau, L.K. and Porter, M.D., "Composition and Structure of Spontaneously Adsorbed Monolayers of N-Perfluorocarboxylic Acids on Silver," *Chem. Phys. Lett.*, 167, 3, 198–204, 1990

Bond Thickness Profile

[51] Waltman, R.J. "The Interactions between Z-Tetraol Perfluoropolyether Lubricant and Amorphous Nitrogenated- and Hydrogenated-Carbon Surfaces and Silicon Nitride," *J. Fluorine Chem.*, 125, 3, 391–400, 2004

Solvation Force measured by Surface Force Apparatus or AFM

[52] Ueno, K., Kasuya, M., Watanabe, M., Mizukami, M., and Kurihara, K., "Resonance Shear Measurement of Nanoconfined Ionic Liquid," *Phys. Chem. Chem. Phys.*, 12, 16, 4066–4071, 2010

[53] Canova, F.F., Matsubara, H., Mizukami, M., Kurihara, K., and Shluger, A.L., "Shear Dynamics of Nanoconfined Ionic Liquids," *Phys. Chem. Chem. Phys.* 16, 8247–8256, 2014

[54] Smith, A.M., Lovelock, K.R.J., Gosvami, N.N., Welton, T., and Perkin, S., "Quantized Friction across Ionic Liquid Thin Films," *Phys. Chem. Chem. Phys.*, 15, 37, 15317–15320, 2013

[55] Smith, A.M., Lovelock, K.R.J., Gosvami, N.N., Licence, P., Dolan, A., Welton, T., and Perkin, S. "Monolayer to Bilayer Structural Transition in Confined Pyrrolidinium-Based Ionic Liquids," *J. Phys. Chem. Lett.*, 4, 3, 378–382,

2013

Molecular orientation of IL at interface

[56] Kolbeck, C., Cremer, T., Lovelock, K.R.J., Paape, N., Schulz, P.S., Wasserscheid, P., Maier, F., and Steinruck, H.P., "Influence of Different Anions on the Surface Composition of Ionic Liquids Studied Using ARXPS," *J. Phys. Chem. B*, 113, 25, 8682–8688, 2009

[57] Aliaga, C., Baker, G.A., and Baldelli, S., "Sum Frequency Generation Studies of Ammonium and Pyrrolidinium Ionic Liquids Based on the Bis-trifluoromethanesulfonimide Anion," *J. Phys. Chem. B*, 112, 6, 1676–1684, 2008

Microtribology

[58] Zhao, W., Zhu, M., Mo, Y., and Bai, M., "Effect of Anion on Micro/Nano-Tribological Properties of Ultra-thin Imidazolium Ionic Liquid Films on Silicon Wafer," *Colloid Surface A*, 322, 78–83, 2009

[59] Mate, C. M., "Tribology on the Small Scale: A Bottom Up Approach to Friction, Lubrication, and Wear (Mesoscopic Physics and Nanotechnology)," 1st edition, *Oxford University Press*, 2008

Far-Field Laser Irradiation Experiment for PFPE

[60] Tagawa, N., Kakitani, R., Tani, H., Iketani, N., and Nakano, I., "Study of Lubricant Depletion Induced by Laser Heating in Thermally Assisted Magnetic Recording Systems-Effect Of Lubricant Film Materials," *IEEE Trans. Magn.*, 45, 2, 877–882, Feb. 2009

[61] Tagawa N. and Tani H., "Lubricant Depletion Characteristics Induced by Rapid Laser Heating in Thermally Assisted Magnetic Recording," *IEEE Trans. Magn.*, 47, 1 Jan., 105–110, 2011

[62] Ma, Y.S., Gonzaga, L., An, C.W., and Liu, B., "Effect of Laser Heating Duration on Lubricant Depletion in Heat-Assisted Magnetic Recording," *IEEE Trans. Magn.*, 47, 10, Oct., 3445–3448, 2011

[63] Ma, Y.S., Chen, X.Y., Zhao, J.M., Yu, S.K., Liu, B., Seet, H.L., Ng, K.K., Hu, J.F., and Shi, J.Z., "Experimental Study of Lubricant Depletion in Heat-Assisted Magnetic Recording," *IEEE Trans. Magn.*, 48, 5, May, 1813–1818, 2012

[64] R. Ji, Y. Ma, and J. Tsai, "Studies of degradation and decomposition mechanisms of high temperature lubricants undergoing laser irradiation," *IEEE Trans. Magn.*, 48, 11, 4475–4478, 2012

[65] Tagawa, N., Tani, H., and Koganezawa, S., "Degradation of Carbon Overcoat Subjected to Laser Heating in an Inert Gas Environment in Thermally Assisted Magnetic Recording," *IEEE Trans. Magn.*, 50, 11, Nov., Article Number 3302404, 2014

[66] Tani, H., Koganezawa, S., and Tagawa, N., "Thermal Behavior of Frictional Properties on Ultrathin Perfluoropolyether Lubricant Film," *Tribologist*, 60, 8, 538–548, 2015 (in Japanese)

Lubricant Synthesis of Chapter 4

[67] Japan patent: P2017-107623A

Laser Ablation

[68] Gamaly, E.G., Juodkazis, S., Nishimura, K., Misawa, H., Luther-Davies, B., Hallo, L., Nicolai, P., and Tikhonchuk,

V.T., “Laser–Matter Interaction in the Bulk of a Transparent Solid: Confined Microexplosion and Void Formation,” *Phys. Review B*, 73, pp. 214101, 2006